The Influence of Normal Physiological Forces on Porcine Aortic Heart Valves in a Sterile *Ex Vivo* Pulsatile Organ Culture System

A Thesis
Presented to
The Academic Faculty

by

Suchitra Konduri

In Partial Fulfillment
Of the Requirements for the Degree
Master of Science in
School of Chemical and Biomolecular Engineering

Georgia Institute of Technology

May 2005

The Influence of Normal Physiological Forces on Porcine Aortic Heart Valves in a Sterile *Ex Vivo* Pulsatile Organ Culture System

Approved by:

Dr. Ajit P.Yoganathan, Advisor
School of Biomedical Engineering
Georgia Institute of Technology

Dr. Timothy M. Wick
School of Chemical and Biomolecular Engineering
Georgia Institute of Technology

Dr. Athanassios Sambanis
School of Chemical and Biomolecular Engineering
Georgia Institute of Technology

Date Approved: January 28, 2005

ACKNOWLEDGEMENTS

I am grateful to many people at Georgia Tech for their guidance and support during this project. First and foremost, I would like to thank my advisor, Dr. Ajit P.Yoganathan for providing me an opportunity to pursue research in an interesting area and his counsel through out. I would also like to thank Dr. Sambanis and Dr. Wick for being a part of my thesis committee.

I acknowledge the National Science Foundation for providing financial support for the work through GTEC-ERC program at Georgia Tech (EEC- 9731643). Special thanks to Mr. Holifield of Holifield's Farm in Covington, GA for donating aortic valves for the experiments. He provided me with facilities to harvest the tissue inside the abattoir for preserving the viability of the valves. His generosity in supporting research is greatly appreciated. I am very grateful for the efforts of Mr. Jeferry Andrews and Mr.Brad Parker of ChbE machine shop, John Graham of ME machine shop and Jim McEntee of J.M. Machining in Lawrenceville for constructing the components of the organ culture system and their input in changing the designs to suit the applications. I very much appreciate the efforts of Tracey Couse, histology lab technician, Georgia Tech, for providing valuable information while performing histological analysis of the samples. Her intelligence and dedication to work made my work easier and simpler and provided me with adequate background to analyze the data. I also thank the undergraduates, Jennifer Coyne, Stacie Hamel, Jason Xenakis and Debnil Chowdry who were involved in the work and carried out their tasks efficiently.

I thank the administrative staff of Chemical and Biomolecular Engineering and Biomedical Engineering, especially Chris Ruffin and Michelle Mayberry for being very helpful. Special thanks to my colleagues at Cardiovascular Fluid Mechanics Laboratory for providing support and technical assistance

I thank the efforts of my mother Subha Laxmi Konduri who as a teacher and a friend supported me all through my studies and my father Chandra Sekhar Konduri, my brother Sunil Konduri and the rest of the family whose love, confidence and encouragement has enabled me to carry out my work. Finally, I am thankful for the emotional support given by my close friend Chakadhar Padala who inspired me at all times to solve difficult problems through this project.

TABLE OF CONTENTS

LIST OF TABLES

LIST OF FIGURES

NOMENCLATURE

SYMBOLS

a	Interfacial area
A	Cross-sectional area of the silicon tubing
h	Population mean
H	Hypothesis for statistical analysis
n	Size of the sample
N	Gas-transfer rate into the medium
M	Molar
k	Mass-transfer coefficient
P	Permeability of the silicon tubing
ΔP_{ln}	Logarithmic mean of partial pressures of the gas
Q	Gas flow rate of the 5% CO_2
R	Rank of the sample
R^2	Coefficient of correlation
Δt	Change in time
U	Test statistic
V	Velocity of the gas
Z	Thickness of silicon tubing
Π	Phi
α	Level of significance

ABBREVIATIONS

ABC	Avidin-Biotin-enzyme complex
ACE	Angiotensin-Converting Enzyme
AOA	Aminooleic acid
BrdU	5-Bromo-2'-deoxyuridine
BSA	Bovine serum albumin
DAPI	4',6-Diamidino-2-phenylindole
DAQ	Data acquisition
DMEM	Dulbecco's Modified Eagle Medium
DNA	Deoxyribo nucleic acid
DPBS	Dulbecco's Phosphate Buffered Saline
DO_2	Dissolved oxygen
EC	Endothelial cells
ECM	Extracellular matrix
ET	Endothelin
Ethd	Ethidium homodimer
F	Fibrosa
GAG	Glycosamino glycans
H & E	Hematoxylin and Eosin
HFA	Hot film anemometry
HMDS	Hexamethyldisilazane
IC	Interstitial cells
ID	Inner diameter

IgG	Immunoglobulin G
IHC	Immunohistochemistry
LDV	Laser doppler velocimetry
LVEDV	Left ventricular end-diastolic volume
LVESV	Left ventricular end-systolic volume
LV Vol	Left ventricular volume
LV Press	Left ventricular pressure
MHV	Mechanical heart valve
mRNA	Messenger ribonucleic acid
NEAA	Non-essential amino acids
OUR	Oxygen uptake rate
PGA	Polyglycolic acid
PLA	Polylactic acid
PLL	Poly L-lysine
S	Spongiosa
SEM	Scanning electron microscopy
SMC	Smooth muscle cells
STS	Society of Thoracic Surgery
TEHV	Tissue engineered heart valves
TPPS	Tetraphenyl porphrine sulfonate
UV	Ultraviolet
V	Ventricularis
vWF	von Willebrand Factor

SUMMARY

The aortic valve has a complex dynamic structure that undergoes changes through out the cardiac cycle in response to the hemodynamic forces surrounding it. These forces include shear and bending stresses, pressure, fluid flow and tensile strain. A thorough understanding of the effect of these forces on cells within the valve leaflets will elucidate the correlation between mechanical stimuli and various disease states. In addition, this information may have implications for the design of a tissue engineered heart valve.

The current study focuses on developing a sterile *ex vivo* organ culture system to grow intact native aortic heart valves and characterize their biological properties in response to physiological forces duplicated in the system. Left ventricular function in the system was attained by a piston pump while aortic compliance was achieved by a compliance tank to cushion the disturbances in the pressure waveform. A membrane chamber separated the sterile and unsterile parts of the system. Oxygen exchange in the system was provided by a gas exchanger placed in the compliance tank. The system developed was shown to be sterile and capable of simulating physiological flow and aortic pressure waveforms at a cardiac output of 3.8-4.2 L/min and pressures of 120/80 mmHg (systolic/diastolic). Valves were cultured in the system at 37^{o}C for 48 hours. Biological properties were evaluated by measuring the differences in total leaflet collagen, sGAG and elastin content between the cultured and control (fresh and statically incubated) leaflets. Hemotoxylin and Eosin staining was used to examine cusp morphology. Endothelial cells on the surface of the leaflets were observed by scanning electron microscopy. α-smooth muscle actin immunohistochemistry (IHC) was used to indicate the expression of actin by smooth muscle cells. Proliferating cells were identified

by 5-bromo deoxy uridine (BrdU) IHC and apoptotic cells in the valve leaflets were detected by activated caspase-3 IHC. Experiments with nine porcine aortic valves showed that the differences in collagen, sGAG and elastin contents were not significant ($p>0.05$) between the cultured and fresh valve leaflets while a significant decrease ($p<0.05$) in sGAG and elastin contents were observed in static control leaflets. The cultured valves maintained the structural integrity of the leaflets while preserving the native morphology and cell phenotype. Cell phenotype in leaflets incubated statically under atmospheric conditions decreased compared to fresh and cultured valve leaflets, indicating the importance of mechanical forces in maintaining the natural biology of the valve leaflets. ECs were retained on the surfaces of cultured leaflets with no remodeling of the leaflets. BrdU results showed no detectable cell proliferation in the cultured leaflets, which was consistent with the controls. The number of apoptotic cells in the cultured leaflets was significantly ($p<0.05$) less than in the statically incubated leaflets and comparable to fresh leaflets.

The organ culture system was shown to retain the native leaflet cellularity, extracellular matrix composition and cell phenotype with no significant remodeling within 48 hours. Therefore, the native biological and physiological functionality of porcine aortic valves was maintained *ex vivo*.

Key words: Organ culture system, Flow and pressure waveforms, Porcine aortic valve leaflets, Extracellular matrix components, Tissue morphology, Cell phenotype, Endothelial cells.

CHAPTER 1

INTRODUCTION

Valvular heart disease is a serious clinical condition that is caused by dysfunction of one or more of the heart's four valves. About five million people in the United States alone are diagnosed with valvular heart disease each year [Shappell, 2004]. According to the American Heart Association's *2003 Heart and Stroke Statistical Update*, valvular heart disease is responsible for nearly 20,000 deaths each year in the United States and is a contributing factor in about 42,000 deaths [Shappell, 2004]. The majority of these cases involve disorders of the aortic valve (causing 63% of deaths) and the mitral valve (14% of deaths). Deaths due to pulmonic and tricuspid valve disorders are more rare (0.06% and 0.01% of deaths, respectively).

Surgical intervention to treat valvular disorders involves heart valve repair or replacement. Typically these replacements involve the use of mechanical valves, bioprosthetic valves or homografts. The first mechanical prosthetic heart valve was implanted in the aortic position in 1960. Since 1952 about 50 different mechanical designs have originated worldwide [Vagale, 2004]. Mechanical heart valves (MHVs) offer greater durability (30 years or more) and lower resistance to flow; however, there is a risk of thrombosis and hemolysis necessitating lifelong anticoagulation therapy for MHV recipeints. On the other hand, bioprosthetic (tissue) valves made from xenografts or allografts have many advantages over MHVs. The valves have better hemodynamics than MHVs since their design approximates that of the native valves. Also, patients implanted with bioprosthetic valves or allografts do not require anticoagulants, since the

valves do not cause blood cell damage and consequent thromboembolic events. However, durability of the valves is limited due to structural dysfunction caused by tissue degradation [Sacks, 2002; Angell, 1989; Hilbert, 1999]. Donor availability is an additional problem in case of allografts. The Ross procedure, first performed in 1962, is an autograft alternative to aortic and mitral valve replacements in which the pulmonary valve is transferred to the aortic or mitral position. This procedure has shown excellent clinical results, which may be due to the ability of the viable pulmonary leaflet cells to adapt to the aortic/mitral environment without eliciting any immunogenic responses. This suggests that a heart valve substitute that has the ability to adapt to different mechanical environments and which is both durable and immunocompatible is required for valve replacement.

Heart valves, created *in vitro* from cells seeded onto suitable scaffolds, may serve as possible replacement option for diseased valves. Tissue engineering is a new domain in which techniques are being developed to transplant autologous cells onto a cell matrix, which can be a biodegradable scaffold, or an acellularized heterograft. Ultimately this promising technique could lead to the creation of a new functional autologous tissue that is capable of remodeling its structure and can grow with the patient. A formidable obstacle to the creation of implantable tissue engineered heart valves is their structural failure due to inadequate mechanical properties in withstanding hemodynamic stresses of the aortic position [Dumont, 2002]. This can be overcome by developing constructs with improved mechanical and biological properties in *ex vivo* organ culture systems, prior to implantation, which provide physiological environments for the growth of the tissue.

Mechanical forces such as shear and bending stresses, transvalvular pressure and cyclic flexure act on the aortic valve during the cardiac cycle; however, the biological response of the valves to these forces remains unknown. It has been inferred from previous studies that shear stresses, pressure, and cyclic stretching during the cardiac cycle affect cell behavior and extra cellular matrix (ECM) composition of the aortic valve leaflets [Boulogne, 1999; Weston, 2001; Xing, 2004]. These studies have shown that mechanical forces regulate the biosynthetic activity of the valvular cells and facilitate matrix production for maintaining a natural valvular architecture. However, these forces in isolation could not maintain the native cell phenotype of the valve leaflets. Hence, studying the effects of physiological mechanical forces on valve leaflet biology *ex vivo* provides an understanding of the mechanical factors required to sustain the native cell phenotype of the leaflets. Furthermore, the results obtained from the work can be used to elucidate various disease mechanisms of the aortic valve. Thus, the focus of this thesis was to design a sterile *ex vivo* organ culture system that is capable of maintaining physiological mechanical conditions and to study the biological responses of porcine aortic valves under those conditions.

CHAPTER 2

LITERATURE REVIEW

2.1. Structure and function of the heart and aortic valve

2.1.1. Function of the heart during the cardiac cycle

The cardiovascular system consists of the heart, blood vessels, cells, and plasma of the blood [Silverthorn, 2001]. The heart is situated in the middle of the chest with its long axis oriented from the left upper abdominal quadrant to the right shoulder. The weight and size of the heart depend on age, sex, weight, and general nutrition. The adult male human heart weighs approximately 325gm while the female heart weighs 275gm. The heart pumps blood through the vessels, and the valves serve to direct the flow in one direction preventing back flow, or regurgitation. The heart must pump blood at a sufficient rate to maintain an adequate and continuous supply of oxygen and other nutrients to the brain and other vital organs. Oxygen-depleted blood returns from the body via the vena cava to the right atrium and through the tricuspid valve to the right ventricle. It then goes through the pulmonary valve, pulmonary artery and to the lungs. Oxygenated blood from the lungs returns via the pulmonary veins to the left atrium and through the mitral valve to the left ventricle. It then goes through the aortic valve to the aorta and finally to the whole body (Figure 2.1).

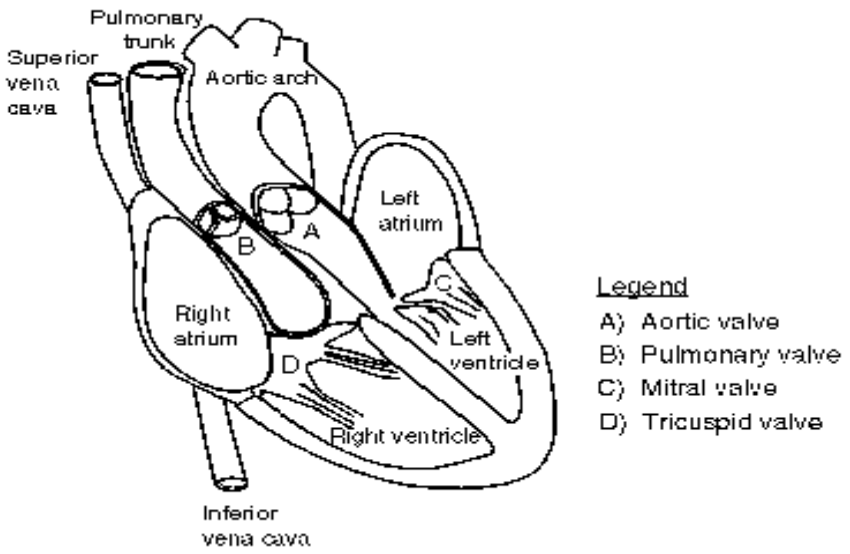

Figure 2.1: Anatomy of the heart. [Scott, 1998]

The events during the cardiac cycle are illustrated in Figure 2.2. The cycle is divided into seven phases. In the first phase (0.11s), the atria contract ejecting blood into the ventricles producing a rise in ventricular pressure. In response to this pressure increase, the A-V valves (mitral and tricuspid) close as the blood starts to flow back into the atria [Klabunde, 1999]. At the onset of systole, which is typically 1/3 of the cardiac cycle (0.35s), ventricular isovolumetric contraction (0.05s) occurs with the closing of the aortic and pulmonary valves. In the rapid ejection phase (0.09s), as soon as the pressure in the left ventricle exceeds the pressure in the aorta, the aortic valve opens and blood flows rapidly from the ventricle into the aorta. Following rapid ejection, the rate of outflow from the ventricle decreases, and the ventricular and aortic pressures start to decrease in the reduced ejection phase (0.13s). At the end of systole, during the isovolumetric relaxation phase (0.08s), the ventricular ejection decreases to zero. The left ventricle pressure falls below the pressures in the aorta and pulmonary artery, which causes the

aortic and pulmonary valves to close (beginning of diastolic phase). Once the ventricular pressure falls below the atrial pressure the A-V valves open and ventricular filling begins. During this period, the flow of blood from the aorta to the peripheral arteries continues, and the aortic pressure slowly decreases. This rapid ventricular filling phase (0.11s) is followed by the reduced ventricular filling phase (0.19s) in which a major portion of filling occurs.

Cardiac cycle

Phase 1 Atrial contraction
Phase 2 Ventricular Isovolumetric contraction
Phase 3 Rapid ejection
Phase 4 Reduced ejection
Phase 5 Isovolumetric relaxation
Phase 6 Rapid ventricular filling
Phase 7 Reduced ventricular filling

Abbreviations:

LV Press, left ventricular pressure
a, a-wave; c, c-wave; v, v-wave
LVEDV, left ventricular end-diastolic volume
LVESV, left ventricular end-systolic volume
LV Vol, left ventricular volume

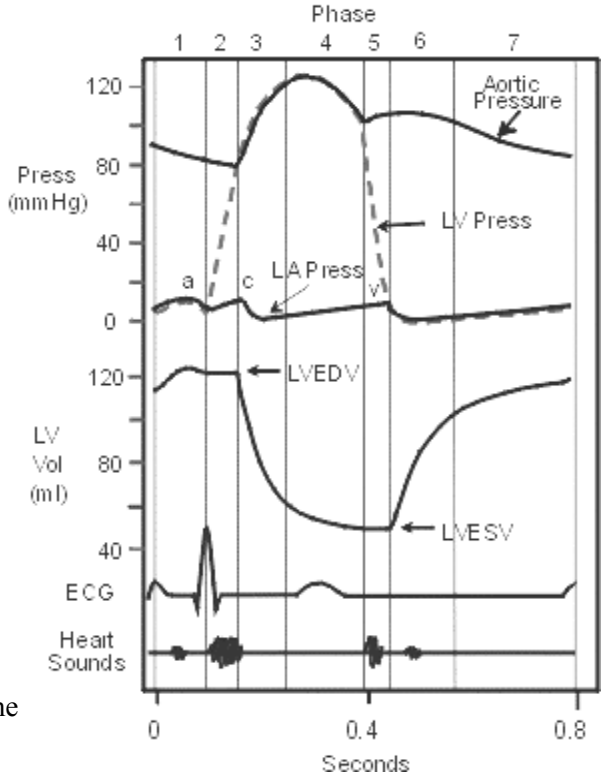

Figure 2.2: The Cardiac Cycle – Events occurring during the cardiac cycle. [Klabunde, 1999]

A healthy heart with a normal cardiac output pumps approximately 5 to 6 L/min of blood at a cardiac rate of 70 beats/min and has a stroke volume of 75mL. The normal

aortic pressure is 120 mm Hg (systolic)/ 80 mm Hg (diastolic). During exercise, the heart beats both faster and stronger to increase cardiac output by three to four times the normal output. The left side of the heart is subjected to higher pressures compared to the right side, hence the mitral and aortic valve account for about 95% of the valve replacement procedures throughout the world.

2.1.2. Structure and function of the aortic valve leaflets

The aortic valve opens widely to allow blood flow into the aorta and closes completely to prevent backflow into the ventricle. The valve opens and closes approximately 103,000 times each day and approximately 3.7 billion times in its life span [Thubrikar, 1990]. It consists of three half-moon-shaped pocket-like flaps of delicate tissue, referred to as cusps or leaflets. When the aortic valve is closed, the cusps are perfectly aligned and separate the left ventricle from the aorta. Along with the three leaflets there are three sinuses, which form a bulging cavity behind the leaflets and are called the sinuses of Valsalva (seen in Figure 2.3). At the lower margin, the sinuses become continuous with the left ventricle, and at the upper margin they become part of the ascending aorta. The sinuses represent dilations of the base of the aorta as seen in Figure 2.3.

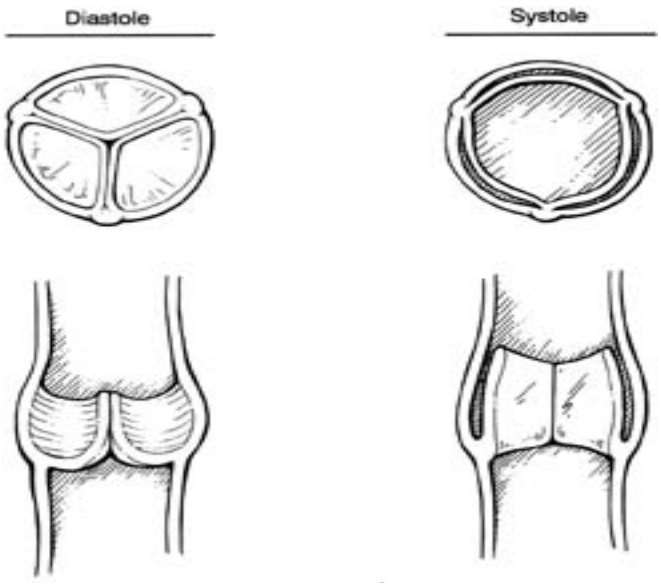

Figure 2.3: Figure shows aortic valve in closed (left) and open (right) positions. The valve in closed position shows the sinuses of Valsalva (left bottom) behind the cusps. [Maier, 2003]

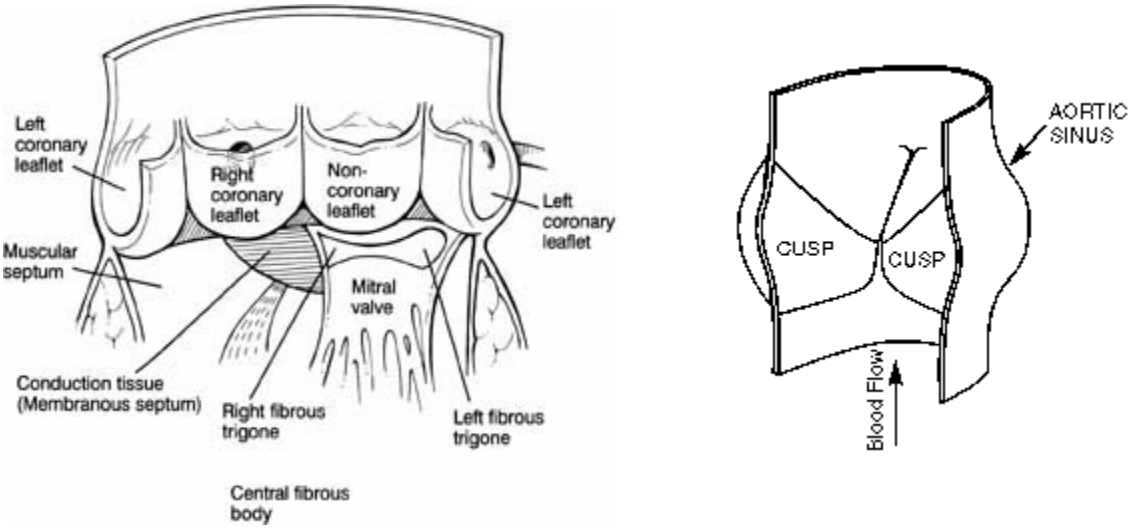

Figure 2.4: Anatomy of the aortic valve. The figure on the left shows leaflet cusps and the one on the right shows the direction of blood flow through the valve. The aortic surface of the leaflet faces the aorta while the ventricular surface faces the ventricle. [Maier, 2003]

The three leaflets are named according to the sinuses that open into the coronary arteries. The left and right coronary leaflets have sinuses containing ostia that open into the right and left coronary arteries, which supply blood to the heart. The non-coronary (posterior) leaflet has a blind sac behind it [Thubrikar, 1990] (Figure 2.4). The surfaces of the leaflets are named based on the anatomical positions that they face when the valve is closed. The surface of the leaflet that faces the left ventricle is called the ventricular surface, and the opposite side that faces the aorta is called the aortic surface. Between these two surfaces is the spongiosa. The average thickness of the leaflets is about 0.6 mm and varies considerably over the surface [Cataloglu, 1976]. The structure of the valve has a direct bearing on its function. During systole, the commissures, points of attachment of adjacent leaflets, pull outward and cause the leaflets to open. Simultaneously, the base of the valve moves inward causing a decrease in the base perimeter. Depending on the ventricular contraction, the open valve has a stellate-shaped, triangular or normal circular orifice. In diastolic phase, vortices that are developed in the sinuses during systole along with the inward motion of the commissures and outward movement of the base close the valve. During valve closure, the sinuses act as shock absorbers and prevent damage to the leaflets due to normal stresses as the stresses are transmitted from the leaflets to the aortic wall through stress-sharing. The impact of stresses is also reduced due to the elasticity of the aortic root.

The composition of the native heart valve is highly complex and well-evolved to meet the extraordinary demands placed on it. Both blood-contacting faces of the leaflet are composed of endothelial cells, sandwiching between them three distinct layers consisting of ICs and varying amounts of ECM components. Among the extracellular

components are collagen, elastin and glycosaminoglycans (GAG). Endothelial cells on the aortic valve leaflet are arranged in a circumferential pattern (from one end of the commissure to the other end); i.e., perpendicular to the blood flow, while, in an artery endothelial cells are aligned in the direction of blood flow [Deck, 1986]. The valvular endothelium like the vascular endothelium serves as a barrier against platelet and fibrin deposition. They express a variety of metabolites and proteins that may affect the function of fibroblasts within the leaflet matrix. Apart from these, ICs populate the matrix of heart valves and express a variety of phenotypes [Hafizi, 2000].

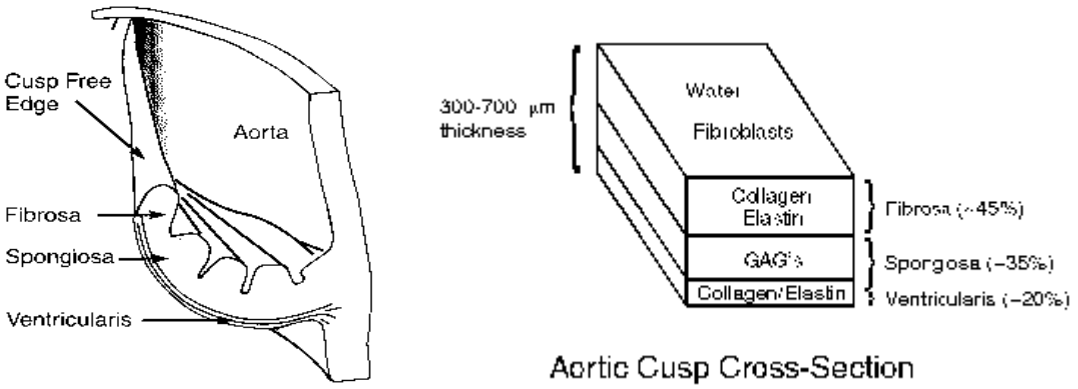

Figure 2.5: Schematic of the aortic valve leaflet structure. [Scott, 1998]

The composite layer structure of the aortic valve leaflet, consisting of the fibrosa, spongiosa, and ventricularis between the aortic and ventricular surface, respectively, imparts incredible durability, flexibility, strength, and fatigue resistance to the native valve (Figure 2.5). Furthermore, the presence of living cells allows dynamic modification

of the ECM components to adjust for changing hemodynamics. The fibrosa, is mechanically the strongest layer of the leaflet and principally bears the stress of diastolic pressure because of the thickness and density of tissue in this layer. It is arranged as a series of parallel tendinous cords, which are aligned perpendicular to the direction of flow. Its collagenous fibers run mainly in the circumferential direction and gives strength to the tissue to withstand the mechanical loading. This directionality results in a structure that is considerably stiffer in the circumferential direction than in the radial direction (from the base to the free edge of the leaflet). A matrix of elastin surrounds the collagen bundles to maintain the valve's microstructure during unloading. There are about 19 different types of collagen present in the body and valve leaflets consist of collagen types I, III and V [Gilbert, 1996]. Collagen forms long uninterrupted fibrils that are composed mainly of proline, hydroxyproline and glycine in a triple helical structure. Elastin, as the name implies, is considerably less stiff than collagen. It is a coiled hydrophobic structure consisting mainly of alanine, valine, leucine, and glycine. Because elastin molecules are hydrophobic they are able to slide over one another or stretch to maintain structural integrity and provide recoil [Welgus, 2003]. In the fibrosa, towards the free edge, tissue is prominently arranged in the form of chords. In the basal region, the connective tissue of the leaflet more consistently forms sheets of fibers that are slightly crosswoven.

Beneath the fibrosa lies the spongiosa, which is a loose, watery connective tissue of varying thickness, fiber composition, and cellularity. The semi-fluid nature of this layer gives the leaflet considerable plasticity. It consists of radially-oriented collagen fibers and cells. Since the fibers and cells of the core tissue are sparse, its bulk consists of connective tissue, principally glycosaminoglycans (GAG) and water. GAGs are

unbranched heteropolysaccharides consisting of N-acetylgalactoseamine or N-acetylglucoseamine and uronic acid. There are seven types of GAG that are of physiological importance, two of which, Chondroitin and Dermatan sulphate, are found in the aortic valve [King, 2003]. The principle function of the spongiosa is to dampen the vibrations in the fibrosa associated with leaflet flexion during closure.

At the ventricular surface of the leaflet, elastin and collagen fibers make up a thin, often bipartite layer called the ventricularis. It consists of a superficial elastin layer and a deeper circumferential layer of collagenous fibers. The ventricular surface of the leaflet is smooth in contrast to the ridged aortic surface as it is important for maintaining laminar blood flow during systole. The elastin of the ventricularis enables the cusps to decrease their surface area when the valve is open and stretch to form a large coaptation area when backpressure is applied. Although the pressure differential across the closed valve induces a large load on the cusps, the fibrous network within the cusps effectively transfers the resultant stresses to the aortic wall and annulus, a ring of tissue that surrounds and supports the aortic orifice.

2.2. Heart valve diseases and surgical alternatives

Heart valves regulate one-way flow of blood through the four chambers of the heart. Failure in the valves on the left side of the heart can cause accumulation of fluid in the lungs or pulmonary edema. Failure in the valves on the right side are rare, but can occur as a result of some forms of congenital heart disease or long-term left-sided heart failure and can cause fluid accumulation in the body, particularly in the legs, abdominal cavity, and the liver [Guyton, 1991]. Heart valve disease can be the result of the natural aging

process where the valve “wears out”, which is often accompanied by calcium deposition in the leaflet tissue resulting in stenosis or regurgitation. Less commonly, rheumatic fever and endocarditis can cause heart valve damage. Additional cases involve congenital heart valve defects or improper closing of the mitral valve leaflets leading to blood leakage into the left atrium. These valve diseases can greatly interfere with the heart's ability to pump blood. Treatment for valvular heart disease depends on the type and severity of the diagnosis. Many patients can be treated successfully with medications such as ACE (Angiotensin-Converting Enzyme) inhibitors to decrease the workload of the heart by widening the blood vessels, antiarrhythemics, antibiotics, anticoagulants, diuretics to lower excess fluid levels in the body, or inotropes to increase the force of the heart’s contractions [Shappell, 2004]. If medications are not successful, interventional procedures such as percutaneous balloon valvuloplasty, valvulotomy or open heart surgery may be necessary.

2.2.1. Aortic valve diseases

Aortic valve disease can be caused by stenosis, regurgitation, or a combination of both. In elderly patients, calcium deposits and the growth of fibrous tissue can damage the aortic valve. Congenital defects (about 2%), such as infants born with a bicuspid aortic valve instead of a tricuspid valve, can lead to severe stenosis or regurgitation after functioning normally for years. Valve disorders can also be caused by abnormalities in the aorta causing enlargement, Marfan syndrome, which is a connective tissue disorder, inflammatory diseases such as ankylosing spondylitis, and less commonly Reiter's syndrome [Nishimura, 2002]. Abnormal valve function produces either pressure

overloading due to restricted valve opening or volume overloading due to inadequate valve closure. Untreated aortic valve disease can eventually result in heart failure, severe infection, and even sudden death.

Valvular aortic stenosis and regurgitation affect about five out of every 10,000 people in the United States [MayoClinic, 2003]. Stenosis results in chronic left ventricular pressure overloading. At any stage of life, the natural history of aortic stenosis largely reflects the functional integrity of the mitral valve. As long as adequate mitral valve function is maintained, the pulmonary bed is protected from systolic pressure overloading imposed by aortic stenosis. The pressure overloading on the left ventricle may thicken and enlarge it causing hypertrophy over the years, subsequently increasing the load on the heart [Novaro, 2002]. The pressure overload weakens the heart muscle leading to congestive heart failure. Aortic regurgitation may occur due to leaflet pathology or aortic root disease. As a dominant isolated lesion, aortic regurgitation usually occurs due to prolapsed leaflets caused by a bicuspid aortic valve. Infective endocarditis involving a bicuspid valve may cause aortic regurgitation from loss of coaptation or perforation of a cusp. Chronic aortic regurgitation predominantly causes volume overloading of the left ventricle, which is usually well tolerated for long periods of time, possibly even decades [Novaro, 2002]. Eventually, the heart begins to fail producing shortness of breath and fatigue.

Unlike the mitral valve, which can often be repaired, the aortic valve usually requires replacement. The most commonly used replacement devices are mechanical and bioprosthetic valves with homografts and autografts less commonly used. From 1990 to 2000, the choice of valve replacements indicated by the Society of Thoracic Surgery

(STS) Registry for patients less than 60 years of age with aortic valve disease was: mechanical valve in 77% of patients, bioprosthetic valves in 13%, homograft valves in 5%, and Ross procedure in 5% [Pettersson, 2003].

2.2.2. Mechanical valves

A mechanical valve is a device constructed from man-made materials that is used to replace patients own damaged or diseased heart valves. The first mechanical valve, developed in 1961, was the "ball and cage" design (Figure 2.6.a), which is still in use today. A number of other designs have been tried since then, primarily those with a single disk or two tilting disks (Figure 2.6.b) and bileaflet valves (Figure 2.6.c) [Thubrikar, 1990]. More than 60 percent of heart valve replacements have been made with mechanical prostheses due to their excellent durability and superior hemodynamics which offer minimal resistance to flow [Travis, 2002]. Although the modern mechanical valves are designed to attain the closest approximation to central flow achieved in a natural heart valve, they are regurgitant, allowing small amounts of backflow between the leaflets as in the case of bileaflet valves [Cabalka, 1995]. Further, the turbulent fluid mechanics through these valves causes damage to blood cells. Possible thrombus formation initiated by disturbed flow patterns necessitates lifelong anticoagulant therapy [Travis, 2002]. Small stagnant regions near the hinges sometimes lead to bacterial infections causing further heart damage.

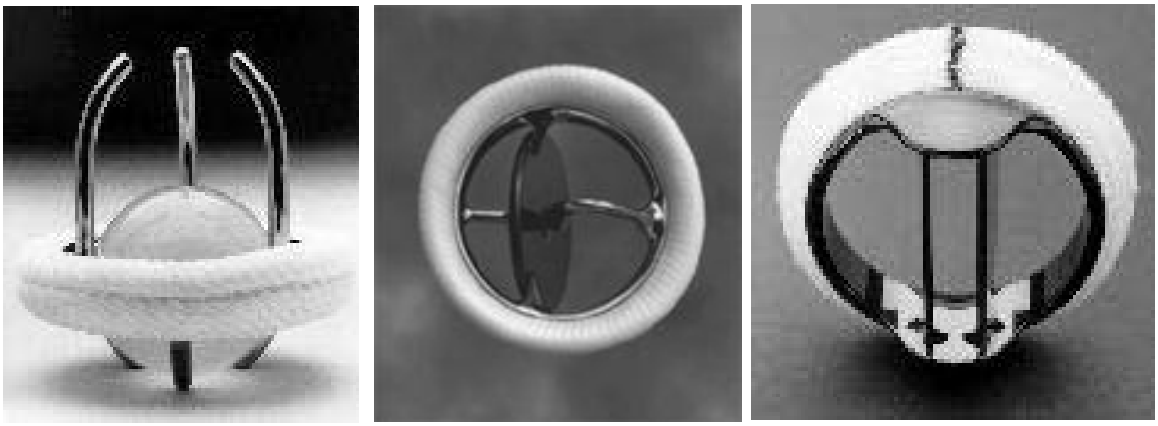

Figure 2.6: Pictures of mechanical heart valves: a) Starr-Edwards ball and cage valve b) Bjork-shiley tilting disc valve and c) St.Jude Medical bileaflet valve [Camp, 1997]

Many different valve designs with different materials of construction have evolved to reduce thrombus formation and decrease the mechanical stresses that can cause blood cell damage. Several synthetic polymers have been tested as leaflet materials such as silicone, polyolefin rubbers and polytetrafluoroethylene [Hilbert, 1987]. Polyurethane valves are capable of achieving more than 800 million cycles (~ 20 years of "normal" function) in laboratory fatigue testing [Bernacca, 1996]. Valve leaflets constructed of a commercially available polyetherurethane when implanted in sheep showed superior valve function to that of bioprosthetic valves [Wheatley, 2000]. Thus, polymeric valves could offer a clinical advantage with the promise of improved durability compared to bioprostheses and low thrombogenicity compared to mechanical valves.

2.2.3. Bioprosthetic valves

Bioprosthetic valves are tissue valves made of animal tissue (i.e. xenografts) and are easily and readily available. These were introduced in the early 1970s as an attempt to

avoid some of the disadvantages of mechanical valves [Talman, 1995]. Flexible, trileaflet, biological tissue valves mimic their natural counterparts more closely than mechanical heart valves. Their central flow characteristics offer better hemodynamic efficiency, and their biological surfaces enhance thromboresistance as compared to mechanical prostheses [Thubrikar, 1990]. The valves are chemically treated to make the tissue less immunogenic and thus less likely to incite an allergic or immunological reaction in the recipient. As a result, the tissue comprising the valve is non-viable, and therefore, subject to degeneration with time. Bioprosthetic valves are commonly employed in elderly patients for whom the risk of bleeding complications are high and in those whose desired way of life precludes the discipline of anticoagulation therapy [Jin, 2002]. Bioprosthetic valves are categorized into either stented or stentless valves. Stented valves are composed of leaflets sutured to sewing rings, which are either metallic stents made of elgiloy or plastic stents made of polypropylene and covered with cloth (e.g. Dacron) [Thubrikar, 1990]. Calcification, perforation, abrasion of the leaflets along the attachments of the commissural posts, and paravalvular leakage are major disadvantages of a stented biological valve [Gross, 1999]. Furthermore, a rigid stent is obstructive and carriers the hazards of infection, hemolysis, and embolization. Also the stent and sewing ring take up valuable space along the perimeter of the orifice so that the opening from the heart to the aorta is smaller than that provided by the stentless bioprostheses.

Stentless, or unstented, valves do not contain a true sewing ring; therefore, long-term durability and hemodynamic results are better than with stented bioprosthetic valves of a similar size [Gross, 1999]. The removal of the stent has several advantages: (a) a larger valve can be implanted into a given size of aortic annulus (b) the distensibility and

dynamic nature of the aortic annulus is preserved (c) less calcification occurs compared to stented valves and (d) it is possible to remodel the native aortic root and preserve the sinotubular junction [Jin, 2002]. Studies have confirmed that stentless valves have lower pressure gradients and a greater effective orifice area than stented valve do soon after implantation [Del Rizzo, 1996]. However, the implantation of these valves requires greater surgical skill for increased durability of the valves.

Commercially available bioprosthetic valves are shown in Figure 2.7. Valves explanted from animals are available in various sizes to fit patients from different age groups. Pericardial valves have a significantly higher area available for blood flow compared to porcine valves of the same size [Purinya, 1994]. At the same flow rate, the pericardial valve has higher performance indices, and lower pressure gradients than the porcine valve of the same size [Cosgrove, 1985].

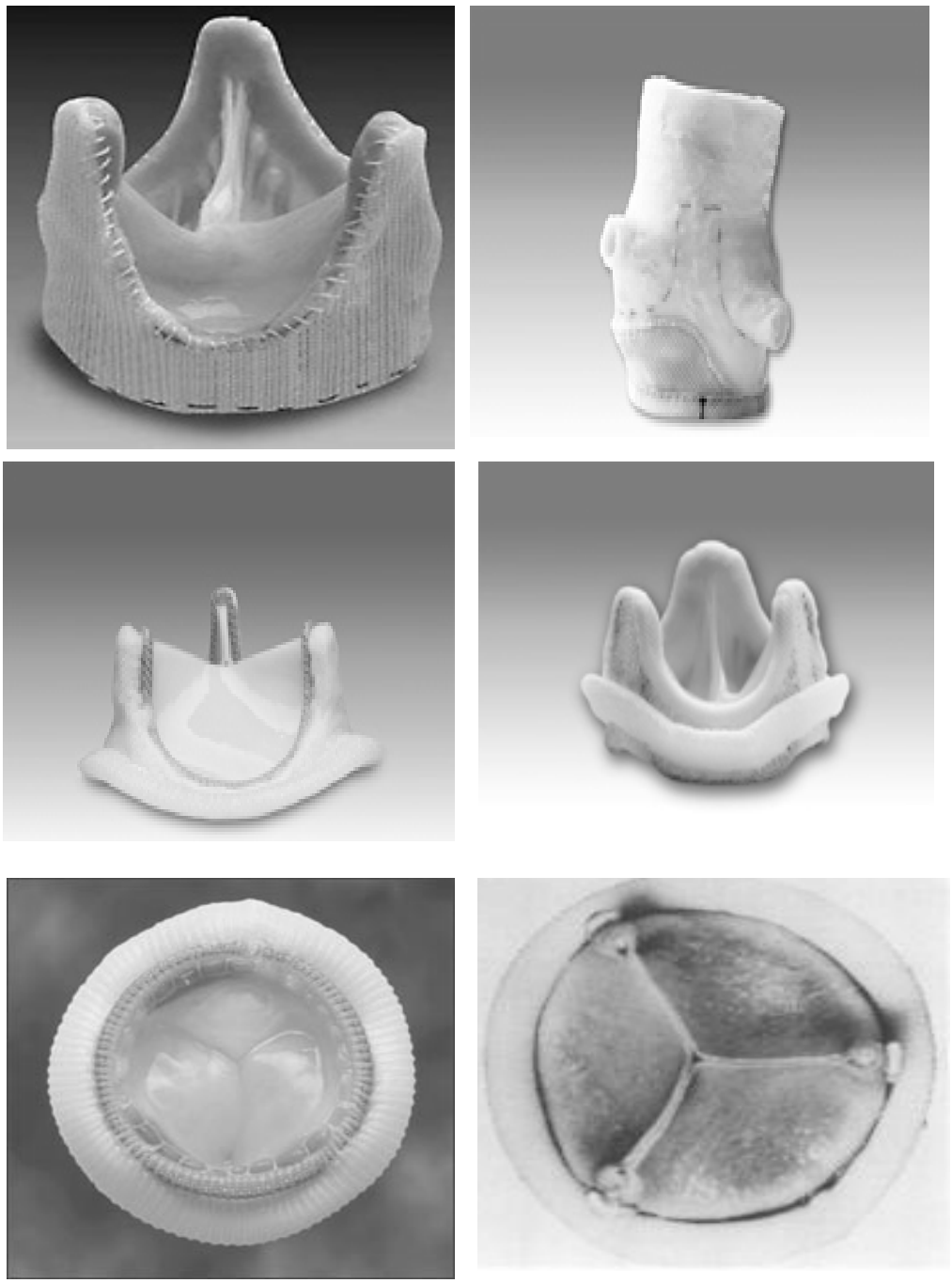

Figure 2.7: Pictures of bioprosthetic heart valves: (Left-right) Toronto stentless porcine valve, Edwards prima plus stentless bioprosthesis (Model 2500P), Carpentier-Edwards perimount pericardial (model 2700) and porcine (model 2625) bioprosthesis [EdwardsLifesciences, 2004], Hancock porcine valve (model 250), Ionescue-Shiley pericardial valve (model 23ISU) [David, 1980].

The biological tissues are usually fixed with 0.625% glutaraldehyde buffered to a pH of 7.4 [Purinya, 1994]. This treatment induces collagen cross-linking thereby preserving the tissue by preventing digestion by enzymes or bacteria, and eliminating tissue rejection [Thubrikar, 1990]. Leaflet fixation also stiffens the tissue unintentionally, alters internal shear properties, increases shear stiffness, stress relaxation and hysteresis, and causes substantial dehydration, all of which lead to valve failure due to calcification or tissue tearing [Talman, 1995; Talman, 2001]. Aminooleic acid (AOA), a detergent that covalently binds to aldehyde residuals and remains within pretreated bioprosthetic tissue, has been demonstrated to prevent porcine valve calcification and protect valvular hemodynamic function [Chen, 1994; Gott, 1997]. AOA significantly reduces the diffusion of calcium ion, which is one of the important steps in the calcification of valves. Studies with ethanol, an anticalcification agent, have shown that apart from complete inhibition of cusp calcification, ethanol pretreatment inhibits aortic wall calcification [Lee, 1998]. Other agents such as aluminium chloride or biphosphonates significantly inhibited bioprosthetic aortic wall calcification [Lee, 1998]. These methods, although effective in reducing calcification, do not prevent disruption of collagen fibers. Collagen fibers exposed to blood flow are damaged and cannot be repaired due to lack of viable cells within the leaflet. This can be overcome by seeding the leaflets with fibroblasts, which are capable of maintaining the valve's native structure [Zund, 1997].

2.2.4. Allograft valves

Allograft (or homograft) valves obtained from a donor are also used as an option for valve replacements. This type of aortic valve replacement was initiated by Ross in 1962,

and over the past decades the allograft has become a well-known aortic valve substitute [Takkenberg, 2002]. Although early allograft valves were variably sterilized in ethylene oxide and preserved in β-propriolactone, irradiated, or freeze-dried, subsequent developments in preservation techniques including antibiotic use, improved culture media, and freezing have led to the use of cryopreserved allograft valves. The most common cryopreservation method involves freezing the valve in dimethyl sulfoxide and storing it in liquid nitrogen [Kitagawa, 2001]. Aortic valve replacement with cryopreserved allograft valves achieved excellent early results (~3 years), although eventual failure of these tissues is common.

Several studies suggest that allograft valve viability associated with cryopreservation techniques is recognized as one of the most influential factors in long-term durability of cryopreserved allograft valves [Angell, 1989; O'Brien, 1987]. The specific cell population of greatest importance in determining the long-term viability of the valves is likely to be the fibroblasts since they participate in valve remodeling through collagen metabolism and improve competency and durability of the cryopreserved valves [Koolbergen, 1998; Song, 1997]. It has been reported that apoptosis occurrs in cuspal ECs and ICs of implanted cryopreserved allograft valves, and this might lead to their loss of cellularity [Hilbert, 1999]. Loss of the endothelium adversely affects the underlying fibroblasts by accelerating graft deterioration due to increased capacity for thrombus formation. Comparison of explanted cryopreserved allograft valves with aortic valves removed from short-term and long-term transplanted hearts showed that cryopreserved allograft valves are morphologically nonviable with flattened collagen [Mitchell, 1998]. The presence of procollagen and the α1-(I) procollagen gene expression in allograft aortic

valves after implantation for 3 days suggested donor fibroblast viability [Lupinetti, 1997]. Although the collagen synthesis ability was preserved, reduction in protein synthesis ability may have a significant impact on the long-term cellular viability. Thus these valves are unlikely to grow, remodel, or exhibit active metabolic functions, and their usual degeneration cannot be attributed to immunologic responses.

2.2.5. Autograft valves

The use of a patient's pulmonary autograft to treat aortic valve disease, initiated by Donald Ross in 1967, has a high success rate since the valves are living tissues with intact cells. The diseased aortic or mitral valve is replaced with patient's pulmonary valve and the excised pulmonary valve is then substituted with an allograft pulmonary valve. The complexity of the Ross procedure is balanced by its advantages of excellent hemodynamics, potential for a permanent replacement for the aortic valve, and elimination of anticoagulation therapy. Long-term durability of the procedure requires appropriate geometric matching of the aortic and pulmonary roots. However, concerns over the development of insufficiency of the pulmonary autograft have limited its application in adults [Fullerton, 2003]. Follow-up studies have shown that 20 years after the procedure, 80% of patients were alive, 85% of them did not require reoperation, and 75% were free from any other event including endocarditis, degeneration of the pulmonary autograft, and death [St.PatrickHospital, 2004]. The Ross procedure results in significant improvement in left ventricular wall thickness and outflow tract velocity, which is not seen in allograft aortic valve replacements [Jones, 1998]. Hence the procedure is potentially used in patients with complex left ventricular outflow tract

obstruction. The procedure has a number of unique advantages in neonates and infants as the valves are non-thrombogenic and have the ability to grow with age because of the anatomical and biological similarities between pulmonary and aortic valves. The clinical success of the autograft valves and their suitability for pediatric population has lead to the construction of tissue-engineered heart valves with the idea that constructs having anatomical and biological properties as that of native aortic valves have a similar functionality as that of aortic valves.

2.2.6. Tissue engineered heart valves (TEHV)

The optimal prosthetic heart valve would involve construction from autologous tissue, which may provide the valves with the ability to grow and repair and thereby increase their durability without the risk of rejection [Zund, 1997]. Tissue engineering is a new domain in which techniques are being developed to transplant autologous cells onto a cell matrix, which can be a biodegradable scaffold or an acellularized heterograft leading to the creation of new functional tissue that can foster remodeling in an active manner. To date, tissue engineering techniques have been used to produce skin substitutes [Ng, 2001], blood vessels [Solan, 2003], cartilage [Freed, 1994], bone [Zhang, 2003], liver [Hasirci, 2001], pancreas, neural substitutes, heart valves [Zund, 1997], myocardial patches, ligaments, tendons, and kidneys using biodegradable polymer scaffolds. Of these, the products that are marketed in the United States are Transcyte (ATS/1997), Dermagraft (ATS/2001), Appligraf (Organogenesis/1997) and Orcel (Ortec/2001) for skin; Carticel (Genzyme/1997) for cartilage repair; and Synergraft (Cryolife Inc., 1999) for heart valve replacement. Several approaches have been used to engineer these tissues.

For example, Auger et al [L'heureux, 1998] used human vascular smooth muscle cells, fibroblasts and endothelial cells cultured in a mandrel to produce a tissue-engineered blood vessel, which exhibited a burst strength of 2000 mmHg. Microencapsulation of insulin-secreting cells using a poly L-lysine (PLL) membrane surrounding calcium alginate microbeads has been used to create a bioartificial pancreas [Tziampazis, 1995]. Heart valve leaflets have been constructed using a polymeric scaffold composed of an outer non-woven mesh made from pure polyglycolic acid (PGA) and an inner layer with a woven mesh from a PGA copolymer consisting of 90% PGA and 10% polylactic acid (PLA) seeded with human fibroblasts and aortic ECs [Zund, 1997].

Tissue engineering of heart valves has progressed dramatically in three different arenas: a biodegradable stented valve seeded with autogenous cells, a decellularised allograft, and xenograft valves that are either seeded, or those that repopulate by adaptive remodeling *in vivo* [Elkins, 2003]. Tissue engineered pulmonary valve leaflets created from autologous sheep cells cultured on PGA scaffolds implanted in growing sheep (for up to 11 weeks) grew in parallel with native tissue of the maturing animal and did not demonstrate dilation or thinning with increased tensile strength and collagen content [Shinoka, 1995]. However, this method required leaflet replacement that is surgically challenging. During the remodeling period, the mechanical properties of the constructs were not as strong as the native tissue. In the second approach, decellularized porcine aortic valves were recellularized by seeding with human neonatal dermal fibroblasts [Zeltinger, 2001]. A pneumatic flow bioreactor imposing leaflet mobility with fluid flow facilitated the attachment of fibroblasts to the scaffold and colonized the decellularized porcine matrix. During the 8-week culture process, the fibroblasts were metabolically

active, mitotic, and synthesized human extracellular matrix proteins. This study suggests that an *in vitro* approach could be used for cellular growth; however, the mechanical integrity of the construct remains questionable. The next step in this approach involves the functional testing of this new valve either *in vivo* in an animal model or *in vitro* under physiological conditions in a bioreactor. In the third method of developing a TEHV, decellularized canine aortic and pulmonary valves maintained leaflet mobility, exhibited no inflammation, and were repopulated by host cells at the valve base and partially endothelialized when implanted *in vivo* for one month [Wilson, 1995]. However, endothelialization in humans is not a spontaneous process which may contribute to graft failure. These studies show that cell-cell interactions, growth factors, flow conditions, shear stress and combinations of these are important for the function of a TEHV.

Synergraft, the first TEHV made from porcine aortic tissue was evaluated *in vitro* in a dynamic bioreactor and *in vivo* by implantation in sheep weanlings. *In vitro* studies showed that the valve exhibited a larger orifice area and lower gradients equivalent to a normal human aortic valve [Goldstein, 2000], and *in vivo* studies showed that the leaflets were stable with up to 80% matrix recellularization with host fibroblasts and no calcification over 150 days. Studies with pediatric patients showed that the xenogenic collagen matrix elicits strong inflammatory response in humans, which is non-specific early on and is followed by a lymphocyte response. Structural failure of the graft occurred within 1 year, which suggests that the valves were not optimal for implantation in humans [Simon, 2003]. A TEHV must incorporate the complex microstructure of a native valve to be durable and have long-term functionality. The optimal approach would be to fabricate the cusps from building blocks of collagen fiber bundles surrounded by

tubes of elastin, linked together by elastin sheets and struts and GAGs that bind water to impart the gelatinous consistency.

2.3. Hemodynamic forces on aortic valve

2.3.1. Forces on aortic valve

The anisotropic property of aortic valve leaflets has potentially significant effects on its mechanical behavior and failure mechanisms. Understanding these mechanical forces is crucial to the development of a TEHV. The aortic valve undergoes complex deformations during each cardiac cycle thus exposing the valve leaflets to transvalvular pressures, shear and bending stresses, and cyclic flexure as the leaflets load and unload. Experimental studies, discussed in the following paragraphs, have been performed to measure the mechanical forces on the valve leaflets, to study the function of the valves, and to identify subtle changes in tissue mechanics that accompany disease and aging of the valves.

Pressure

In vivo the pressure on the leaflet varies from systole to diastole, thereby changing the stress and, consequently, the length of the leaflet. Under normal hemodynamic conditions, the closed valve supports a transvalvular pressure of 80-120 mmHg acting perpendicular to the leaflet area (normal stress). This force is supported by the lamina fibrosa layer of the leaflet and is transmitted from the collagen fibers to the cells within the tissue that are aligned with the collagen fibers. The pressure acting on the leaflets is usually estimated in terms of stresses assuming the tissue to be homogeneous [Thubrikar,

1990]. The leaflet, however, is inhomogeneous, anisotropic, nonlinear, and viscoelastic with a complex geometry.

In vivo studies using a marker-fluoroscopy technique with radiopaque markers placed on canine aortic valve leaflets were conducted as early as 1980. The stresses were estimated from the change in position of these markers using equations for membrane stress assuming a cylindrical geometry. The membrane stresses in the circumferential direction of the leaflet were 1.7 g/mm^2 during systole and 24.5 g/mm^2 during diastole [Thubrikar, 1990]. In another study finite element formulation was used to analyze the stresses. Based on a pressure of 114.7 mmHg and a human aortic valve leaflet thickness of 0.6 mm, the maximum principle stress was found to be 22.35 g/mm^2, which is comparable to the *in vivo* study [Cataloglu, 1976].

Shear Stress

Aortic valve shear stress is an important factor in the synthetic activity of the valvular cells and also in cell adhesion. Shear stress is experienced by the ventricular surface of the leaflets during systole when blood flows past the leaflets and on the aortic surface during diastole when blood pools into the sinuses. An estimate of these stresses aids in understanding effect of stresses on leaflet cellular function and in elucidating cellular responses [Weston, 1999].

Tissue degradation and failure due to calcification of the leaflets has been associated with regions of high shear and bending stresses in the leaflets during valve opening and closing [Wheatley, 1987]. Various *in vitro* studies were performed to estimate the shear stresses on the aortic valve using bioprosthetic and mechanical valves.

Techniques such as Laser Doppler velocimetry (LDV) and Hot film anemometry (HFA) were used to measure near-wall velocities downstream of the valves. Using LDV, the highest shear stress found in a 29 mm Hancock stented porcine aortic valve under pulsatile flow conditions was 29 dyne/cm^2 at 45 mm downstream of the valve [Walburn, 1984]. Measurements under steady flow conditions for 21 and 25 mm polymeric trileaflet valves showed that the aortic wall shear stresses were 200–500 dyne/cm^2 at 40 to 60 mm downstream of the valve [Woo, 1986]. Experiments using the HFA technique with a 27 mm Ionescu-Shiley bovine pericardial valve under pulsatile conditions yielded a stress value of 29 dyne/cm^2 at 30 mm downstream of the valve [Nandy, 1987]. These studies calculated the shear stress downstream of the valve rather than the stress on the leaflet surfaces. However, shear stresses on the leaflet surfaces are critical for understanding the functionality of valvular leaflet cells.

In order to estimate the shear stresses on the leaflet surface, LDV measurements were performed using a polymeric (polyurethane) trileaflet valve under pulsatile conditions [Einav, 1990]. Shear stress on the leaflet surface at peak systole was found to be 800–1800 dyne/cm^2. In a recent study by Weston et al [Weston, 1999], two-component LDV measurements were conducted using a polyurethane valve. Measurements were taken inside the valve as well as downstream of the valve. The maximum wall shear stress inside the valve was found to be 79 dyne/cm^2 while the wall shear stress measured 83 mm downstream of the valve was 10-17 dyne/cm^2 at a flow rate of 7.5 L/min. At a flow rate of 22.5 L/min the shear stress was 52-104 dyne/cm^2. These values are an order of magnitude less than those found in earlier investigations. Bioreactors designed taking these stress values into account can be used to study the

responses of valvular cells to mechanical forces and the signaling cascades for inflammation involved in the valve leaflets, without damaging the endothelium lining.

Bending Stress

The change in leaflet curvature during the cardiac cycle gives rise to bending stresses, shearing, or buckling [Thubrikar, 1990]. The collagen chords in the leaflet structure are free to bend in the circumferential direction without significant resistance from the elastic fibers aligned in the radial direction. Bending stress is both tensile and compressive with the leaflet on the convex side experiencing tensile stress while the concave side experiences compressive stress. During bending, the belly of the leaflet undergoes reversal of curvature due to loading and unloading of the valve while the zone of attachment acts as a hinge facilitating leaflet movement. The bending stress increases with an increase in leaflet stiffness causing early failure of some bioprosthetic valves.

Thubrikar used the radiopaque marker technique to calculate the bending strains *in vivo* in canine aortic valves. The bending strains, calculated from modulus of elasticity, thickness and radius of the leaflet, were found to be 2% during systole and 2.2% during diastole in the circumferential direction [Thubrikar, 1990]. *In vitro* experiments using dip-cast polyurethane trileaflet valves were performed to determine values for bending strain and stress at the free edge of the leaflet under physiological pulsatile conditions. The bending was greatest during the opening phase corresponding to a maximum strain and stress of 14.5% and 1.22 MPa, respectively. During the closing phase the maximum strain and stress were 8.3% and 0.71MPa, respectively [Corden, 1995].

Stretch

Stretching is important for a leaflet as it allows the leaflet to extend and form a coaptive seal with the other two leaflets. It is required for the maintenance of an adequate coaptation area. Leaflet stretch may be lost at a relatively rapid rate for reasons that are not yet understood [Thubrikar, 1990]. The first and most rapid change starts in late adolescence. The stretch during this period is halved from 80% to 40% over a time span of 15 to 25 years. This corresponds to a linearized reduction of approximately 4% per year in stretch rate. Between the ages of 25 and 40 the stretch remains approximately constant at a value of about 40%. After age 40, the stretch continues to decline at a slower linearized rate of about 1% per year until age 58 [Christie, 1995a]. Thus, a valve from 15-year-old donor has about four times more stretch than one from a 58-year-old donor. The tissues become less extensible with increasing age because collagen fibrillogenesis increases the diameter of some of the constituent fibrils in discrete steps. Thus, larger numbers of thick collagen fibrils will require greater force to produce the same extension, causing a reduction in stretch.

In vivo studies done by Thubrikar measured the change in leaflet length in the circumferential and radial direction during the cardiac cycle in canine aortic valves. He observed that the leaflet in both the circumferential and radial directions is longer during diastole than during systole. The leaflets elongate by 11% in the circumferential direction and 31% in the radial direction from systole to diastole [Thubrikar, 1990]. This is because the collagen in the circumferential direction provides greater tensile strength than that in the radial direction, which is mainly composed of elastic structures. Porcine aortic valves stretched *in vitro* using a “Tensilon” tensile stress testing machine showed elongations in

the leaflets to be 33% and 60% in the circumferential and radial directions, respectively [Missirlis, 1978]. Barratt-Boyes et al [Christie, 1995b] have measured the biaxial properties of pulmonary and aortic valve leaflets during extension in the fresh and gluteraldehyde fixed states. For the pulmonary leaflets, radial stretch was greater than that in the aortic leaflets and circumferential stretch was similar. Thus, the ratio of radial to circumferential stretch was 6.0±1.1 for the aortic leaflets and 9.0±1.8 for the pulmonary leaflets. After fixation in 0.2% gluteraldehyde, the ratios in the aortic leaflets were the same except with significantly reduced stretches in both directions. Purinya et al [Purinya, 1994] studied the biomechanical and structural properties of the explanted bioprosthetic valve leaflets. Eighty months after implantation, the pericardium valve became more extensible and ultimate strain increased 2.5 times while that of the porcine bioprosthetic valve increased from 13 to 22%. These studies do not infer the response of native tissue to cyclic stretch in the leaflets; hence, it is interesting to look at this stretching effect on native valve biology.

2.3.2. Cellular responses of aortic valve to mechanical loading

The cell types that are predominantly found in aortic heart valve leaflets are ECs and ICs. These cells show force-dependent responses to pressure, shear and bending stresses, and cyclic stretch during the cardiac cycle. Previous studies have shown that scaffolds seeded with valve cells maintain natural cell phenotype and extracellular matrix composition when cultured under dynamic conditions *in vitro*. When implanted *in vivo* these constructs appear to be capable of remodeling and potential growth. To understand this

relationship several studies have been performed with cells and native tissue from different species, which are discussed below.

Pressure

ECs are of significant importance to tissue engineered cardiovascular constructs as they help in regulating vascular tone, inflammation, thrombosis and vascular remodeling. ECs transdifferentiate to replenish ICs and maintain homeostasis by regulating the interaction between blood and ICs. In blood vessels, these cells are oriented in the direction of blood flow. However, studies with aortic valves have shown that ECs on both the aortic and ventricular sides are arranged perpendicular to the direction of flow. A study done with adult mongrel dogs has shown that the ECs were arranged in a circumferential pattern on the ventricularis side instead of aligning in the direction of systolic blood flow. This suggests that the endothelium lining is governed by diastolic blood pressure [Deck, 1986]. Tokunaga et al [Tokunaga, 1987] exposed cultured umbilical vein ECs and smooth muscle cells (SMC) to increasing pressures and found that EC growth was maximum at 80 mmHg and minimal at atmospheric pressures. The cells degenerated at 120 mmHg with marked degeneration at 160 mmHg. Growth of SMCs on the other hand was not influenced by ambient pressure and steady growth continued throughout the culture period. In another study, when cultured bovine aortic ECs were exposed to atmospheric, static (135 mmHg), or pulsatile pressures (160/110 mmHg), EC number significantly decreased at both pressure conditions. To further study this effect, EC conditioned media from the three pressure conditions were transferred to static cultured EC. There was a significant cell growth inhibition in the control EC group suggesting that

ECs exposed to pulsatile pressure secrete autocrine factors with growth inhibitory properties [Vouyouka, 1998]. This suggests that cells are affected by the magnitude and type (steady or pulsatile) of pressure. In studies by Hishikawa et al [Hishikawa, 1994] a static pressure of 120 mmHg enhanced DNA synthesis in SMC, but inhibited it in ECs suggesting that the pressure effect may also be cell type specific. Studies carried out in rat aorta showed that under hypertension there was an increase in proliferation of ECs, SMCs and fibroblasts within the vessel wall [Owen, 1985]. ECs and fibroblasts' proliferation was decreased at the end of 30 days while the SMCs continued to proliferate.

Large arteries subjected to hypertension undergo changes such as increased stiffness and collagen content [Iwatsuki, 1977]. Recent studies have examined the effect of pressure on heart valves. Willems et al [Willems, 1994] studied the effect of hypertension on Wistar Kyoto rats' tricuspid, mitral and aortic valves by intrarenal aortic ligation thus increasing the ventricular pressure overload. The results showed an increase in DNA synthesis and mRNA amounts of both collagen type I and III while maintaining the cell phenotype when compared to sham aortic ligation and normal rats. *In vitro* studies on porcine aortic valves leaflets exposed to static pressures of 100, 140 and 170 mmHg for 48 hours showed that there was an increase in collagen synthesis at elevated pressures. An increase in collagen synthesis of 37.5% and 90% in leaflets subjected to 140 and 170 mmHg, respectively, was observed when compared with leaflets subjected to atmospheric pressures. No significant difference in DNA or sGAG synthesis was observed at elevated pressures; however, DNA synthesis at 100 mmHg decreased. α–SMC actin declined during the experiments, although no significant difference was

observed between the pressure and control groups [Xing, 2004]. Further studies are required to study the effect of pressure on valvular cells under static and pulsatile conditions to understand the influence at the gene level.

Shear stress

Studies of the effect of shear stress on cellular functions were initially performed to understand the thromboembolic complications associated with cardiovascular prostheses. Platelet activation was thought to be associated with certain physical forces. A rotational viscometer was used to apply graded levels of shear stress to platelet-rich plasma, which showed that the platelets were extremely sensitive to shear stress and increased the possibility of thrombus formation due to action of physical forces on circulating platelets [Brown, 1975]. In studies involving endothelium damage in stenotic regions, it was observed that acute shear stresses created by reducing the lumen of the rat aorta by 20-25% resulted in a loss of ECs within 3 minutes with no significant increase in damage after one hour [Joris, 1982]. A similar study was done to observe the shape of ECs related to local wall shear stress. ECs in aortic stenosis regions (high shear stress regions) created by reducing the cross-sectional area to 70% were elongated [Levesque, 1986]. Also, another study showed that cultured ECs exposed to steady laminar shear stress elongate and align in the direction of flow [Dewey, 1981]. Studies with porcine ECs from the aorta and aortic valve subjected to 20 dynes/cm^2 steady laminar shear stress for up to 48 hours showed that the aortic valve ECs were aligned perpendicular to flow. However, the aortic ECs, were aligned parallel to flow [Butcher, 2004b]. This suggests that valvular ECs exhibit different characteristics from vascular ECs.

ECs are immediate recipients of shear stress, and their responses are transmitted through the cytoskeleton to the SMC, which regulate EC number in the vessel wall. Many studies have been done to profile ECs subjected to turbulent and laminar shear stresses. It has been found that in regions subjected to disturbed shear stresses, both pro- and anti-atheroscelerotic transcript profiles coexisted, suggesting that the region is primed for inflammation even if it is not active [Passerini, 2004]. Studies with human dermal fibroblasts exposed to a shear stress of 80 dyne/cm^2 in a flow chamber showed that the cells did not align in the direction of flow [Jouret, 1997]. Exposing human cardiac leaflet fibroblasts to a stress of 40 dyne/cm^2 showed that the cells under culture proliferated at 96 hours but did not show any elongation or orientation under steady laminar shear [Wick, 1997]. Further studies are required to understand the effect of shear stress on valvular cells.

Stretch

The effects of cyclic stretch have been studied previously in cell culture with osteoblasts, chondrocyctes, fibroblasts, ECs, vascular SMCs, valvular ICs, and cardiomyocytes. Many strain devices were developed to impose uniaxial or biaxial stretching. Sotoudeh et al developed a strain device to impose dynamic and equi-biaxial strain to cultured bovine aortic ECs. The device was tested by measuring luciferase activity, which was chimerically transfected onto ECs. When stretched by 15% or more in area, cells showed significantly increased lucifrease activity at different membrane locations confirming that strain was uniform and biaxial across the membrane [Sotoudeh, 1998]. To test the dynamic flexure of native and tissue engineered valves, a bioreactor has been developed

to subject the tissue to uniaxial cyclic flexure [Englemayr, 2003]. The reactor can be used to test different specimen materials of interest in tissue engineering.

Many investigators have studied the effects of stretch on cardiomyocytes because mechanical stress has been considered to be one of the major causes of physiological development and growth of the heart as well as cardiac hypertrophy. When subjected to a cyclic stretch of 120% at a frequency of 30 cycles/min, embryonic rat cardiomyocytes along with intracellular myofibrils oriented parallel to the stretch direction during the first 12 hours of initiation [Kada, 1999]. Henriëtte et al [Jonge, 2002] have examined the effect of cyclic stretch (30 cycles/min and 20% elongation) as well as endothelin-1 (ET) on rat neonatal ventricular myocytes. After 24 hr stimulation by ET-1 or cyclic stretch, the myocytes responded by developing hypertrophy. David et al studied the altered gene expression in perfused arterial segments exposed to cyclic flexure *ex vivo* [Vorp, 1999]. RT-PCR analysis demonstrated that E-selectin and MMP-1 were consistently and significantly down-regulated in the specimens subjected to 4 hr of cyclic bending in a perfusion system.

ECs lining the lumen of blood vessels or the heart valve leaflets are subjected to strain by pulsatile blood pressures and shear forces on them. Cyclic stretching of intact vessels under normal transmural pressure in the absence of shear stress induces within a few hours, realignment of endothelial actin stress fibers in the circumferential direction. Sipkema et al studied the effect of cyclic axial stretch of rat arteries on endothelial cytoskeletal morphology and vascular reactivity [Sipkema, 2003]. Concomitant with the morphologic alteration, the sensitivity to the endothelium-dependent vasodilator was significantly decreased in the stretched vessels. Hence, similar to cultured cells, ECs in

intact vessels subjected to cyclic stretching reorganize their actin filaments almost perpendicular to the stretching direction. Chaubey et al have studied the effect of stretch in the expression of cytoskeletal proteins, vimentin and desmin and ECM protein, fibronectin in aortic and pulmonary valve IC [Chaubey, 2003]. The expression of vimentin was unaltered by stretch whereas desmin upregulated in aortic and pulmonary interstitial cells. Fibronectin was unaltered in aortic valves but was downregulated in pulmonary valves.

Mechanically induced ECM remodeling plays a crucial role in tissue engineering of load-bearing structures, such as heart valves and cartilage. Driessen et al did some study on collagen fibre remodeling [Driessen, 2003]. They hypothesized that collagen fibre reorientation was induced by macroscopic deformations and the amount of collagen fibres was assumed to increase with the mean fibre stretch. Also the collagen fibres align in a direction to avoid mechanical stimulus under cyclic deformation. However, there must be a limit in the sensitivity of the cellular response to the mechanical stimulus. A cell and its intracellular stress fibers orient approximately in the same direction under cyclic deformation. Some research has also been done to measure the stress-strain properties, elongation in the leaflets during each cardiac cycle and structural changes in the leaflets of native aortic, mitral and pulmonary valve leaflets.

2.4. Bioreactors for native and engineered constructs

Tissue engineered cardiovascular devices offer the possibility of developing a patient specific implantable device that has a potential to grow and remodel with native tissue without risk of rejection. However, concerns over patient safety during the graft

remodeling *in vivo* has prompted its testing *ex vivo* using a bioreactor. Thus, the graft can be completely remodeled prior to its implantation in the patient. Many studies have been carried out to simulate physiological environments *ex vivo* in order to study cellular and tissue responses to mechanical conditions during creation, physiological conditioning, and testing of cells, tissues, scaffolds and organs to aid in the development of tissue engineered blood vessels and heart valves.

Bioreactors are being used as integral parts of artificial organs such as excorporeal liver assistant device, artificial kidney, etc. to produce artificial organs such as dermal, epidermal skin grafts, cartilage, bone, blood vessel, heart valves, etc. to amplify cell cultures *ex vivo*; and to seed cells efficiently with few chances of nutrient and oxygen depletion. Physically interactive bioreactors are used for investigating biomechanical regulation of cell function under controlled physiologically relevant conditions and for the development and regeneration of cell-matrix constructs for tissue engineering [Ingham, 2003]. The simplest and commonly used bioreactor is the culture dish as it provides a sterile, easy to use, static and economical method of amplifying cells. However, the disadvantage of this system is that, scale-up is limited to use of multi-well culture dishes which require manual handling. Also if the tissue thickness exceeds 10 microns then nutrient and oxygen diffusion becomes a limitation which can partly be overcome by the use of spinner flasks with filters for gas exchange [Martin, 2004]. Although static loading of cells in a monolayer or seeding onto scaffolds is commonly used, it leads to non-native phenotypic expression of proteins, low seeding efficiencies, and non-uniform distribution of cells within the scaffolds. These drawbacks of static cultures can be overcome by perfusion bioreactors, which exploit the principle of

convective transport for production of 3D uniformly seeded scaffolds. Also, the *ex vivo* microenvironments of such bioreactors are biomimetic and guide cell organization, control cell-matrix interactions, and provide appropriate structural and mechanical features.

An early usage of bioreactors in cardiovascular research was to seed vascular cells on acellular constructs. Under pulsatile flow conditions cell retention and adhesion on the scaffold along with the mechanical strength improved compared to static conditions. The first tissue-engineered vascular graft was produced by Weinberg and Bell [Weinberg, 1986]. A multilayered tube consisting of cultured bovine EC, SMC, and fibroblasts were mixed to construct blood vessels. Seliktar et al [Seliktar, 2001] developed a system for dynamic conditioning of collagen-gel blood vessel constructs. The tubular constructs were cultured with SMC seeded on collagen-gel over thin walled silicon tubes inflated with cultured medium under pneumatic conditions. The constructs were exposed to inflation and deflation of the conduits at a frequency of 1 Hz for periods of 4 and 8 days. This imparted a cyclic strain of 10% onto the cell-seeded constructs. At the end of 8 days, the SMC oriented circumferentially and distributed homogeneously throughout the thickness of the vessel wall. Also, the ultimate tensile strength of the vessel was found to be within the range of the human aorta while that of the static cultures was lesser. In another study, Niklason [Niklason, 1999] developed a blood vessel construct seeding PGA scaffolds with porcine aortic SMC in a pulsatile bioreactor for approximately 24 weeks. The vessel's histological appearance was similar to that of the native vessels and exhibited burst strength of nearly 2000 mmHg as compared to 300 mmHg of nonpulsed constructs. Teebken [Teebken, 2002] used seeded xenografts to produce small diameter

vascular grafts. Decellularized porcine aortas were seeded with EC isolated from human saphenous vein and cultured in a pulsatile perfusion bioreactor. The EC grew to form a monolayer on the lumen. Stable biomechanical properties were achieved at physiological perfusion pressures *in vitro*. These studies suggest that physical stimuli improve cell and tissue growth. Also bioreactors that mimic physiological conditions produce constructs with better mechanical properties and morphological characteristics as compared to those developed in static cultures.

It has been demonstrated from previous studies that, *in vivo*, architecture, development, and function of the cardiovascular tissues are intimately related to their hemodynamic environment. Pulsatile blood flow gives rise to both radial and circumferential strain while steady flow causes normal and shear stress on the walls of the vessels. These forces impact the alignment and sensitivity of the cells to biochemical signals for growth, maintenance, and repair [Niklason, 1999; Seliktar, 2001; Teebken, 2002; Weinberg, 1986]. An early study to produce TEHV involved initial static seeding on polymeric constructs *in vitro* and then *in vivo* implantation for its development. The major disadvantage of such tissue engineered valves was progressive structural valve deterioration resulting in stenosis or regurgitation. Hence bioreactors simulating heart valve dynamics have been developed to improve the structural and mechanical properties of the engineered valves. An *in vitro* flow system was developed by Jockenhoevel et al [Jockenhoevel, 2002] to investigate the impact of laminar flow on ECM formation and tissue development. The system provided a cross flow arrangement of main flow induced by a dialysis roller pump. PGA scaffolds were seeded with myofibroblasts from human aortic regions and incubated for 14 days under static conditions. The tissue was then split

into two groups; one group was exposed to shear stress for 14 days while the other was maintained under static conditions. The *in vitro* system maintained stable cell culture conditions and collagen production increased significantly (1.5 times) compared to the static culture conditions. This study suggests that dynamic mechanical environment is required for attaining significant fibroblast activity. Dumont et al [Dumont, 2002] developed a bioreactor consisting of two major parts, a silicone left ventricle and an afterload consisting of compliance and resistance, with the valve placed in between the two. Stroke volume output was accomplished by means of compression and decompression of the left ventricle. Using controllable resistance, compliance, stroke volume and frequency, different pressures and flow rates were obtained. Using the bioreactor, they obtained physiological aortic pressures and maximum flow rate of 3.44 L/min. However, the bioreactor was not tested for sterility, nutrient limitation (especially oxygen limitation) and viability of the tissue grown in it. A similar attempt to develop a sterile pulsatile bioreactor with adjustable flow and pressure levels was made by Hoestrup et al [Hoerstrup, 2000b]. The system consists of two principle chambers, an air chamber and a fluid chamber. The two chambers are separated by a silicon diaphragm. The fluid chamber was divided into two compartments; the lower of the two was connected to the top perfusion compartment through a tube. The tissue engineered valve was fixed on the top of the tube into the perfusion chamber. Media flow was directed from the bottom compartment through the tube to the mounted tissue engineered valve. Pulsatile flow was attained by pumping air into the air chamber which displaces the silicon diaphragm periodically between the two chambers. The air-driven system was connected to a respirator which functioned as an air pump. By adjusting the stroke

volume and ventilation rate of ventilator a flow rate of 50 to 2000 ml/min and pressures of 10 to 240 mmHg were achieved in the bioreactor. Though a wide pressure and flow rate ranges could be attained by the system, the flow rate values were not in the physiological range and the system did not address the issue of O_2 transport. A trileaflet valve created using PGA scaffolds coated with P4HB was grown in the bioreactor [Hoerstrup, 2000a]. The leaflets showed mobility with synchronous opening and closing within the bioreactor and all the leaflets were intact, pliable and competent during valve closure compared to those grown in static culture, which were fragile and were losing structural integrity after 14 days. The leaflets which were grown in the bioreactor showed organized layered cellularity with dense outer layer and less cellular inner layers at the end of 14 days. Also the tissue had a confluent smooth surface with cell orientation in the direction of flow. In contrast rough surface was observed for static cultured tissue. The collagen content increased 129% compared to the native tissue after 14 days and leveled off at 85% at the end of 28 days. GAG was found to be 60% of the native tissue after 14 days and increased a little at the end of 28 days. In a similar study Sodian et al [Sodian, 2000] created a trileaflet heart valve using polyhydroxyalkanoate. Valves cultured in the bioreactor showed that cells were viable and ECM formation was induced after exposure to pulsatile flow. The engineered valves produced by the methods above, when implanted *in vivo* in sheep model showed patency up to 16-20 weeks and later developed regurgitation due to improper coaptation. Thus, further studies must be done to design a bioreactor that will provide the mechanical environment required for the stimulation of the cells to develop the functional characteristics similar to native valvular cells. A better

understanding of the response of native valvular cells to mechanical forces experienced by the heart valves during the cardiac cycle will enable a better bioreactor design.

Studies to understand the biology of native heart valve leaflet tissue and cells in response to individual cardiac hemodynamic forces have been carried out over the past few years by many investigators. Weston et al [Weston, 2001] developed a system to study the effects of steady and pulsatile flow (10 L/min and 20 L/min) and laminar shear stress (1, 6, 22 dyne/cm^2) on native porcine aortic valve leaflets. The results showed that exposure to bulk flow or shear stress environment for 48 hours maintained the collagen, GAG and DNA synthesis at native synthetic levels; however the synthesis increased significantly when leaflets were subjected to static incubation. A difference in protein synthesis in the leaflet tissue was observed as compared to freshly excised tissue when it was exposed to shear stress. These results suggest that fluid flow maintained the synthetic activity of leaflets at normal levels. A study done to investigate the effects of constant pressure on biology of aortic valve leaflets showed an increase in collagen synthesis at hypertensive pressures when compared to statically incubated leaflets [Xing, 2004]. These studies demonstrate that leaflet tissue show varied responses to different physiological forces in isolation. In both these studies, it was observed that the leaflets were unable to preserve α-smooth muscle actin immunoreactive cells, which suggests that other mechanical forces, such as bending or stretch caused by back pressure may be required to preserve cell phenotype. To attain this, aortic valve leaflets anchored to the aortic root need to be subjected to physiological forces *in vitro* and their response to these forces needs to be characterized.

2.5. Rational for the research

Aortic valve leaflets consist of a matrix of collagen, elastin fibers, proteoglycans and glycoproteins that along with the cells populating the matrix sustain the dynamic behavior of the valves by undergoing changes in synthetic activity. ICs lie within the matrix and play a vital role in maintaining the functionality of the valves. They are myofibroblastic in nature and exhibit contractility and secrete ECM components (collagen, elastin and GAG). ECs are present on the leaflet surfaces and are critical for maintaining nonthrombogenicity, transport of nutrients, and transduction of mechanical and biochemical signals to the ICs via the ECM. Constant production, remodeling, and adaptation of these cells and matrix ensure the functional integrity of the aortic valve. The cellular elements of the valve leaflet exhibit different phenotypes specific to the role performed. Consequently, it has been shown that phenotype of vascular SMC was altered with changes in culture conditions, mechanical or biochemical stimulation [Stegemann, 2003a; Stegemann, 2003b]. Reduction in α-SMC actin expression was observed with valvular ICs in 3D gels under static culture [Butcher J.T., 2004; Butcher, 2004a] which was similar to that seen in 3D vascular cells gel culture [Stegemann, 2003b]. This suggests that mechanical forces along with matrix interaction play a significant role in modulating cell phenotype. Porcine aortic valve ECs subjected to 20 dyne/cm^2 of steady laminar shear stress showed different organization of focal adhesion complexes and cell alignment than static cultures, suggesting the influence of mechanical forces on valvular EC behavior [Butcher, 2004b]. Studies on native aortic valve leaflets subjected to mechanical forces showed that fluid forces, laminar steady shear stress and constant pressures at physiological levels reduced the expression of α- SMC actin of valvular ICs

compared to native levels [Weston, 2001; Xing, 2004]. From this it can be said that altered or absence of certain mechanical forces such as cyclic strain or bending stresses leads to loss of contractile phenotype of the cells.

The results from above studies suggest that the lack of an appropriate mechanical environment induces a change in the physiological characteristics of the aortic valve tissue. To address this issue, an *ex vivo* organ culture system will be used to study porcine aortic heart valves. The system should be able to maintain sterility with physiological cardiac output (4.2 L/min) and mean pressure (100 mm Hg), while providing sufficient oxygen transport to the native porcine aortic valves. The advantage of this system is that cells are maintained in their natural 3-D matrix, in contrast to typical 2-D *in vitro* cell culture studies, and the mechanical environment can be closely controlled, unlike *in vivo* models. Native porcine aortic valves will be cultured in the system under sterile conditions for 48 hours and quantitatively compared for ECM components (collagen, sGAG and elastin) with fresh valve leaflets and leaflets incubated under static conditions for 48 hours. Qualitative comparison of the leaflets will be done to look at morphology, changes in cell phenotype, retention of endothelial cells, cellular proliferation and apoptosis.

The results obtained from this study may elucidate the understanding on the effects of hemodynamics on cell-cell interactions, mechanotransduction mechanisms in valvular cells and changes in gene and protein expression.

CHAPTER 3

SPECIFIC AIMS

Studies on the role of hemodynamic forces in regulating the biological properties of aortic valve leaflets are important in understanding the normal function of the valve leaflets and also to elucidate failure mechanisms that are implicated in various valvular diseases. To date, a complete understanding on the biological characteristics of valve leaflets subjected to normal physiological and pathological mechanical conditions has not been attained. The identification of the mechanisms of valve failure due to adverse mechanical conditions is an area requiring research.

The native aortic valve offers minimal resistance to fluid flow when open and minimal backflow into the left ventricle when closed. It experiences shear and bending stresses, fluid and pressure forces, and cyclic flexure during each cardiac cycle. The transvalvular pressure difference during valve closure generates large stresses on the valve leaflets, which are distributed to the aorta through the fibrous skeleton. Under pathological conditions, the inability to reduce these large stresses causes further deterioration of the valve resulting in the need for repair or replacement. Studies have already been performed in our laboratory to study the effects of laminar shear stress, and constant and cyclic pressure on the valve leaflets. These studies showed differences in cell phenotype when compared with native aortic valves, suggesting that the lack of appropriate mechanical forces such as bending stresses, or cyclic flexure alter the native biological property of the valves.

The hypothesis of this research work is that exposure of native aortic valves to normal hemodynamic conditions in an *ex vivo* sterile organ culture system should maintain the cellular/biological functionality and phenotype of the valve leaflets. The hypothesis is addressed by specific aims: 1) developing a sterile organ culture system that simulates the hemodynamics of aortic valves under normal physiological flow and pressure conditions; 2) comparing aortic valve leaflet biology between the valves cultured in the system for 48 hours and fresh aortic leaflets, and leaflets incubated under static, atmospheric conditions in medium for 48 hours.

3.1. Aim 1: Development of the sterile *ex vivo* organ culture system

The focus of this aim is to design a sterile *ex vivo* organ culture system that is easy to assemble and compact enough to be placed inside an incubator. The system must satisfy the following criteria: It should: 1) be closed to maintain sterility; 2) maintain physiological pressures (mean of 100 mmHg) and cardiac output (3.8 – 4.7 L/min) for a period of 48 hours; and 3) maintain the viability of aortic valve leaflets by providing sufficient oxygen transport to the valve. The system developed should be able to evaluate the biological characteristics of native aortic valves under physiological and pathological conditions for extended periods of time. To achieve this, the system will be tested for physiological flow and pressure waveforms for a period of over 48 hours. The sterility of the system will be checked by operating the system aseptically for 96 hours, while providing sufficient oxygen transport in the system.

3.2. Aim 2: Effect of mechanical forces on the biology of porcine aortic valves

The focus of this aim is to study the biological properties of native porcine aortic valve leaflets cultured in the organ culture system under normal physiological conditions for a period of 48 hours. Native valves when cultured *ex vivo* in the system are hypothesized to have similar biological characteristics to those of fresh aortic valves. Total collagen, sGAG and elastin content of the cultured valve leaflets will be measured and compared to fresh and statically incubated leaflets to evaluate the ECM composition of the leaflets. Further Hematoxylin and Eosin staining will be performed to examine the leaflet morphology and structural integrity. Immunohistochemical stains will be used to study cell phenotype by observing the expression of α- smooth muscle actin produced by smooth muscle cells, cell proliferation by 5-bromo deoxyuridine labeling of the cells, and cell apoptosis by activated caspase-3 antibody. Presence of endothelial cells will be observed by von Willebrand factor immunohistochemistry and scanning electron microscopy.

CHAPTER 4

MATERIALS AND METHODS

4.1. Construction of the organ culture system

The organ culture system was designed to mimic the systemic circulation in order to create an *in vitro* mechanical environment that simulates the *in vivo* hemodynamic environment. The arterial, capillary and venous systems constitute the systemic circulation of the human body. The arterial system must maintain a relatively high pressure in order to establish coronary circulation during the diastolic phase of the cardiac cycle. The elastic nature of the arteries acts as compliance, called the Windkessel effect that provides a cushioning effect for the pressure waveform preventing excess pressure build-up and also helps maintain the pressure at the required level with the help of the arterioles. The arterial system ends in arterioles, which form a large peripheral resistance by acting as strong muscular control valves through which blood is released into the capillary system. The blood from the capillaries is collected by the venous system which acts as a storage place for blood controlled by venous constriction [Guyton, 1991]. Since the heart pumps blood via a pulsatile cycle into the arterial system, the flow and pressure waveforms show a pulse with peak values corresponding to the pressure and flow conditions in the arterial system. The physiologic waveforms are depicted in Figure 4.1. The area beneath the flow waveform denotes stroke volume which is 70 mL for a normal, resting adult. Retrograde flow occurs during valve closure for approximately 30msec. The systolic/diastolic pressure for a normal, resting adult is 120/80 mmHg.

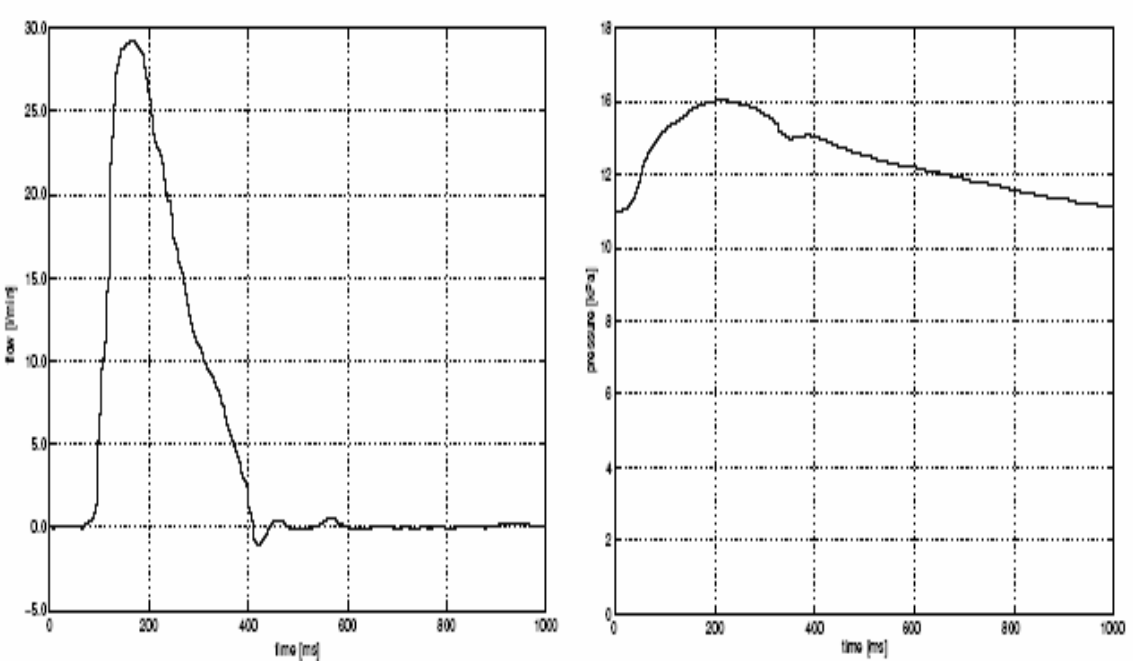

Figure 4.1: Schematic of flow and pressure waveforms in the ascending aorta of adult humans under normal, resting conditions. [Willems, 2002]

4.1.1. Design criteria and initial design of the organ culture system

The primary design consideration when constructing the organ culture system was to mimic the cardiac cycle of the systemic circulation to allow *ex vivo* studies on native aortic heart valves. For this purpose, the system must be sterile and closed to the atmosphere in order to avoid contamination and enable extended study periods. The design criteria governing the construction of the organ culture system are as follows:

1) Physiological flow and pressure conditions: The system must be capable of providing proper flow and pressure waveforms as shown in Figure 4.1 with a cardiac output of 3.7 – 4.2 L/min and a mean pulsatile pressure of 100 mmHg (120/80 mmHg systolic/diastolic) at a frequency of 1.167 Hz for the duration of an experimental run when operated under normal hemodynamic conditions.

2) Temperature, pH and oxygen exchange: The media inside the system must be maintained at a temperature of 37^{o}C and at a pH of 7.4 for optimal growth of the aortic valve tissue. There should not be nutrient limiting conditions, especially O_2, in the system. Preliminary studies with aortic valves suggest that valvular cells undergo apoptosis when oxygen is insufficient in the system. Hence, an O_2 exchange rate greater than the uptake rate of the aortic valves is necessary, and must be maintained at all times in the system by exchange of 5% CO_2 gas.
3) Sterility: The system is required to be sterile to prevent contamination of the tissue. For this purpose the system should be closed. It must also be fast and easy to assemble to avoid tissue damage caused by long ischemic periods between harvesting of the valve and placement in the organ culture system.
4) Size: The closed system must be placed in an incubator and maintained at a temperature of 37^{o}C. Thus, the system size is limited to the size of the incubator, which is 65 × 60 × 45 cm^3 (width × depth × height). A smaller size also facilitates using less volume of media to fill the system.

The initial design of the organ culture system, alternatively called a flow loop, was developed by I.H.A.Willems in our laboratory [Willems, 2002]. The prototype flow loop evolved as a result of a series of non-sterile experiments to attain proper pressure and flow waveforms. The flow and pressure waveforms in the ascending aorta, which arise due to the interplay between the ventricular contraction and the peripheral resistance and compliance of the systemic circulation, can be attained by simulating these forces with a piston pump and two valves to mimic the aortic and mitral valves *in vivo*. Figure 4.2 shows a photograph of the initial design of the flow loop.

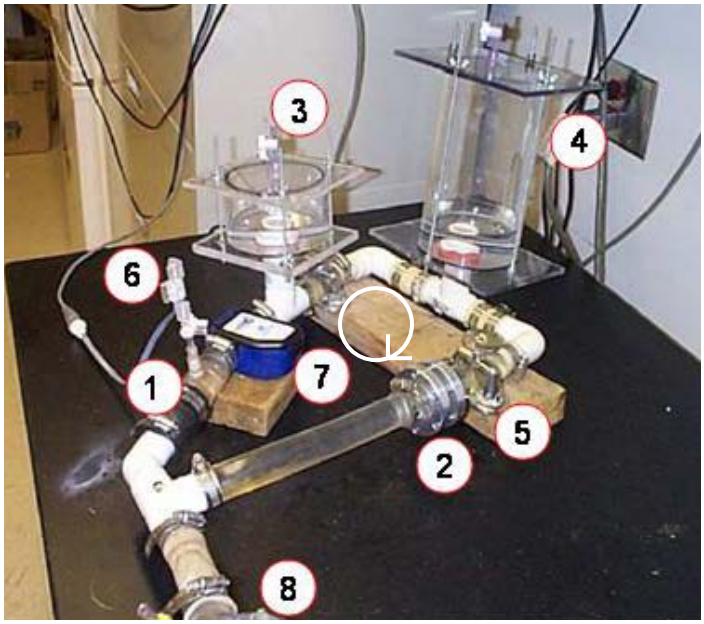

Figure 4.2: Initial design of the flow loop.1) Hancock® II stented bioprosthetic aortic valve 2) Björk-Shiley mechanical mitral valve 3) Reservoir 4) Capacitance reservoir 5) Clamp 6) Pressure transducer 7) Ultrasonic flow probe and 8) Pumphead. Flow direction is indicated by the arrow.

The loop was made by connecting series of Tygon®, acrylic and polyvinyl chloride tubing with rigid sanitary connectors. A piston pump (Superpump SPA3891, Vivitro systems Inc., Victoria, BC) was used to simulate left ventricular function in the loop and to drive the media through the loop. The loop was connected to the pump via a custom-made pump head (J.M. Machining, Lawrenceville, GA) that was constructed to have a male and a female part so that a flexible membrane could be incorporated to separate the sterile and non-sterile parts of the flow loop. A latex sheet of 0.02" thickness was placed between the two parts to maintain this separation. A Hancock® II stented bioprosthetic aortic valve was mounted in an in-house built valve holder and a Björk-Shiley mechanical mitral valve was mounted in a custom-built (J.M. Machining,

Lawrenceville, GA) valve holder. An acrylic reservoir was used to provide the aortic compliance to attenuate oscillations in the flow and pressure waveforms and to avoid pressure build-up during piston movement. Injecting air into the reservoir with a syringe allowed the pressure to be varied, thus providing the proper flow and pressure waveforms. A capacitance reservoir, also made of acrylic, was filled with fluid and was used to provide the required diastolic pressure and to simulate venous pooling. Regulation of venous return was achieved by injecting air into the compliance with a syringe. A stainless steel clamp placed upstream of the mitral valve simulated the peripheral resistance found in the arterioles at the entrance to the capillary system. By tightening or loosening the clamp, the desired aortic pressure was attained. Downstream of the aortic valve, a gage pressure transducer (CDX III, Maxxim Medical, Athens, TX) interfaced to a bridge amplifier (CD 12, Validyne Engineering, Northridge, CA) was used to measure aortic pressure and an ultrasonic flow probe (H20XL, Transonic Systems, Ithaca, NY) was used to measure the flow rate which was displayed on a digital flow meter (T110, Transonic Systems, Ithaca, NY). The entire system was placed inside an incubator maintained at 37^{o}C. The piston pump along with the pump head was placed outside the incubator (Fisher scientific, Suwanee, GA) and was connected to the rest of the flow loop through a hole at the back of the incubator.

Experiments done with a bioprosthetic valve in the flow loop showed that the flow and pressure curves were in the physiological range with mean values of 4.2 L/min and 100.5 mm Hg (123/78 mm Hg), respectively. The system was also tested for sterility for a period of 48 hours. However, the design was not robust enough to be used with native aortic valves. Most of the components of the loop were unfit for repeated

autoclave cycles, and leaks arose near the compliance and capacitance reservoirs and pump head during operation. Also, assembling the loop took a long period of time, and the entire process was tedious. The aortic valve holder was unsuitable for native aortic valves since it required the use of the valve along with a piece of the aorta to support the leaflets. Without this support the aorta bent over the leaflets obstructing leaflet movement during the systolic phase of the cardiac cycle. Also, the system did not provide any means to oxygenate the medium to maintain viability of the valve tissue. Due to these design limitations, many components of the system required significant modifications including the aortic valve holder, compliance and capacitance reservoirs, pump head, and tubing.

4.1.2. Final design of the organ culture system

The design of the flow loop and some of its components were changed to simplify the system assembly, reduce the risk of contamination, and maintain the viability of the valve leaflets. Based on the observations of the initial design, the aortic valve holder was changed significantly for ease of assembly and to provide a leak proof seal. The valve holder was divided into three parts called the inflow, central and outflow parts. The design was adopted from a previous model of the holder developed by I.H.A.Willems. The model developed by him was big, required 24 screws for assembly, and leaked. The new model was reduced in size to accommodate a native aortic valve with a 25mm aortic root diameter and a 51mm (2.0") aorta. The material of construction was stainless steel to sustain multiple autoclave cycles. The valve was held in place by suturing the aortic root to a polypropylene ring with an inner diameter of 1". The annulus of the central part of the valve holder was constructed to have two different diameters. The inflow side of the

central component has an annulus diameter of 1.3" spanning a depth of 0.5", which then decreases to 1" for the rest of the length. The increased diameter of the annulus was to accommodate the coronary arteries of the valve, which were ligated to avoid back flow of the media. The outflow part of the holder was designed so that excess aorta could be slipped between the central and outflow parts to avoid bending of the aorta over the leaflets. Detailed designs of the valve holder are given in the appendix A. The components were sealed together by two C-clamps, which wrapped around the gaps between the inflow and central parts and outflow and central parts to provide a tight seal. Gaskets were placed between the components to avoid leakage of the media.

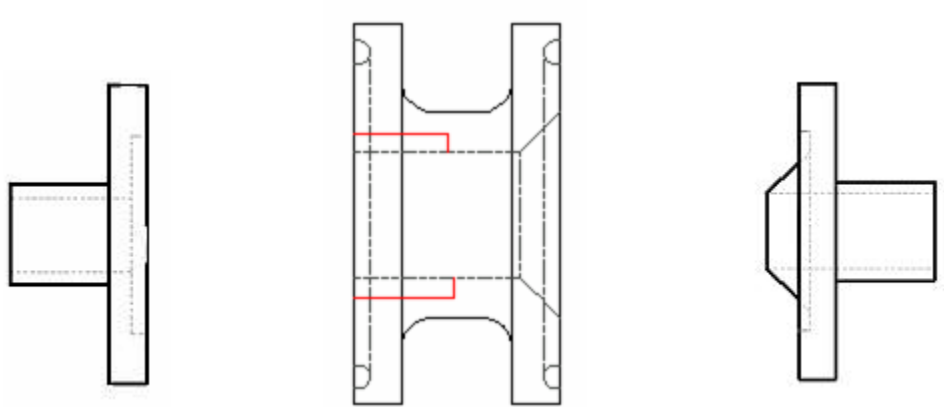

Figure 4.3: Schematic of the inlet, central and outlet parts from left to right respectively. (not to scale). Detailed designs with dimensions are given in Appendix A.

Another design flaw of the original flow loop was that the compliance and capacitance reservoirs were difficult to assemble since the central cylinder had to be carefully positioned between the two gaskets to prevent leakage. This type of alignment was cumbersome and tedious to achieve and often leaked after undergoing an autoclave cycle. To avoid this process the two reservoirs were replaced with a 500 mL spinner flask

(Bellco Glass Inc., Vineland, NJ) as the compliance chamber, which was easier and quicker to assemble. A 1" diameter hole was made in the lid of the flask to allow the media to flow into the compliance tank. Neoprene rubber O-rings were placed on either side of the hole to prevent leaks. The loop was filled with media through one of the side arms of the tank via a two port assembly (Bellco Glass Inc., Vineland, NJ). One of the two ports was connected to the media reservoir, which is a 2 L glass bottle (Bellco Glass Inc., Vineland, NJ) using Pharmed tubing (Colepalmer, Vernon Hills, Illinois), and the other port had a biofilter (VWR, Suwanee, GA) attached to it through the tubing. Air was injected into the tank through the latter port to build up pressure in the system. Once the required pressure was reached, the tubing was clamped to prevent loss of pressure in the flow loop. After loop was filled with media, the tubing was clamped to prevent leakage of media back into the reservoir and also to prevent loss of pressure in the flow loop. On the other arm of the compliance tank, another two port assembly was fitted at the mouth, and silicon tubing was connected between the two ports inside the tank to serve as a gas-exchanger in the system. The diameter of the silicon tubing was 0.16", and the tubing was coiled inside the compliance tank and held in place by three hollow, 1" diameter polyvinyl chloride tubes. One end of the port was connected to a gas/liquid rotameter (Omega Engineering, Inc., Stamford, CT), which was in turn connected to a 5%CO_2 + 95% air cylinder (Southeast specialty gases, Atlanta, GA) to provide oxygen to the system. A gas biofilter was placed at the other end of the port to enable contamination free exit of the spent gases. By partially closing the exit port with a clamp, the pressure inside the flow loop could be maintained at the required level for the duration of the experiment. Since the silicon tubing was immersed in the media in the compliance tank,

gas-exchange to the surrounding media took place across the tube wall and was transported throughout the media by flow of the liquid in the system. Thus, sufficient oxygen could be provided to the tissue while maintaining the mechanical performance of the system.

Another potential place for leakage in the initial design of the flow loop was the pump head. The original design required careful placement of the latex membrane between the male and female parts of the pump head, which were held in place by four stainless steel screws. If the screws were not aligned properly, the parts would not fit tightly enough to hold the latex together. Often the membrane slipped causing the pump head to leak and allowing the media to mix with the water, thus causing contamination in the system. To avoid this, a membrane chamber was designed which was separated from the pump head. The new chamber was designed so that it could be placed inside the incubator to maintain the temperature of the media at 37^{o}C throughout the flow loop. The membrane chamber consisted of two parts, made from poly carbonate, with the edges grooved to grip the latex membrane tightly as shown in Figure 4.4. The media circulates from one port of the membrane chamber into the aortic valve holder and returns to the chamber through the other port via the mitral valve holder. The two components of the chamber were fixed together using three screws, which reduced the assembly time and also provided leak proof separation of the sterile and non-sterile parts of the flow loop.

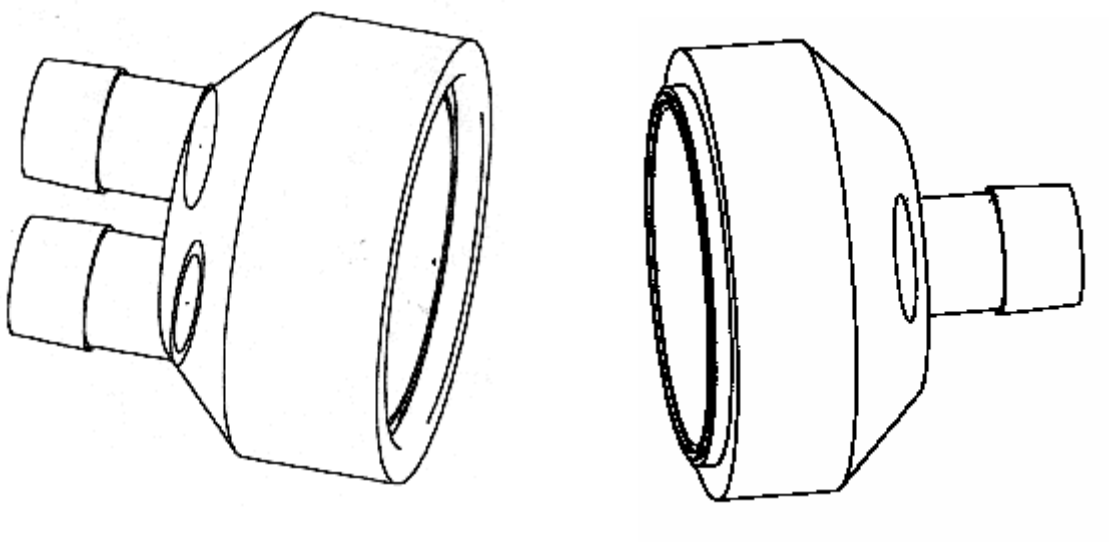

Figure 4.4: Drawing of membrane chamber. The left part is connected to the loop and the right part is connected to the pump head. (not to scale). Detailed designs with dimensions are given in Appendix A.

Apart from the changes in the design of components in the system, additional changes were also made to the flow loop to withstand the high temperature (121^{o}C) and pressure (15psig) of the autoclave. The Tygon tubing was replaced by a 1" inner diameter Silicon reinforced tubing (Colepalmer, Vernon Hills, Illinois) with tygon tubing used only at two places: downstream of the aortic valve and the compliance tank. Silicon reinforced tubing was thick and less flexible compared to the tygon tubing to be clamped by the flow probe. This prevented the measurement of flow rate downstream of aortic valve as the ultrasound flow probe could not measure the flow signal. Also it was difficult to build up resistance in the system downstream of the compliance tank. Hence tygon tubing was used at these two places. The final configuration of the flow loop was rectangular as opposed to the triangular configuration seen in the initial design due to incorporation of the membrane chamber, elimination of resistance chamber and change in the design of

compliance chamber. The final setup of the flow loop required a media volume of 1.5L to obtain physiological waveforms and also to completely immerse the gas-exchanger in the media. Figures 4.5 and 4.6 show the schematic and picture of the final design of the flow loop, respectively. Parts of the flow loop such as the latex sheet and support ring required periodic replacement due to wear and tear.

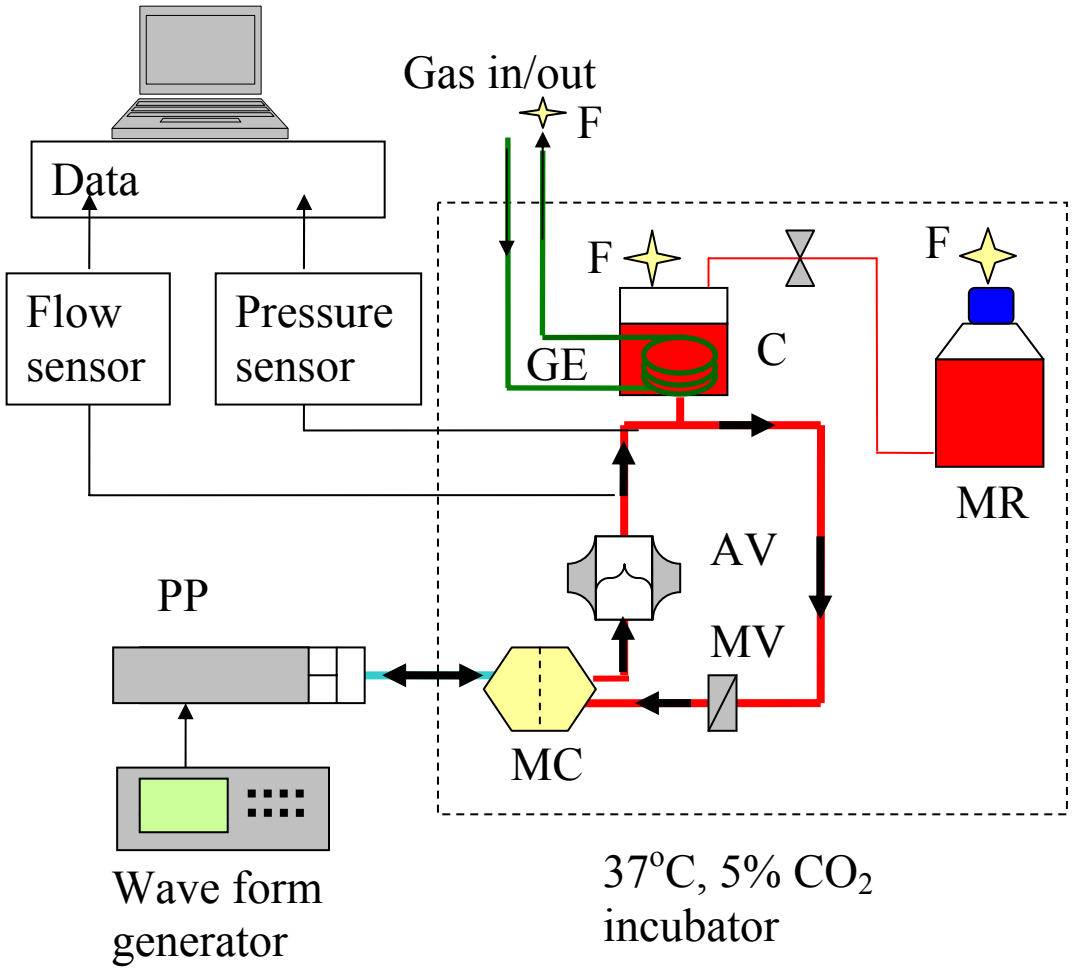

PP = Piston pump
AV = Aortic valve
MR = Media reservoir
GE = Gas-exchanger

MC = Membrane chamber
MV = Mitral valve
C = Compliance tank
F = Biofilter

Figure 4.5: Schematic of the final design of the flow loop. The flow direction is indicated by the arrows. The sterile part of the system is indicated by the dashed box. Media is shown in red and gas-exchanger is shown in green. Flow and pressure signals are acquired downstream of the aortic valve.

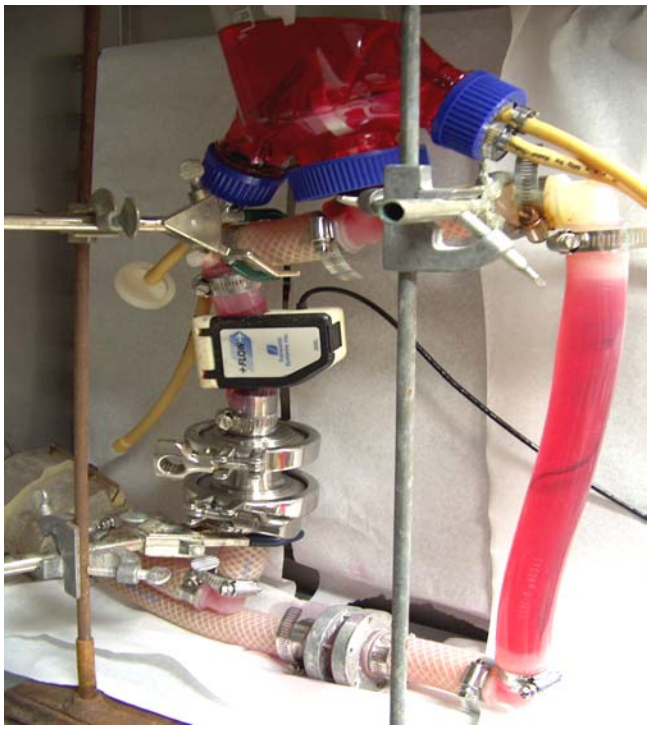

Figure 4.6: Picture of the organ culture system with porcine aortic valve cultured in the system.

4.1.3. Signal input and data acquisition

The mechanical performance of the system was evaluated by comparing the flow and pressure curves with *in vivo* data. The fluid was circulated through the loop by a piston pump that was controlled by an input signal from a waveform generator (HP33120A, Hewlett – Packard, Palo Alto, CA). The input signal was programmed in the waveform generator using software (Benchlink Arb, Hewlett-Packard, Palo Alto, CA) that came with the generator. The input signal had a frequency of 70 beats/min (1.167 Hz) and is shown in Figure 4.7.

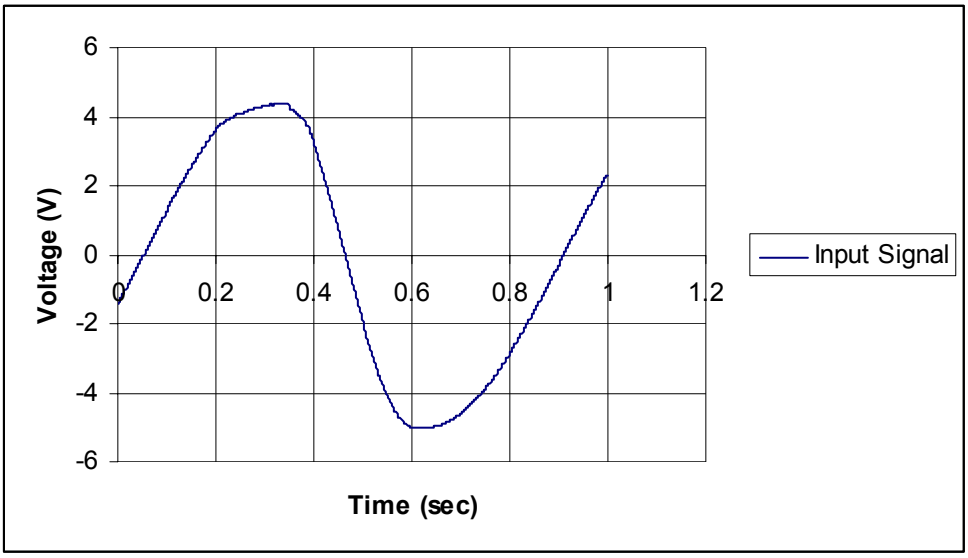

Figure 4.7: Input signal programmed in the wave form generator that is given to the piston pump.

A list of parameters used in the setting of waveform generator and trigger signal are given in Table 4.1.

Table 4.1: Parameters set programmed under Recall 1 menu in the waveform and trigger signal generators.

	Serial #	Parameter	Value
Waveform generator	1	Waveform	Arb
	2	Frequency	1.167 Hz
	3	Amplitude	4.998
	4	Offset	0.000
Trigger generator	1	Waveform	Step
	2	Frequency	1.167Hz
	3	Amplitude	4.000
	4	Offset	0.000

The mechanical performance of the organ system was also tested, in our laboratory, at various mechanical conditions such as hypertensive, severe hypertensive aortic pressures with mean values of 140 and 170 mmHg, respectively, at normal cardiac output (4.2 L/min) and frequency of 1.167 Hz, and elevated cardiac output of 7.5 L/min at a frequency of 120 beats/min (2Hz) at mean aortic pressure of 100 mmHg [Warnock, 2004]. The parameters programmed into the waveform generator and trigger signal were maintained the same for all aortic pressure conditions. While testing the performance of the system at elevated cardiac output at 2 Hz, the frequency value in the waveform and trigger generators was changed to 2 Hz keeping the remaining parameters constant in Table 4.1. The input signal at a frequency of 2 Hz is shown in Figure 4.8.

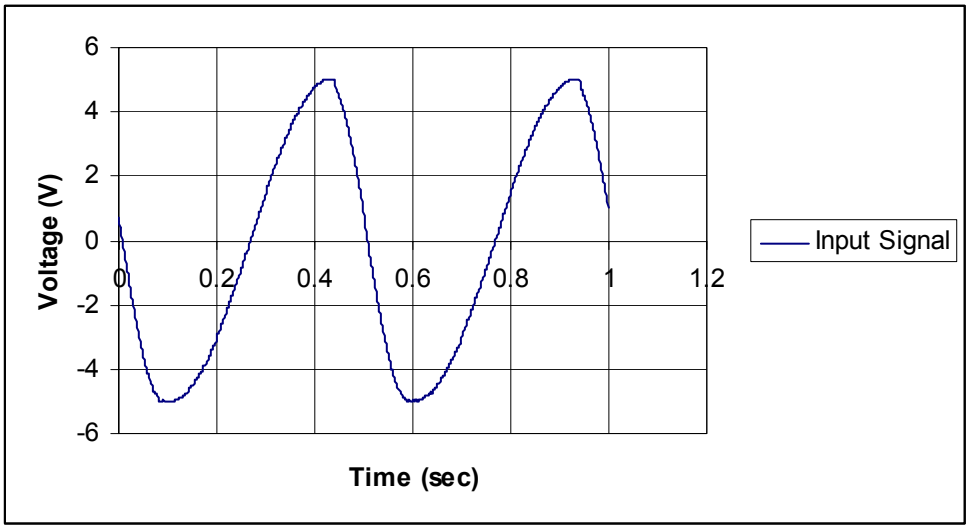

Figure 4.8 Input signal at elevated cardiac rate of 2Hz, programmed in the wave form generator that is given to the piston pump.

After feeding the required parameters to the signal generators, the flow loop was started, and data was acquired to generate flow and pressure waveforms. An in-house built interface box, or DAQ box was used to acquire the flow and pressure signals from the ultrasound flow probe (H20XL, Transonic Systems, Ithaca, NY) and pressure transducer (CE0344, Maxxim medical, Athens, TX), respectively. The DAQ box receives analog voltage signals from the transducers and transfers the signals to a PCMCIA data acquisition card (NI DAQCard-1200, National Instruments, Austin, TX). The card has eight different channels, which are synchronized by the trigger signal from the trigger waveform generator. During the data collection, channel one was used for flow, two for pressure, and the eighth was used for the trigger. The DAQ Card was plugged into a computer system, and the data was stored using in-house developed data collection program called DAQ-ANAL 2.2 based on LabVIEW 5.1 graphical user interface software (LabVIEW 5.1, National Instruments, Austin, TX). The sampling time was 2

msec and the data was collected and stored over 10 cycles then averaged over the cycles during data analysis. Data was stored in Excel spreadsheets using the data analysis function of DAQ-ANAL. Microsoft Excel was used to analyze and plot the waveforms. Flow and pressure signals, which were obtained as voltage signals, were converted to units of flow rate and pressure, using the conversion factors obtained from the flow probe and pressure transducer calibrations.

The flow loop used for calibration of the flow probe consisted of a rotameter located upstream of a bucket for water collection that was connected by polyvinyl chloride and tygon tubing with flow probe on it back to the rotameter. Water was circulated through the loop with a water pump (4E-34N, Little Giant Pump Co., Oklahoma City, OK) to drive the fluid through vertically up the rotameter. The water pump was placed in an ice filled container to reduce the heat generated by it. The flow rate through the rotameter was controlled by a variable transformer (CSA LR18948, Staco Energy Products Co., Dayton, OH) coupled to the water pump. The flow probe was fixed around the tygon tubing to record the flow rate on the flow meter. A voltmeter (Fluke 27, John Fluke MFG. Co., INC.,Everett, WA) was connected to the flow meter to read the voltage values corresponding to the flow rate value. By successively increasing the rotameter reading monitored by the movement of the float, the corresponding reading for flow rate and voltage were noted. A graph of voltage versus flow rate was plotted and the conversion value was calculated (Figure 4.9).

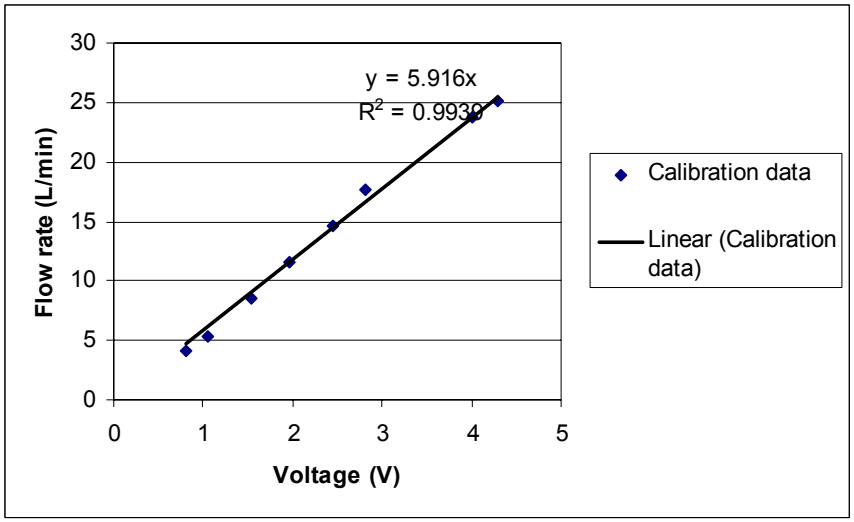

Figure 4.9: Calibration curve for ultrasound flow probe calibrated with water as circulating fluid.

The pressure transducer was calibrated using a U-tube manometer. The transducer was attached to one of the limbs of the manometer tube by a connector, which was used to inject or remove the fluid from the manometer limb. A voltmeter was connected to the bridge amplifier to note the voltage values corresponding to the pressure in the manometer tube. The connector was initially open to the atmosphere to set the reading on the amplifier to zero. Once this was done, water was injected to a maximum height into the limb connected to the transducer. For decreasing water levels, the corresponding voltage readings were noted and a graph was plotted between pressure and voltage after converting the pressure to mmHg.

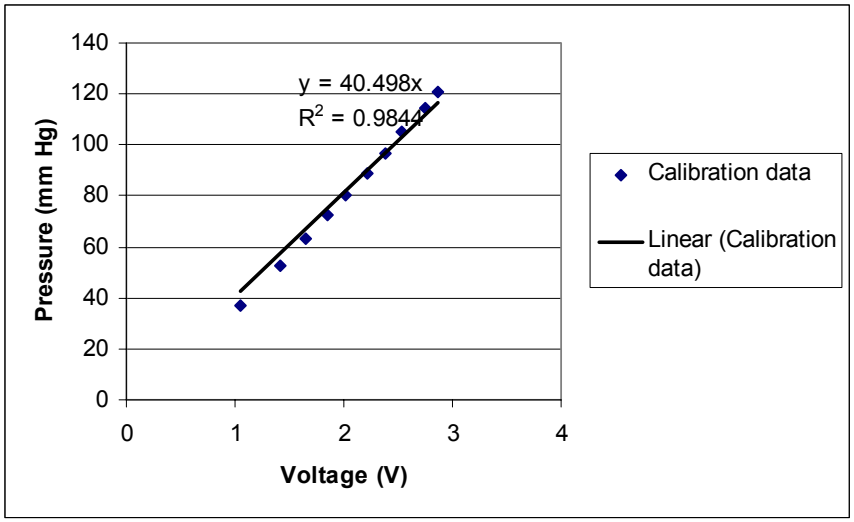

Figure 4.10: Calibration curve for pressure transducer calibrated with water.

4.2. Mechanical validation of the organ culture system

Mechanical validation of the system was performed by conducting experiments using mechanical and bioprosthetic valves with water circulating in the system. Since the ultimate goal of the design was to study the functionality of native aortic valves, the system was tested for sterility of the medium over a period of 96 hours with a mechanical valve. The efficiency of the gas-exchanger was also tested to ensure that it provided oxygen to the medium at a rate greater than the oxygen uptake rate of the aortic valves.

4.2.1. Physiological flow and pressure waveforms

Mechanical testing of the flow loop was performed using a 25mm Starr Edwards ball and cage mechanical valve and 25mm pericardial bioprosthetic aortic valve. The loop was assembled as shown in Figure 4.5 and was connected to the pump head, which was attached to the piston pump. A 1" internal diameter polypropylene ring was placed around the mechanical or bioprosthetic valve to hold the valve in place. The loop was

placed in a vertical position with the help of two stands, and the flow probe was clamped around the tygon tubing downstream of the aortic valve holder. The pressure transducer was screwed onto a connector attached to an elbow joint at the end of the tygon tubing also downstream of the aortic valve. Once the loop was closed, it was filled with water by injecting air into the media reservoir through a biofilter. After the flow loop was filled, the tubing from media reservoir was clamped. A clamp was also placed on the other port through which air was injected into the compliance tank. The tubing from the 5% CO_2 tank was then connected to the compliance tank and gas flow was regulated with a rotameter. Once all the connections were made, the waveform and trigger generators were switched on and set to the required parameters. The flow meter and bridge amplifier were turned on, and the piston pump was started. The amplitude of the piston was increased slowly until the desired flow rate of 4.2 L/min was attained and then the pressure in the loop was increased by clamping the tygon tubing downstream of the compliance tank and also by injecting air into the compliance tank through a syringe. Once the pressure in the loop attained a mean value of 100 mm Hg, which was monitored using DAQ-ANAL, the waveforms were recorded and saved on the computer. The consistency of the waveforms was tested for a period of 48 hours by recording the waveforms at regular intervals. The data collected was analyzed and averaged over all the cycles. The average values were plotted over the entire cardiac cycle (860 msec). The organ culture system was also validated at elevated mechanical conditions in our laboratory, which are summarized in Table 4.2 [Warnock, 2004].

Table 4.2: Various mechanical conditions under which the organ culture system was validated with a Starr-Edwards ball and cage mechanical valve. * indicates data obtained by Warnock et al [Warnock, 2004].

Mean Aortic Pressure (mmHg)	Cardiac Output (L/min)	Heart Rate (Hz)	Mass Transfer Rate (mg O_2/sec)
100	4.2	1.167	9.9023×10^{-5}
*140	4.0	1.167	1.95×10^{-3}
*170	4.0	1.167	8.02×10^{-4}
*100	7.5	2.0	5.93×10^{-3}

4.2.2. Sterility testing of the organ culture system

In order to use the organ culture system to study the biology of aortic valves, the system must maintain valve viability during the entire experiment. An important consideration for achieving this is to maintain aseptic conditions in the system. For this a sterility test was performed for a period of 96 hours.

The organ culture system was assembled as shown in Figure 4.5 with the membrane chamber disconnected. A component of the membrane chamber, which was connected to the pump head, was packed in an autoclave pouch (VWR, Suwanee, GA) along with a latex membrane cut in a circle whose diameter was greater than the outer diameter of the membrane chamber. Aluminum foil was wrapped around the other part of the membrane chamber, which was connected to the loop. The connecter, to which the pressure transducer was fixed, was closed with a cap and all the biofilters along with the inlet to the 5% CO_2 tank in the system were covered with aluminum foil. An empty media reservoir was connected to the system, ensuring that no section of the loop was

exposed to air. The entire assembly and other components required for the loop were then sterilized for a period of 15min in an autoclave. 1.5 L of Dulbecco's Modified Eagle Medium (DMEM, Sigma, St.Louis, MO) supplemented with 1% antimycotic- antibiotic solution (Sigma, St.Louis, MO) filtered aseptically in a sterilized 2L glass bottle was the circulating media in the loop. A Starr-Edwards ball and cage mechanical valve, which was suspended in absolute ethanol overnight along with the pressure transducer and support ring, was used for the test. After the system was sterilized, the valve was placed in the valve holder with the support ring, and the system was filled with media. A small volume of media was taken for sampling in an Eppendorf tube (VWR, Suwanee, GA). The gas flow rate into the system was regulated and the flow rate and pressure values were adjusted to physiologic values and the waveforms recorded. The media was observed visually at regular intervals for macroscopic contamination. Contaminated media usually looks cloudy (turbid) often accompanied with a change in color from red to orangish yellow. The waveforms were recorded at different time points during the experiment to check the uniformity in the curves. At the end of 96 hours, the experiment was stopped and a sample of media was taken for analysis.

Samples of the media were analyzed microscopically and also by measuring the absorption values. For microscopic analysis, a small drop of media was placed on a glass slide and cover slipped for viewing under the microscope to reveal any bacterial or fungal growth in the media. For quantitative analysis, the media samples were placed in triplicate in a micro well plate reader (Spectra Max Gemini Microplate Spectrofluorometer, Sunnyvale, CA), and the absorbance values were measured at a wavelength of 364nm. The absorbance values were then averaged and a paired t-test was

performed on the two samples with a p-value of < 0.05 considered significant. Microsoft Excel was used for analyzing the results.

4.2.3. Gas-exchange in the organ culture system

Oxygen transport is one of the most important considerations in designing an organ culture system. Preliminary experiments with native aortic valves in the system showed that significant cell death occurred within the leaflet tissue, which was attributed to O_2 deficiency in the loop. Because the flow loop is a closed system, a gas-exchanger was needed in the system to provide O_2 to the tissue and maintain the viability of the native aortic valves. Soft silicon tubing (McMastercarr, Atlanta, GA) with an inner diameter of 0.16" was chosen to provide gas exchange in the media. To find the amount of O_2 required in the system, the O_2 uptake rate of the aortic valve was determined so that the amount of O_2 transferred to the media would be sufficient to maintain valve viability.

The oxygen uptake rate of the aortic valve was calculated by measuring the dissolved oxygen content in the media with aortic valves cultured in it. Four aortic valves were excised from porcine hearts aseptically in a local abattoir (Holifield farm, Covington, GA) and transported to the laboratory in sterile, ice cold Dulbecco's Phosphate Buffered Saline (DPBS, Sigma, St.Louis, MO) in a sealed container. The valves were trimmed to remove excess tissue and surrounding myocardium in a laminar flow hood (Fisher Hamilton, Two rivers, WI). Four sterile glass bottles were filled with 400 mL of DMEM. The media was oxygenated until it reached saturation by passing $5\%CO_2 + 95\%$ air into it and measuring the dissolved oxygen (DO_2) content using a DO_2 meter (ExTech Instruments, Tampa, FL). The aortic valves were then put in the media,

and the bottles were closed to prevent any oxygen transfer into the media from the atmosphere. The DO_2 content was measured every hour for the first 8 hours and at regular intervals over the remaining 40 hours, and the values were tabulated. At the end of 48 hours, the valves were removed, and their wet weight was measured to normalize the uptake rate of O_2. The pH of the media in all four bottles was also noted at the end of 48 hours. The uptake trend of the valve was observed by plotting a graph between the DO_2 value and time. The oxygen uptake rate of the valve was calculated by plotting DO_2 versus time for first 6 hours and measuring the slope from the plot. This calculation was employed as the DO_2 content in the medium decreased linearly with time in the first 6 hours and hence consumption rate was assumed to be constant. The equation used to calculate the uptake rate was,

$$OUR = \Delta DO_2/\Delta t \qquad (4.1)$$

Where OUR = Oxygen uptake rate of the valve

ΔDO_2 = Change in concentration of DO_2 in the medium (mg of O_2/ gm of tissue/ L of medium)

Δt = Change in time (hour)

The oxygen uptake rate of the valve was used as a limiting value to design the gas-exchanger to provide the required oxygen to the media. The equations used for the design are as follows;

$$Q = V.A \qquad (4.2)$$

Where Q = Gas flow rate of the 5% CO_2

V = Velocity of the gas

A = cross-sectional area of the silicon tubing

= Π× diameter of silicon tubing × length of the silicon tubing

$$V = P (\Delta P_{ln}) / Z \qquad (4.3)$$

Where P = Permeability of the silicon tubing (7961 cc × mm/ (cm^2×sec×cm Hg)) ×10^{-10})

ΔP_{ln} = Logarithmic mean of partial pressures of the gas (cm Hg)

= $(P_{in} - P_{out}) / \ln (P_{in}/P_{out})$

Z = Thickness of silicon tubing = 0.79375 mm

The O_2 transfer rate was arbitrarily chosen to be greater than the uptake rate. The assumptions made for this calculation were that the gas exchange was occurring at atmospheric conditions, and that almost all of the 5% CO_2 gas was exchanged into the system. The partial pressure of the gas mixture was calculated to be 151.62 mm Hg and based on the gas transfer rate the final pressure was calculated to be 0.66 mm Hg which gave a ΔP_{ln} value of 27.766 mm Hg. The velocity of the gas was thus found to be 2.785×10^{-6} cm/sec. Based on a trial and error procedure and using equation 4.2, the length of the silicon tubing to provide the required gas transfer rate was found to be 2 m at an inlet gas flow rate of 0.2 L/min.

The above parameters were then used to design the gas-exchanger, and experiments were run to measure the actual gas-transfer rate in the system. The flow loop was assembled as shown in Figure 4.5 and filled with DMEM. The medium was degassed using N_2 before passing 5% CO_2 into the system. The DO_2 values of the medium before and after degassing were noted. The DO_2 reading every hour was noted until the

saturation limit was attained, and the values were tabulated. The gas transfer rate was then calculated based on the following equation;

$$N = k\,(DO_{2,i} - DO_{2,f}) \qquad (4.4)$$

Where N = Gas-transfer rate into the medium (mg/sec)

k = Mass-transfer coefficient (cm/sec)

$DO_{2,i}$ = DO_2 reading at time t = 0

$DO_{2,f}$ = DO_2 reading at saturation time i.e., t = 4hours

The mass-transfer coefficient was calculated by plotting a graph between the logarithm of percent saturation of O_2 and time. The percent saturation values were obtained from DO_2 values using the equation;

$$\%\ \text{saturation} = 100 - 100\,(DO_{2,f} - DO_{2,t})/DO_{2,f} \qquad (4.5)$$

The equation used to calculate the coefficient was;

$$k = \text{Slope}/a \qquad (4.6)$$

Where a = interfacial area (mm^{-1})

= area/volume = 0.01676 mm^{-1}

The slope was obtained from the graph, and the mass-transfer coefficient was calculated using equation 4.6. The gas transfer rate was then obtained using equation 4.4. The O_2 uptake rate value was converted into the same units as that of the gas-transfer rate for comparison to test the efficiency of the exchanger setup.

Thus, the organ culture system was validated to satisfy the design criteria stated in section 4.1.1 before proceeding to the biological validation.

4.3. Biological validation of the organ culture system

The objective of designing an organ culture system was to study the biology of native aortic valves in response to physiological hemodynamic forces. The final stage in the design was to test whether the native biological properties of aortic valve are preserved in the system when the valve is subjected to normal hemodynamic forces such as a flow rate of 3.8-4.5L/min and pulsatile pressure of 120/80 mm Hg. The valves were cultured in the organ culture system for a period of 48 hours under the mechanical conditions stated and were analyzed quantitatively and qualitatively by measuring total collagen, sGAG and elastin content in the leaflet tissue and performing immunohistochemical stains on the tissue sections, respectively.

4.3.1. Experimental Procedure

Porcine aortic valves were obtained from a local abattoir. Animals from which hearts were obtained were usually adult pigs weighing 300-400 lbs. However, no specific record about the age or weight was made during procurement. Once the heart was separated from the other organs of the animal, on-field dissection was carried out to isolate the aortic valve from the heart. The apex of the heart was cut first and then the pulmonary valve was separated from the aortic valve. Mitral tissue adjacent to the aortic valve was removed and discarded. The aortic valve was then washed with sterile ice cold DPBS to remove residual blood adhering to the valve and placed in DPBS for transportation. The ischemic time was typically 30 min of warm ischemia between death of the animal and valve removal and about 2 hours of cold ischemia when the valve was transported to the laboratory.

After transporting the valve to the laboratory, it was trimmed to remove excess tissue and the surrounding myocardium. A support ring made of polypropylene was sutured tightly to the aortic root with 4/0 prolene blue monofilament sutures (Ethicon Inc., Somerville, NJ) to hold the valve in place in the aortic valve holder while circulating medium through the flow loop. The valve was soaked in DPBS throughout the suturing process, to prevent drying of the tissue. After the valve was sutured, the loop was assembled aseptically as shown in Figure 4.5. The organ culture system was autoclaved the day before the scheduled experiment. After the system has been autoclaved, it was placed in the laminar flow hood with UV light switched on and left overnight to prevent any possible contamination. Media required for the system was also prepared and sterilized and left at room temperature overnight.

The media composition used for the system was 20.04 gm of DMEM, 5.55 gm of $NaHCO_3$, 7.5 mg of 5- Bromodeoxyuridine (BrdU), 15 ml of antimycotic-antibiotic solution, 15 ml of Non-essential amino acids (NEAA), 18 μL of 1.5mM $CuSO_4$, 3.9 mL of 0.113M Ascorbic acid (Sigma, St.Louis, MO) and 1.5 L of deionized water. DMEM and NEAA provided the required nutrition for the cells, while $NaHCO_3$ was used to obtain the required pH (7.2-7.4). BrdU was used in the media to mark the proliferating cells in the tissue. Antibiotics were used to prevent infection due to any microbial growth. Ascorbic acid is necessary for collagen synthesis in the tissue, while $CuSO_4$ was used to reduce formation of anti-oxidants in the media. After the media was prepared, it was oxygenated by bubbling 5% CO_2 gas into it for a period of 45 min. This process also established the pH within the physiological range (7.2-7.4). The media was then sterilized by filtering it with sterile filters (VWR, Suwanee, GA) using vacuum filtration technique.

Once the aortic valve was sutured to the support ring, the organ culture system was assembled by connecting the two components of the membrane chamber with the latex membrane between them. After connecting the medium reservoir to the system, the aortic valve was placed in the valve holder and the pressure transducer was connected downstream of the aortic valve holder aseptically. The entire system was maintained at $37^{o}C$ by placing it an incubator, which has been decontaminated prior to the experiment. The flow loop was then connected to the piston pump via the pump head and medium was filled into the system to prevent drying of the valve. The medium in the system was oxygenated by circulating 5% CO_2 gas at a regulated flow rate. Once it was ensured that there were no leaks in the system and the connections were sufficiently tight, the pump head was filled with water, and the flow probe was clamped to the tygon tubing. The piston pump was started, and the flow rate was increased slowly over a period of two hours to prevent any leakage due to a sudden increase in flow and pressure in the system. After the flow rate was established, the pressure was increased in the system by injecting air into the compliance tank. After the flow and pressure values were stabilized, mechanical data was recorded using DAQ-ANAL at time, t = 0 hours. The loop was operated for a period of 48 hours with flow rates and aortic pressures acquired periodically every 12 hours to check the consistency in operating conditions.

At the end of 48 hour period, the system was disassembled and the aortic valve was removed. The leaflets were excised from the valve by cutting along the attachment line. Each leaflet was then laid flat on the lid of a tissue culture plate and a rectangular piece of approximately 14mm × 5mm was cut from the belly region of the leaflet. This piece was in turn cut into four small pieces of approximately 3mm × 1mm for analysis.

Three of the four pieces were placed in 1.5 mL micro-centrifuge tubes (VWR, Suwanee, GA) and dried for 48 hours in a vacuum oven (Yamato Scientific America, San Francisco, CA) to be used for biochemical assays to quantify total protein content (collagen and elastin) and GAG. The fourth piece was placed in a tissue-culture plate and fixed in 10% buffered formalin (Fisher Scientific, Suwanee, GA) for a period of 24 hours to be used for histological studies.

Fresh leaflets, isolated and processed immediately after harvest in the same manner as the cultured leaflets, were used as fresh controls, and leaflets cultured in media under static, atmospheric conditions for a period of 48 hours, were used as static controls. The static control leaflets were incubated in a 6-well tissue culture plate (VWR, Suwanee, GA) with 10 ml of medium at 37^{o}C. All three sets of leaflets were processed following the same protocol to maintain the uniformity for analysis. The different analyses that the leaflets were subjected to are detailed in the following sections.

4.3.2. Quantitative analysis

Collagen, GAG and elastin are the major components of aortic valve leaflet tissue. Changes in the mechanical environment of the leaflets alter fibroblast activity, specifically protein (collagen and elastin) and sGAG synthesis [Weston, 2001; Xing, 2004]. By measuring the leaflet collagen, sGAG, and elastin content, any significant differences in collagen, elastin and GAG due to changes in the mechanical environments can be identified.

The leaflets were dried over a period of 48 hours, and their dry weights were determined. Dry weight was used as a normalizing parameter to compare the data within

the leaflets from the three groups. The tissues were then digested with enzymes dissolved in buffer solutions for a period of 24-48 hours, and the dissolved tissue was used for analysis. Since the overall procedure for the assays is similar for all three endpoints the specific protocols are given in Appendix B.

4.3.2.1. Collagen assay

The collagen assay (Sircol collagen assay, Accurate Chem. & Scientific Corp., Westbury, NY) is a quantitative dye-binding method designed for the analysis of soluble collagen. The tissue was digested using pepsin, at a ratio of 1:3 of enzyme: tissue dry weight. The required amount of pepsin (Sigma, St.Louis, MO) was dissolved in 0.5 mL of 0.5 M acetic acid (Sigma, St.Louis, MO) and added to the tissue. The samples were then placed in a water bath at 60^{o}C for 24 hours with occasional stirring. The collagen was converted to a soluble form, as pepsin cleaved part of the C-terminal non-helical region of the α-chains that make up the triple helix of tropocollagen. The samples were then assayed for pepsin-soluble collagen content, which will henceforth be referred to as total collagen content. The assay kit measured mammalian collagen, types I to IV. Collagen standards were prepared using acid soluble collagen, type I, supplied in the kit. Test samples and standard solutions in 0.5 M acetic acid were mixed in a Sircol dye reagent containing Sirius Red in 1.5 ml micro centrifuge tubes. The dye was mixed with the collagen with a vortex tube mixer (VWR, Suwanee, GA). Sirius Red is an anionic dye with a sulphonic acid side chain group that reacts with the side chain groups of the basic amino acids present in collagen thus forming a complex. After collagen-dye complex formation, the tubes were centrifuged to separate the complex pellet from the unbound dye. The

supernatant from the tubes was then removed, leaving the pellet at the bottom. A cotton bud was used to remove any remaining supernatant fluid from the tube. An alkali reagent was then added to these tubes and stirred to reconstitute collagen bound dye. Although the alkali dye solution is stable when exposed to light, the absorbance must be measured within 3 hours of preparation. The samples were placed in a 96-well plate reader, and the absorbance data was recorded at a wavelength of 540 nm. The data was collected as a text file and transferred to an Excel spreadsheet. A standard curve was plotted using the data from the blank and standard samples. The slope of the curve was used as a conversion value to calculate the collagen content of the test samples based on the absorption values. A R^2 value of > 0.98 for the calibration equation was usually considered to give a good estimate, otherwise the assay was repeated.

4.3.2.2. sGAG assay

Sulfated glycosaminoglycans (sGAG) in the leaflet tissue were analyzed using Blyscan assay (Accurate Chem. & Scientific Corp., Westbury, NY) in a similar manner as collagen assay. sGAG assay measures the total sulfated glycan content present in a soluble form. The tissue was digested with protease (Sigma, St.Louis, MO), at a ratio of 1:30 of enzyme: tissue dry weight. Protease dissolved in 0.5ml of 0.1M tris-acetate buffer with 10mM calcium acetate was added to each sample and incubated in the same manner as the collagen samples. sGAG (sulfated glycoaminoglycan) standards were prepared using chondroitin 4-sulfate supplied in the kit. The acetate buffer was used a reagent solution. Sample preparation was done the same way as described in the above section. Blyscan dye reagent containing 1,9- dimethly-methylene blue in an inorganic buffer

containing surfactants and stabilizers was added to all the tubes. Sufficient time was allowed for the dye to bind sGAG while stirring the samples on a vortex tube mixer (VWR, Suwanee, GA). Reaction between the dye and sGAG was carried out in the presence of excess unbound dye and an acidic pH thus producing dye-GAG complex. Tubes with samples containing sGAG turned purple/pink, and the complex precipitated, thus enabling separation from the unbound dye by centrifugation. The pellet was separated from the supernatant solution and dissolved in Blyscan dissociation agent to reconstitute the complex into a soluble form for measurement. Since the solution was light-sensitive, the absorbance measurement was performed within 3 hours of preparation at a wavelength of 656 nm. The measurement and data analysis methodology were the same as that for the collagen.

4.3.2.3. Elastin assay

The Fastin elastin assay (Accurate Chem. & Scientific Corp., Westbury, NY) is also a quantitative dye-binding method for elastin analysis. However, the analysis method is slightly different from the collagen and sGAG assays. The dry samples of tissue were digested with proteinase kinase (Fisher Biotech, Suwanee, GA) at an enzyme concentration of 0.5 mg in 1 ml of buffer solution (5 ml of 50mM tris-HCl, 3.72 gm of 0.1 M EDTA, 1.168 gm of 0.2 M NaCl (Sigma, St.Louis, Mo) and 95 ml of dH_2O) in each tube. Test and standard samples were prepared in the same manner as for the previous assays using bovine a-elastin standard. 1 ml of elastin precipitating agent was added to each of these samples and incubated in ice cold water overnight. The next morning the samples were transferred to ice and incubated for about 30 minutes to bring

the sample temperature to 0^{o}C. The samples were then centrifuged to separate elastin as a gel, which was mixed with dye reagent along with 200µl of 90% saturated ammonium sulfate. The dye was then stirred for one hour to allow the dye to bind with the elastin. The Fastin dye reagent contains 5, 10, 15, 20- tetraphenyl-21, 23-porphrine in a water soluble form as the sulfonate (i.e tetra sulfonate) (TPPS). The dye binding to elastin followed a shape-and-fit phenomenon wherein the acidic dye was firmly retained by the basic amino acid side chain residues of elastin. After sufficient time was allowed for complex formation, the tubes were centrifuged and the pellet was separated from the supernatant. The pellet was then dissolved in the Biocolor dissociation agent and absorption values were measured at 513 nm. The analysis was done using the method described in the previous sections.

4.3.3. Qualitative analysis

Histological techniques were used to observe any changes in the morphology or cell phenotype of the cultured valve leaflets. Cell death and cell proliferation rates were also compared with the controls to see whether the *ex vivo* system induced any changes in the normal tissue behavior. Finally, both histology and scanning electron microscopic studies were done on the leaflet tissue to observe the endothelial cells in the three leaflet groups. This study was conducted to test the retention of ECs on the valve leaflets cultured under dynamic conditions. Since an intact endothelium is critical to maintain the normal functionality retention of the valvular cells.

Histology is the study of tissues using a variety of chromogenic techniques. Tissue pieces cut from the valve leaflets were fixed in 10% neutral buffered formalin for

24 hours to stabilize the proteins in the tissue and prevent further changes. Fixation inactivates the tissue and prevents activities such as decay, putrefaction and autolysis [Carson, 1990]. After fixation, the samples were placed in cassettes (VWR, Suwanee, GA) sandwiched between sponges (VWR, Suwanee, GA) to maintain the proper orientation during processing, and stored in 70% alcohol (Harleco, Gibbstown, NJ) until ready for processing. Processing includes dehydration, clearing and infiltration of the tissue, which was done in an automated processor, Path center (Thermo Electron Corp., Pittsburg, Pennsylvania). Dehydration of the tissue serves to remove all free water from the tissue. The dehydrant used was alcohol. The next step, clearing, serves to link the dehydration and infiltration steps. The clearing agent used was xylene (Harleco, Gibbstown, NJ) as it is miscible with both the dehydrating agent and the infiltration medium. The final processing step, infiltration, is achieved using an embedding medium, which holds the cells and intracellular structures in their initial state when thin sections are cut. Paraffin wax (Fisher Scientific, Houston, TX) with a melting point of 55-58^{o}C was used as the embedding medium. Excessive time in molten paraffin was limited to minimize tissue shrinkage and hardening. Once the tissue was processed, it was embedded in molds using the Embedder (Thermo Electron corp., Pittsburg, Pennsylvania). After the molds were cooled to solidify the wax, the blocks were removed from the molds and stored at room temperature until sectioning. The blocks were sectioned using a rotary microtome (Micron, Richard Allen Scientific, Kalamazoo, MI). The blocks were initially cooled using ice, and the cooled blocks were then fit into the chuck of the microtome, which moved up and down, sectioning the tissue to the desired thickness of 5μm. The sections obtained as a ribbon were placed in a water bath at 37^{o}C

to reduce compression in the paraffin section. The sections were then placed on a glass slide (VWR, Suwanee, GA) and dried overnight at 37^{o}C in an oven (VWR, Suwanee, GA). Prior to staining, sections were deparaffinized in a xylene substitute and rehydrated using decreasing grades of alcohol.

The histological study presented here consists of tinctorial and immunohistochemical stains. Hematoxylin and Eosin, which is a basic stain, is most widely used for its simplicity and ability to demonstrate different tissue structures. A more elaborate discussion of the stain will follow in the next section. Immunohistochemical stains were performed to observe the cell phenotype by identifying smooth muscle cells secreting α-smooth muscle actin, von Willebrand Factor secreted by endothelial cells, 5-Bromodeoxyuridine incorporated into proliferating cells, and apoptotic cells identified by activated caspase-3.

Immunohistochemistry is a technique used to identify cellular or tissue constituents (antigens) by means of antigen-antibody interactions [Bancroft, 2002]. The site of antibody binding can be identified either by direct labeling of the antibody, or by using a secondary labeling method. During fixation and processing of the tissue, it is possible for antigen epitopes to become masked by formalin cross linking. This cross linking can make the antibodies inaccessible to antigen sites; hence antigen retrieval is performed by employing proteolytic enzyme digestion. The enzymes used for these studies were protease and proteinase K. Digestion of the tissue sections in these enzymes allows antibody penetration by exposing the antigen sites. The sections were then blocked in 1% gelatin (JT Baker, Fairlawn, NJ) -phosphate buffered saline (PBS, Roche, Indianapolis, IN) or normal whole serum from the species in which the secondary

antibody was raised. This was done to prevent non-specific background staining, which may occur when the antibody attaches to highly charged collagen and connective tissue and is recognized when the secondary antibody is applied. After removal of the blocking agent, the primary antibody was applied, and the sections were incubated in a humid chamber to prevent evaporation of reagents. After removal of unbound antibody, the secondary antibody in the appropriate concentration along with normal serum from the same species as that of the secondary antibody were applied to the tissue sections. The secondary antibody recognizes the heavy polypeptide chain of the primary antibody and binds specifically to the antigen-antibody complex. The secondary antibody is biotinylated and is capable of binding to Avidin-Biotin-enzyme complex (ABC), which in turn links to the substrate. The sections were then washed to remove unbound secondary antibody and incubated with ABC. The free sites of avidin in ABC form a biotin-avidin linkage with the secondary antibody. Following incubation with ABC, the sections were washed and a substrate was applied. The enzyme affiliated with the ABC complex chemically modifies the substrate and in the process, the substrate's conformational state changes and develops an observable color.

Some of the stains in the current study were done using an immunofluorescent technique. This technique has the potential to define antigen-antibody interactions at the sub-cellular level and also within the histological topography of the tissue sections In this technique, avidin D- fluorochromes were used in conjunction with biotinylated secondary antibodies, which absorb radiation as visible or ultraviolet light causing the molecules to attain an excited state leading to electron redistribution and emission of radiation at a different wavelength within the visible spectrum. The fluorochromes used in this study

were avidin D –Texas red and avidin D- fluorescein. A brief discussion of the individual stains will be presented in the following sections, and the protocols are given in Appendix C.

4.3.3.1. Hematoxylin and Eosin stain

The hematoxylin and eosin stain has widespread applicability to tissues from different sites due to the simplicity of the stain. The stain can be performed progressively or regressively. The difference between the two methods is the use of acid alcohol, which serves as a differentiation agent in the staining procedure. For the current study, a regressive method was employed. This stain clearly demonstrates different tissue structures. Hematoxylin stains cell nuclei blue with good intra nuclear detail, while eosin stains all other tissue components in varying shades of pink and red. The dyes used in the stain are water or alcohol based. Hence the tissue sections were first deparaffinized by subjecting the slides to xylene (Harleco, Gibbstown, NJ), decreasing grades of reagent alcohol (Harleco, Gibbstown, NJ), and then a final wash in water before staining them with hematoxylin (Gill's hematoxylin, Harleco, Gibbstown, NJ). Excess hematoxylin was removed by subjecting the slides to acid alcohol and the blue hue of hematoxylin affected by this step was restored by Scott's solution ($NaHCO_3$ +$MgSO_4.7H_2O$+dH_2O). Excess Scott's solution was removed by washing followed by treatment with 95% alcohol to subject the slides to eosin. Eosin (Harleco, Gibbstown, NJ) is highly soluble in water; hence it is used along with 95% alcohol. The sections were finally dehydrated in ascending grades of alcohol and then cleared in xylene. The sections were then coverslipped (VWR, Suwanee, GA) using a solvent based mounting medium (Cytoseal

60, Richard allen scientific, Kalamazoo, MI). The entire stain was performed automatically using an autostainer (Leica, Vashaw Scientific, Norcross, GA) in the histology laboratory (Georgia Tech., Atlanta, GA). The slides were allowed to dry overnight before viewing. A Nikon imaging microscope (Southern Microscope Instruments, Inc., Marietta, GA) was used to view the slides, and a Q-Imaging camera, Retiga 1300C (Southern Microscope Instruments, Inc., Marietta, GA) was used to take the pictures.

4.3.3.2. Cell proliferation: anti- 5-Bromodeoxyuridine Immunohistochemistry

Labeling cells, which are active in the cell cycle, can assess the growth fraction of a tissue section. Cells in the synthesis phase will take up thymidine or analogs of thymidine such as 5-Bromodeoxyuridine (BrdU). Incorporated molecules can be identified by immunohistochemistry or flow cytometry using an anti-BrdU antibody. Counting the proportion of labeled cells will give an estimate of the synthesis phase fraction. Deparaffinized sections were pretreated with proteinase K and subjected to 4N HCl (Sigma, St.Louis, MO). The acid served to dissolve histones associated with DNA. This permitted uncoiling of the DNA and accessibility of reagents to all parts of the nuclei acids. The sections were then subjected to Tris buffered EDTA (Sigma, St.Louis, MO) which acts to neutralize the acid step previously performed. Blocking was performed once the pH was in the range of 7.0-7.5, which was determined using a pH indicator strip. The primary antibody, anti-BrdU (Dako, Carpinteria, CA) at a concentration of 1:20 in 1% crystalline grade bovine serum albumin (BSA, Sigma, St.Louis, MO) in PBS, was applied to the sections and incubated for an hour at room temperature. The sections were

then washed with PBS, and a working dilution (1:400) of secondary antibody, biotinylated horse anti-mouse IgG in 1%BSA/PBS along with 2% normal horse serum, was applied. The sections were then incubated with ABC reagent prepared from an alkaline phosphatase standard kit (Vector laboratories, Burlingame, CA). The slides were washed in PBS and 100mM tris (Sigma, St.Louis, MO), which served to raise the pH to the functioning range of the enzyme. The substrate made up with 5ml of tris at pH of 8.2, levamisole (Vector laboratories, Burlingame, CA) and reagents one, two, and three from an alkaline phosphatase substrate kit (Vector laboratories, Burlingame, CA) was immediately applied to the sections. Levamisole was used to inactivate endogenous alkaline phosphatase, which induces non-specific staining in the sections. After the application of the substrate solution, the slides were incubated in the dark for 20-30 minutes and were checked periodically under the microscope for color reaction. The substrate reaction was terminated by blotting off the solution and rinsing the sections in tap water. The sections were finally counterstained in an autostainer with hematoxylin. The counterstaining protocol employs hematoxylin, acid alcohol and Scott's solution steps before dehydrating the sections using graded alcohol and xylene. The sections were then cover slipped and allowed to dry overnight.

Proliferating cells were observed as red nuclei. The total number of positive cells was quantified using Image Pro software (Image pro plus software 4.0 from Media Cybernetics, Meyer Instruments, Houston, TX). Photographs of each section were taken at three different locations along the length of the section and total cell nuclei (> 500) in each photograph were determined by defining a threshold pixel size and color. The total cell nuclei were averaged over the images taken at different locations of the same tissue

section. Positive cells were counted manually by tagging the cells using the software. The percentage of positive cells was calculated for each group, and statistical analysis was performed to determine the difference between the groups.

4.3.3.3. Cell apoptosis: anti- Caspase 3 Immunohistochemistry

Apoptosis or programmed cell death is a crucial process in development, normal cellular differentiation, and tissue homeostasis in all multicellular organisms. Apoptosis can be triggered by a variety of cellular death stimuli including tumor necrosis factor. Among the many known effectors and regulators of apoptosis, the caspases play a crucial role in almost every cell type. There are about 13 different caspases, which can be grouped into 3 different subfamilies based on their substrate specificities. Caspase 3 (also called CPP32, Yama, apopain) is one of the key effectors of the apoptotic pathway. Caspase 3 is a cytosolic protein found in cells as an inactive 32kDa proenzyme. It is activated by proteolytic cleavage into 17-19 kDa and 12 kDa active subunits only when cells undergo apoptosis. These apoptotic cells can be identified by anti-caspase 3, active antibody, which can be detected by immunoblotting, indirect immunofluoroscence and immunohistochemistry. The staining method for activated anti- caspase 3 is similar to that of BrdU with a difference in two steps. The blocked sections were subjected to a working dilution of 1:400 of rabbit anti-human caspase 3 (Sigma, St.Louis, MO) in 1%BSA/PBS. Then a working dilution of 1: 400 of biotinylated goat anti- rabbit IgG antibody in 1% BSA/PBS and 2% normal goat serum was applied on them. These steps were followed by application of ABC and substrate solutions as done in BrdU staining. Then the slides were counterstained to see the cell nuclei and cover slipped. Apoptotic

cells were seen as red nuclei and the total number of apoptotic cells was quantified using the method described in the previous section.

4.3.3.4. Double immunofluoroscence: von Willebrand Factor and α-Smooth muscle actin Immunohistochemistry

Endothelial cells lining the surfaces of valvular leaflets secrete glycoproteins such as von Willebrand Factor (vWF). vWF is a 270 kDa multimeric plasma glycoprotein and is also present in platelets and megakaryocytes. It mediates platelet adhesion to injured vessel walls and serves as a carrier and stabilizer for coagulation factor VIII. vWF in valvular tissue sections can be determined by using anti-vWF which can be detected by immunofluoroscence.

Actin is a contractile protein present in muscle and some non- muscular tissue. Six major isoforms of actin have been described, some of which are restricted to muscle cells. Monoclonal antibodies are present with general muscle and smooth muscle specificity. These antibodies are used as sensitive markers for muscle cells differentiation. Actin in valvular leaflets was detected using an α- smooth muscle actin antibody. A double immunofluorescence procedure using two biotinylated antibodies and avidin D fluorochrome conjugates was used to detect cells expressing vWF and α-smooth muscle actin (α-SMA) on the same tissue section. This procedure was employed to reduce the time required for staining and it also gave a good signal to noise ratio. Deparaffinized slides were treated with 100ug/ml of protease and blocked using 1%gelatin/PBS mixture. The slides were incubated with primary antibody at a working dilution of 1:800 anti-vWF (Sigma, St.Louis, MO) in 1%BSA/PBS mixture followed by

secondary antibody at a working dilution of 1:400 goat anti-rabbit in 1%BSA/PBS along with 2% normal goat serum. After the secondary antibody was washed off, the sections were incubated in the dark with avidin D-Texas red (Vector laboratories, Burlingame, CA) at a concentration of 1:100 in 1%BSA/PBS. The sections were again blocked using 2% normal horse serum in 1% BSA/PBS with ~200μL of avidin D in the dark. Primary antibody of α-SMA (DAKO, Carpinteria, CA) was then applied at a working dilution of 1:800 in 1%BSA/PBS along with ~200μL of biotin to the sections and incubated in the dark. The slides were washed in PBS at which point the secondary antibody, horse anti-mouse IgG, was applied at a working dilution of 1:400 in 1%BSA/PBS along with 2% normal horse serum. Next, the second fluorochrome, avidin D-fluoroscein (Vector laboratories, Burlingame, CA) was applied to the sections at a dilution of 1:100 in 1%BSA/PBS. The sections were then counter-stained with 4',6-Diamidino-2-phenylindole (DAPI, Sigma, St.Louis, MO) at a working dilution of 0.25 μg/ml of PBS and cover slipped with Aquamount mounting media. The sections were then refrigerated at 4^{o}C until viewed under the microscope.

4.3.3.5. Scanning electron microscopy (SEM)

SEM was used to observe the valvular tissue surface for the presence of endothelial cells, since it produces high resolution images enabling examination of closely spaced features under high magnification. Tissue harvested from the valves was initially rinsed with 0.2M sodium cacodylate buffer (Electron microscopy sciences, Hatfield, PA) at pH =7.2 and fixed in 2.5% gluteraldehyde in cacodylate buffer (Electron microscopy sciences, Hatfield, PA). The tissue was dehydrated in varying grades of alcohol followed by

changes in varying grades of hexamethyldisilazane (HMDS) (Electron microscopy sciences, Hatfield, PA). The tissue was then dried overnight in 100% HMDS. The dry tissue samples were placed on aluminum stubs (SPI supplies, West Chester, PA) using conductive, double sided, carbon adhesive tape (SPI supplies, West Chester, PA). The samples themselves were made conductive by coating the samples with a thin layer of gold (about $100A^{o}$) in a sputter coater. The coated samples were then left in a desiccator until viewed under the SEM (Leo 1530 thermally assisted field emission gun SEM, MSE Dept., Georgia Tech., Atlanta, GA).

4.3.4. Statistical analysis

4.3.4.1. Paired t-test

Paired t-test is used for testing the difference between two means when the data are paired and the paired differences follow a normal distribution. This test was used to analyze the sterility data obtained in the study. A hypothesis test of the difference between population means when observations are paired was used.

For a paired t-test:

$H_0: h_1 = h_2$ versus $H_1: h_1 \neq h_2$ where h is the population mean

A confidence interval of 95% was used in the analysis, which was done using Minitab software (Minitab release 12, Minitab Inc. State Collage, PA). The data from each sample must be in separate numeric columns of equal length. Each row contains the paired measurements for an observation. If either measurement of a row is missing, Minitab automatically omits that row from the calculations. The difference between the samples at t = 0 and t = 96 hours was considered significant if p-value < 0.05.

4.3.4.2. Mann-Whitney non-parametric analysis

Mann-Whitney non-parametric analysis is used to analyze independent sample populations that are not normally distributed. This method was employed in the study since control and cultured valve leaflets were obtained from different animals and the data were not normally distributed. The Mann-Whitney test performs a hypothesis test of the equality of two population medians and calculates the corresponding point estimate and confidence intervals. In this analysis, the data from two populations that have the same distribution are assumed to be independent random samples. The hypotheses for the analysis are shown as,

$H_0: h_1 = h_2$ versus $H_1: h_1 \neq h_2$, where h is the population median.

A confidence interval of 95% was used in the analysis, which was done using Minitab. Two columns, which can be of same or different lengths, containing numeric data are needed from two populations. Minitab automatically omits missing data from the calculations when the sample size is different in the two columns, and ranks the two combined samples with the smallest observation given rank 1, the second smallest, rank 2, etc. If two or more observations are tied, the average rank is assigned to each. The test statistic is the sum of the ranks of the first sample and the point estimate of the population median, which is the median of all the pairwise differences between observations in the first sample and the second sample. The test statistic (U) can be represented as,

$$U_{calc} = n_1 n_2 + n_2(n_2+1)/2 - \sum_{i=1}^{n_1} R_i$$

where n_1 = size of larger sample

n_2 = size of smaller sample

R = ranks of smaller sample

U_{table} is obtained from table of critical values for U based on the sample size of each group.

If $U_{calc} > U_{table}$ at $\alpha = 0.05$, then reject H_0.

I.e., if U exceeds the critical value for U at significance level of 0.05, it means that there is evidence to reject the null hypothesis in favor of the alternative hypothesis. Mann-Whitney determines the attained significance level of the test using a normal approximation with a continuity correction factor. If there are ties in the data, Minitab adjusts the significance level.

The data collected from the assays and images of BrdU and activated caspase-3 were put in columns in the Minitab worksheet, and analysis was done with two columns at one time for all the leaflets (i.e right coronary, left coronary and non-coronary) in all the groups. The average and standard deviation values of the data were calculated and plotted in an Excel graph, and the differences between the data were considered significant if the p-value was less than 0.05.

CHAPTER 5

RESULTS

5.1. Physiological flow and pressure waveforms

Mechanical validation of the organ culture system was done with respect to maintaining normal physiological flow and pressure waveforms for a duration of over 48 hours. The system was tested with a Starr-Edwards ball and cage mechanical valve, a pericardial bioprosthetic valve and a native porcine aortic valve. All the experiments were conducted at a cardiac output of 3.8-4.5 L/min, a mean aortic pressure of 100 mmHg and at a frequency of 1.167 Hz (70 beats/min). The flow probe and pressure transducers were calibrated with water, which has the same viscosity as the culture medium, as described in the previous chapter. The flow and pressure waveforms with the mechanical, bioprosthetic and native valves are shown in Figures 5.1 to 5.4.

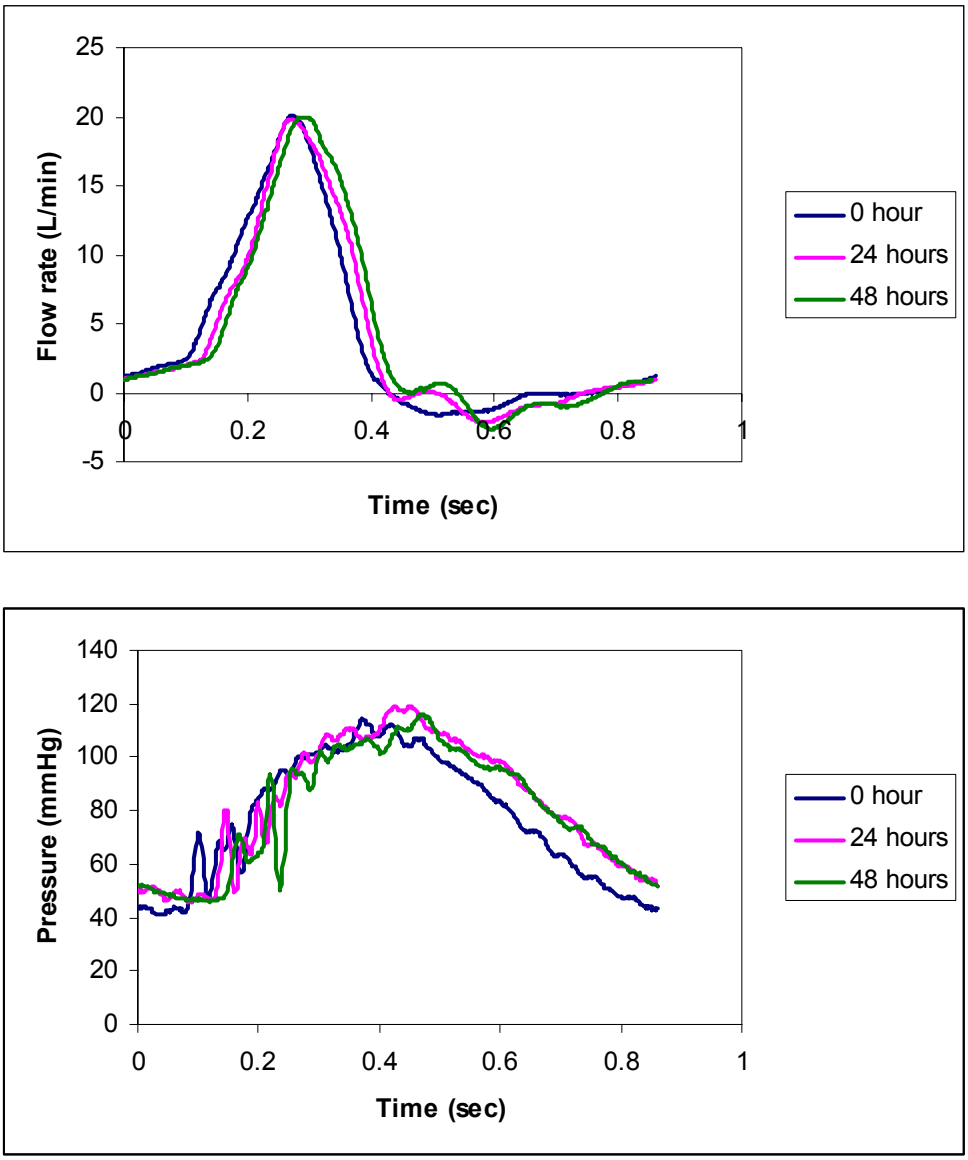

Figure 5.1: Flow and pressure waveforms of the Starr-Edwards ball and cage mechanical valve in the organ culture system with water as the circulating fluid. The curves are physiological and consistent over a period of 48 hours.

The flow and pressure waveforms seen above are comparable to normal physiological waveforms and are consistent throughout the experimental time period. The curves are smooth with minimum backflow in the flow waveform and very few oscillations in the pressure waveform. The mechanical performance of the system was

also tested with a pericardial bioprosthetic valve for a period of 48 hours. The mechanical waveforms are shown in Figure 5.2.

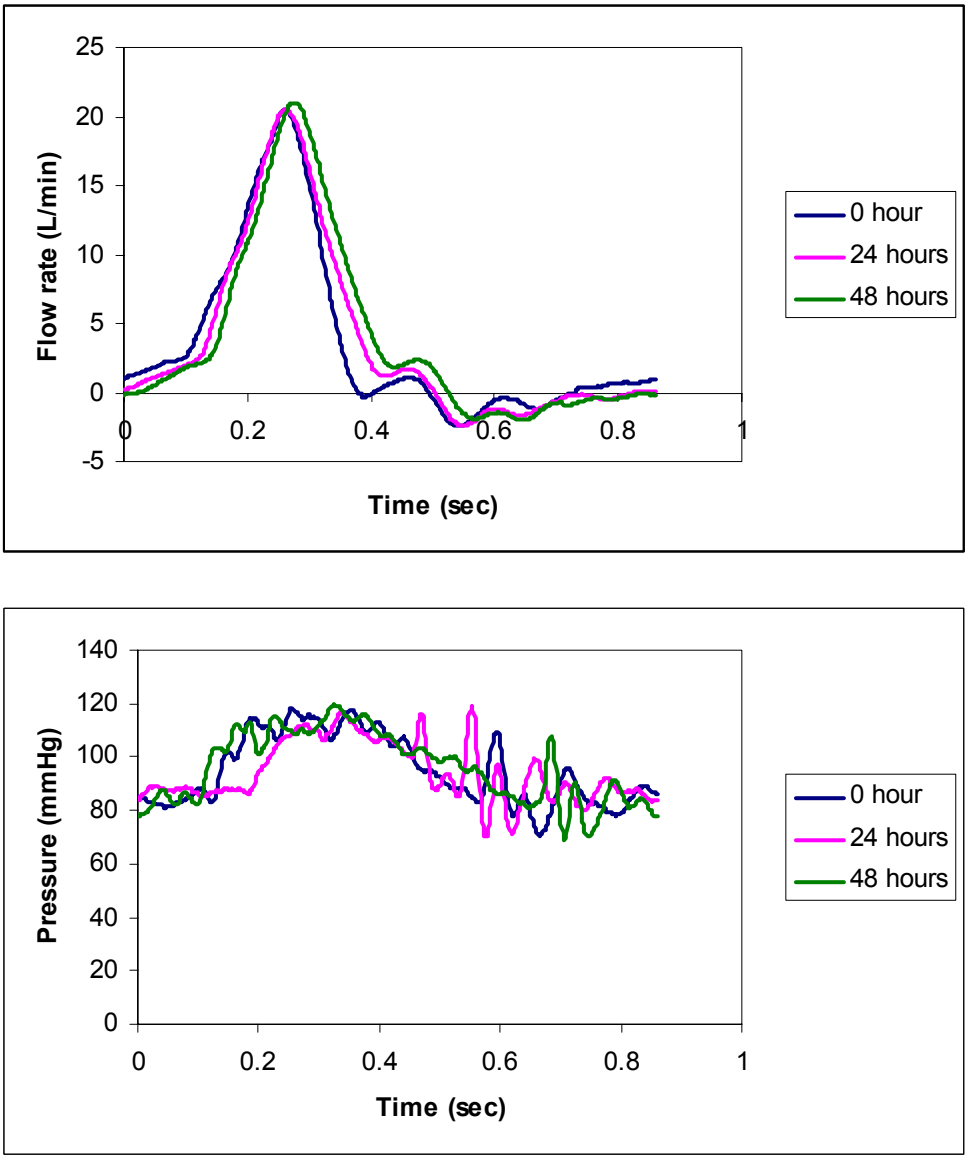

Figure 5.2: Flow and pressure waveforms of the pericardial bioprosthetic valve in the organ culture system with water as the circulating fluid. The curves are physiological and consistent over a period of 48 hours.

The waveforms shown above are consistent and closely approximate to normal physiological curves throughout the duration of the experiment. The flow curves show backflow of fluid during diastolic phase due to improper leaflet coaptation present in the bioprosthetic valve, which was not system induced. The pressure waveforms have 120/80 mmHg systolic/diastolic phase pressures, which are in the range of normal blood pressure.

The next step in the mechanical validation procedure was to test the sterility of the system for a duration of 96 hours. This was achieved by circulating sterile DMEM in the system with the mechanical valve placed in the aortic valve holder. The mechanical conditions of the system were monitored and recorded using DAQ-ANAL and the waveforms are shown in Figure 5.3.

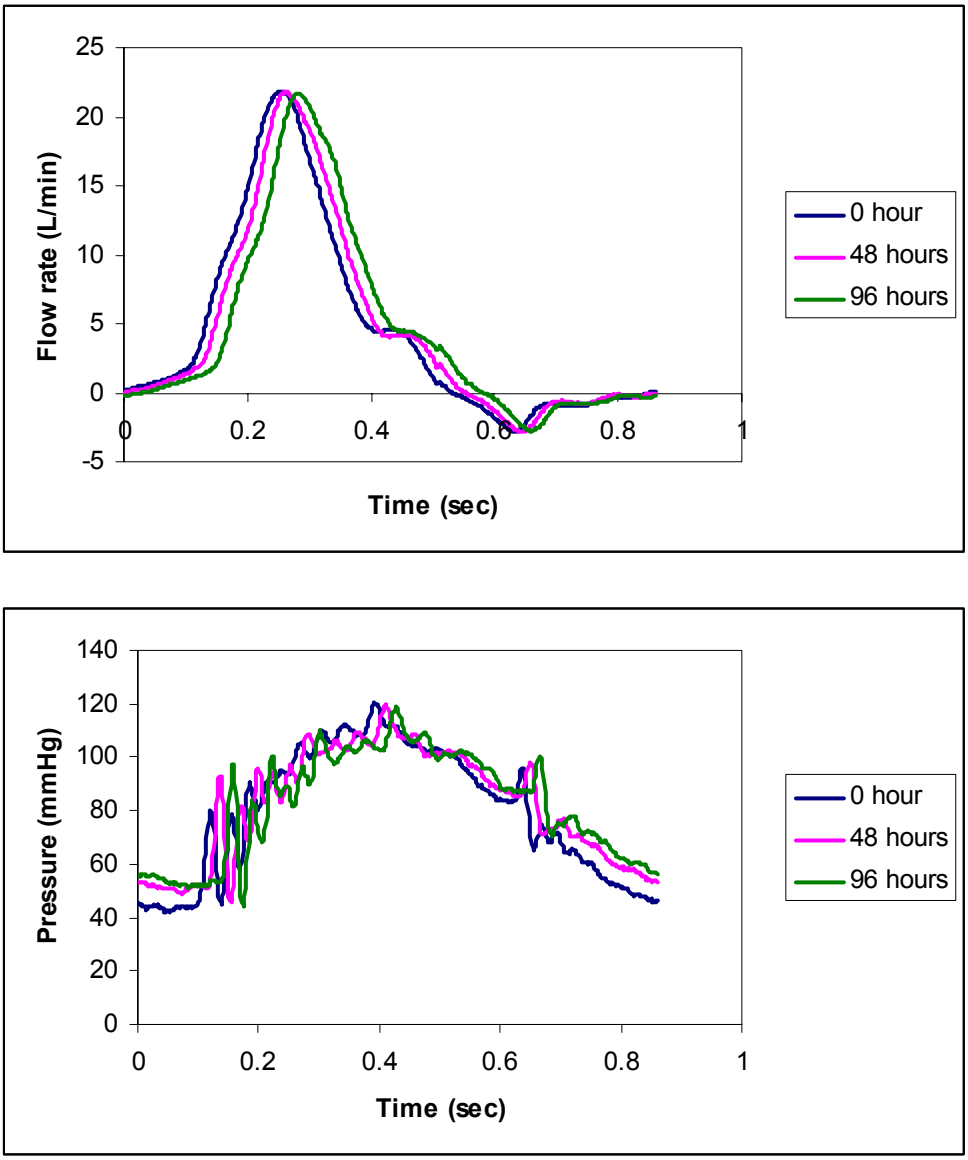

Figure 5.3: Flow and pressure waveforms of a Starr-Edwards ball and cage mechanical valve in the sterile organ culture system and DMEM as the circulating fluid. The curves are physiological and consistent over a period of 96 hours.

From the above figure it can be seen that the system was capable of maintaining consistent mechanical conditions over a period of 96 hours. The sterility data for the system will be shown in section 5.2.

Once the system was mechanically validated, it was tested biologically using native porcine aortic valves. The aortic flow and pressure curves with native valve are shown in Figure 5.4. The coronary arteries of the valve were ligated before the valve was placed in the holder to prevent backflow of the medium from the sinuses of the valve. However, minimal backflow of medium along inside of the walls of the holder caused the negative flow rates noticed in the flow curve. Also, some pressure oscillations were evident between 100-190 msec during the beginning of the systolic phase due to turbulence created in the system by the outward movement of the piston to pump the medium through the valve.

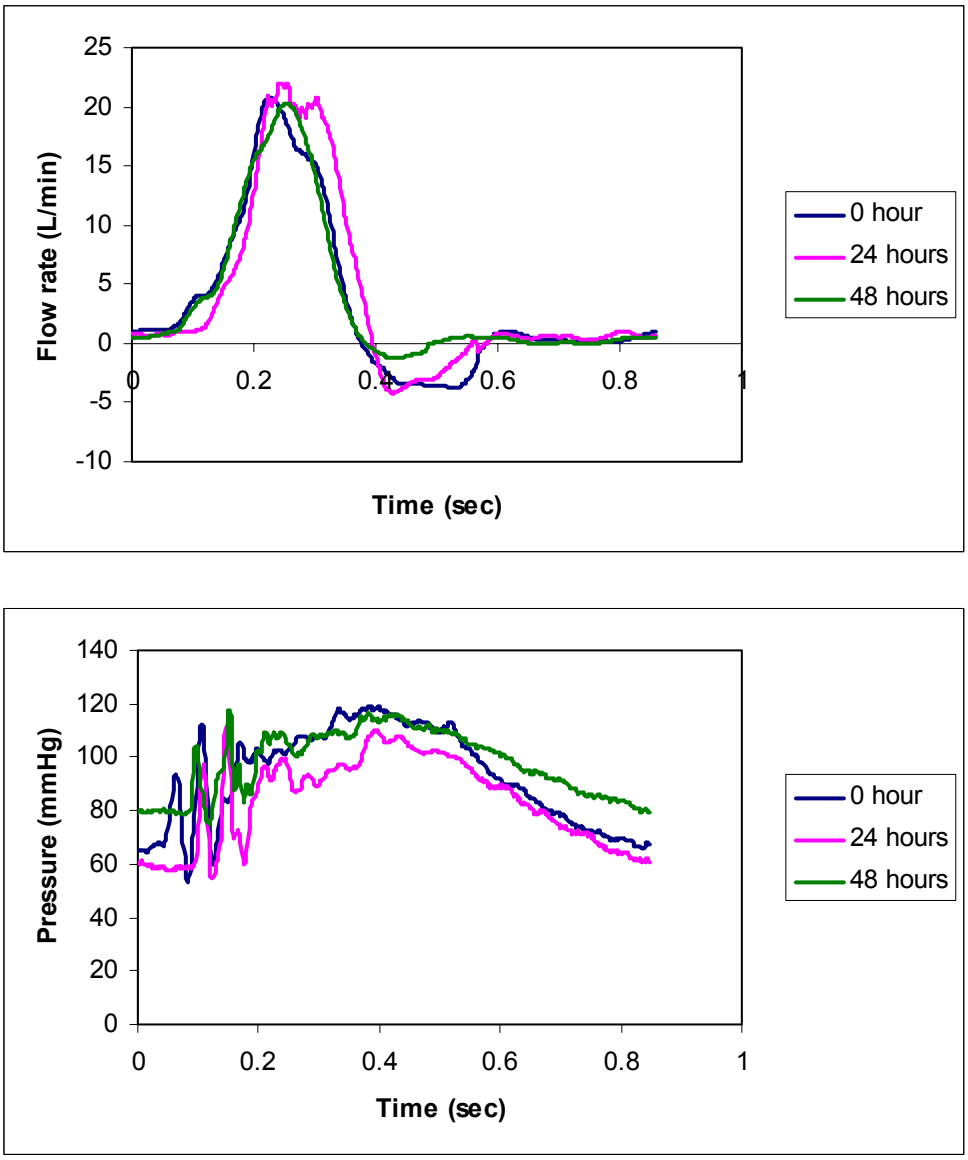

Figure 5.4: Flow and pressure waveforms for a native porcine aortic valve in the sterile organ culture system and DMEM as the circulating fluid. The curves are physiological and consistent over a period of 48 hours.

From the above waveforms with mechanical, bioprosthetic and native aortic valves it can be inferred that the system is capable of maintaining normal physiological mechanical conditions for up to 96 hours of operation without any sudden fluctuations in

the values. Thus, it can be said that the developed organ culture system has been mechanically validated.

5.2. Sterility measurements

A sterility test was performed with a Starr-Edwards mechanical valve for a period of 96 hours as indicated in section 5.1. The medium was tested for contamination by microscopic examination and also by measuring the absorbance of the medium before and after the experiment, as described in the methods chapter.

Medium samples were taken at time t = 0 hour and t = 96 hours to test for evidence of microbial contamination in the system. Intermittent sampling was not prudent as this compromised the sterility of the system. Contaminated medium was characterized by increased turbidity, a color change from dark red to orange-yellow, and an unpleasant odor depending on the level of contamination. After 96 hours, gross examination of the medium showed a clear liquid without any color change or turbidity. Additionally, the medium absorbance was measured and samples underwent microscopic examination. Absorbance values of the medium samples are shown graphically in Figure 5.5.

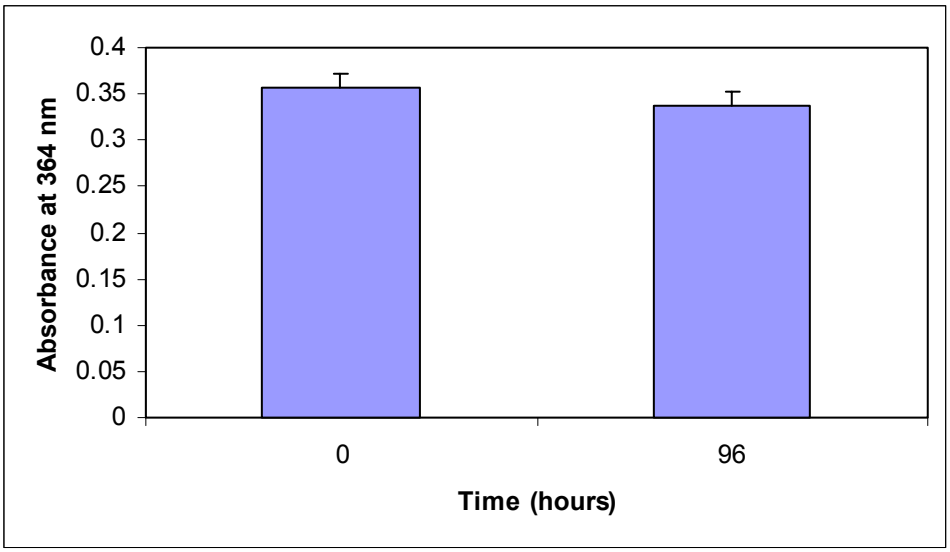

Figure 5.5: Absorption values of the medium samples at t = 0 hour and t = 96 hours at a wavelength of 364 nm. The data are expressed as the average value + one standard deviation. No significant difference was observed between the two samples.

The results show that there was no significant difference between the samples at t = 0 hour and t = 96 hours with $p > 0.05$ (p-value = 0.1). Microscopic examination of the medium showed a clear medium through out the section with no microbes. This suggests that the organ culture system was able to maintain sterility for a duration of 96 hours and can hence be used for long term valvular culture studies.

5.3. Gas exchange in the organ culture system

Preliminary experiments with aortic valves cultured in the organ culture system showed cell death due to adverse environmental conditions in the system. Hence changes in the pH and oxygen transfer were characterized to address these concerns. The pH of the medium was recorded at the end of every trial. Results from three experiments showed that the pH was 7.36 ± 0.11. This value is within the physiological range of 7.2-7.4. To

ensure sufficient oxygen transfer, gas permeable silicon tube was used as a gas exchanger in the system. Silicon tube with a 0.16" inner diameter was wound in a coil supported in place by three hollow polyvinyl chloride rings. The tubing was connected between the two ports of a lid assembly at the side arm of the compliance tank. To determine the oxygen required by the system, four porcine aortic valves were used to calculate the uptake rate as described in section 4.2.3. The oxygen uptake rate (OUR) was measured by noting the dissolved oxygen (DO_2) content over a period of 48 hours (Figure 5.6) and fitting a second order rate equation to the data (Figure 5.7).

Figure 5.6 shows that the oxygen content of the media follows a rectangular hyperbolic trend, as seen with nutrient uptake studies in cell culture. The amount of DO_2 reduces to half its value within the first 4 hours suggesting that most of the oxygen is taken up by the valve during that time period, after which time the uptake rate is drastically reduced and decreases to about 0.0232 mg of O_2/gm of tissue/L of medium at the end of 48 hours. The graph below indicates that oxygen limitation may occur in the system within 4-6 hours.

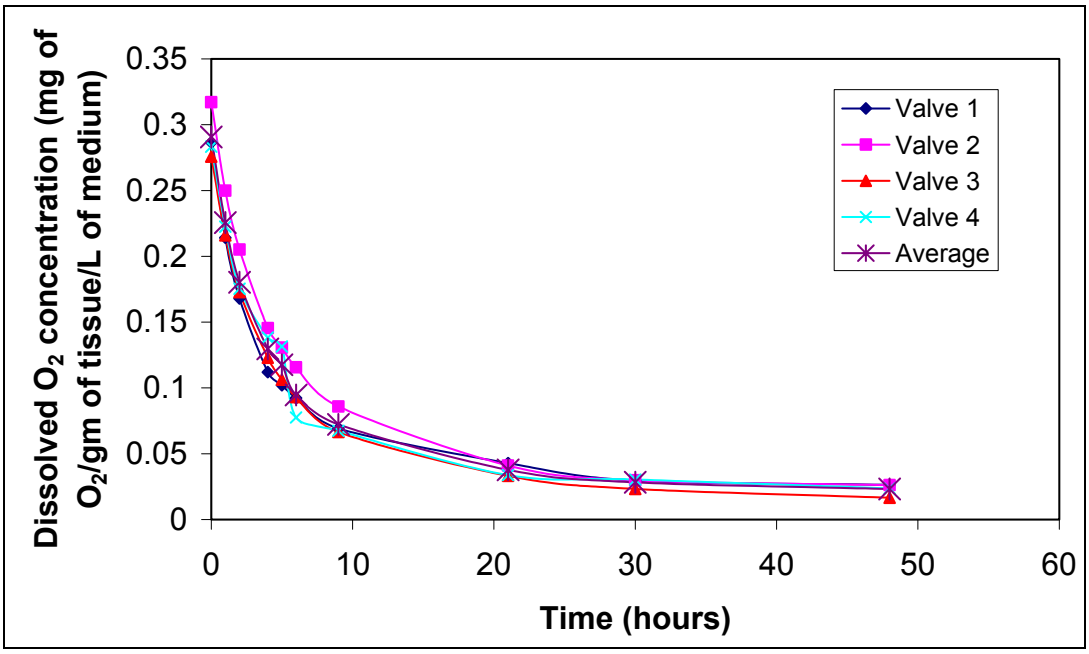

Figure 5.6: Dissolved oxygen content in the medium (400mL) with porcine aortic valves. Oxygen content decreases to half its value in the first four hours and then decreases slowly until it levels off around 48 hours.

The wet weight of the aortic valve was determined to normalize the OUR of the valve, which was 29.23 ± 1.64 gm. The OUR of the aortic valve was found by finding the slope by plotting a curve of DO_2 Vs time for the first 6 hours. It can be seen from Figure 5.6 that DO_2 concentration decreases to 50% of its value in the first 6 hours, hence this time span was chosen for calculating the OUR. The assumption involved in this calculation is that, oxygen becomes limiting in the medium before the nutrients, hence the reaction follows zero order kinetics. The OUR of the valve was found to be 0.0305 mg of O_2/gm of tissue/L of media/hour (or) 8.472 $\times 10^{-6}$ mg of O_2/gm of tissue/L of media/sec (or) 9.9023 $\times 10^{-5}$ mg/sec. This value was comparable to the value of 3.05 $\times 10^{-5} \pm 1.37 \times 10^{-5}$ ml of O_2/ml of tissue/sec found in the literature [Wend, 2001].

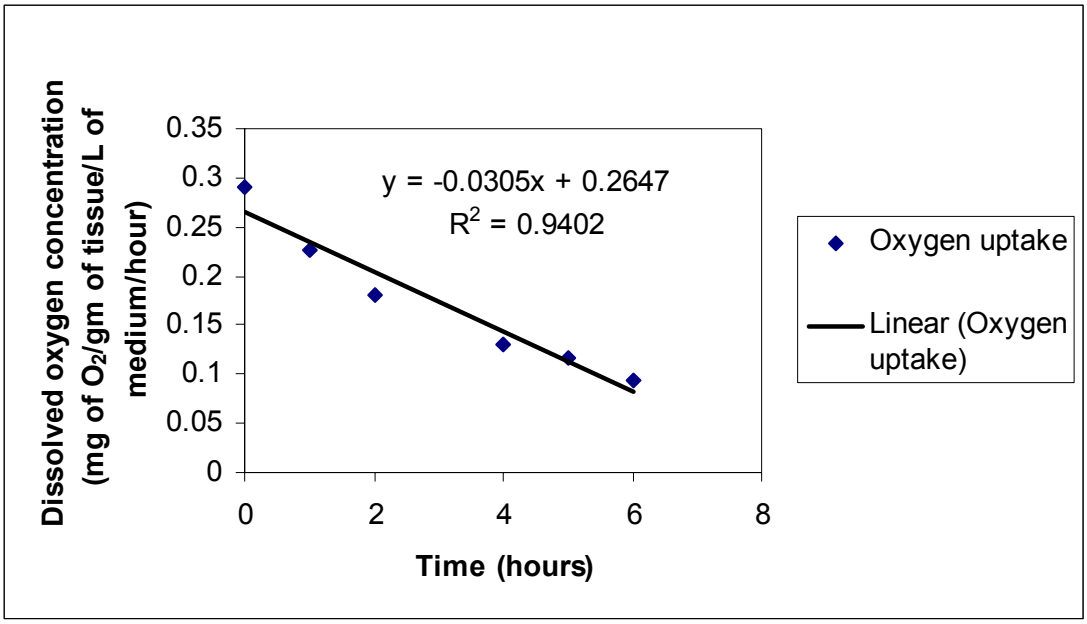

Figure 5.7: OUR plot of the DO_2 concentration data. Slope of the graph yields oxygen uptake rate of the aortic valve, which was 3.1×10^{-3} mg/sec for a 29 gm aortic valve.

After establishing the OUR of the aortic valve, the required oxygen transfer rate in the system was calculated. The length of the tubing and gas flow rate calculated using equations 4.2 and 4.3 were found to be 2 m and 0.2 L/min, respectively. These calculations were validated by measuring gas transfer into the system. The DO_2 of the degassed medium was measured every hour until saturation (Figure 5.8), and the transfer rate was calculated using equation 4.4. It can be observed from the graph that the DO_2 value reached 95% of the saturated value in the first hour after which the increase was slow until saturation was attained.

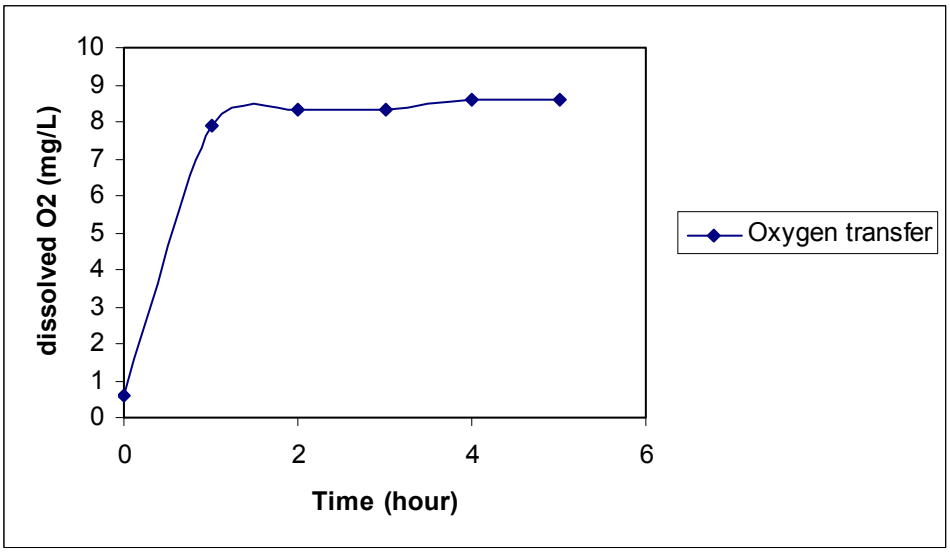

Figure 5.8: Oxygen exchanged into the organ culture system over a period of 5 hours. Saturation was attained within 3 hours as measured by dissolved oxygen content in the medium.

The mass-transfer coefficient was calculated from the slope obtained by plotting the logarithm of % O_2 saturation versus time (Figure 5.9). A steep increase in oxygen content in the medium during the first hour of gas-exchange (Figure 5.8) caused a significant shift in the linear fit leading to a low R^2 value seen in the graph (Figure 5.9). However, a linear fit to the data was best fit when compared to a quadratic fit.

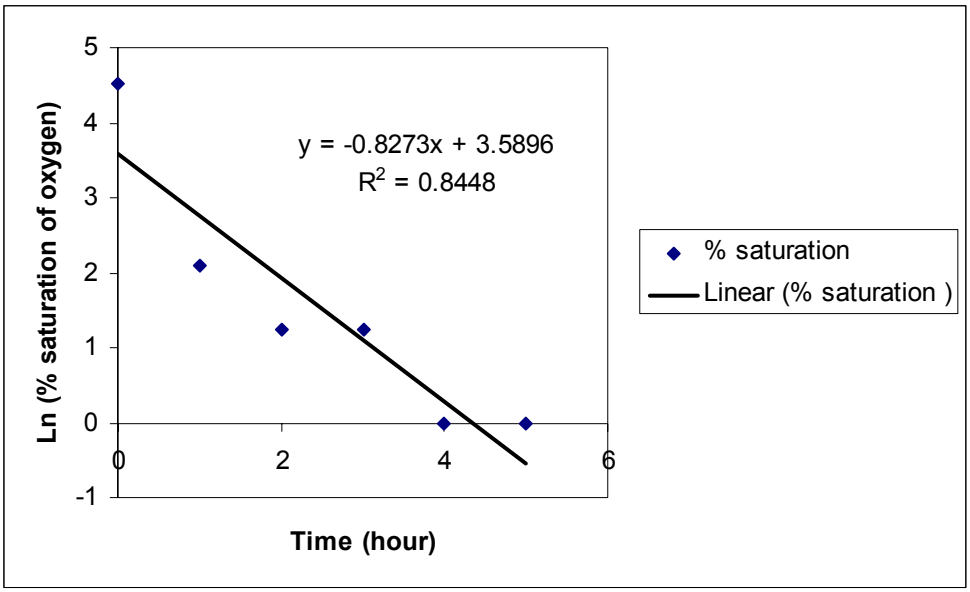

Figure 5.9: Percentage saturation of oxygen transferred into the system. The slope obtained from the graph was 0.8273 hour^{-1}.

The value of the slope obtained from Figure 5.9 was 0.8273 hour $^{-1}$. Using equation 4.6, the transfer coefficient was found to be 49.54 mm/hr, or 0.0013761 cm/sec. From equation 4.4 a gas transfer rate of 4.74 $\times 10^{-3}$ mg/sec was calculated. Since the gas transfer rate is greater than the OUR, the theoretical calculations are valid. Hence, a 5% CO_2 gas flow rate of 0.2 L/min circulating through a 0.16" diameter by 2 m length silicon tube provided the required oxygen to maintain valve viability in the organ culture system.

5.4. Extracellular matrix components

Measurement of total amount of extracellular matrix components in the cultured valve leaflets and comparison with control (fresh and statically incubated) leaflets shows the ability of the system to retain the native synthetic activity of the cultured leaflets. A total of 10 experiments were conducted with valves cultured in the organ culture system, and

of these, 9 data sets have been analyzed here. Data from one valve was not analyzed since visual observation of the valve in the holder revealed the presence of excess sinus tissue, which formed folds inside the valve holder and prevented proper opening and closing of the leaflets. Cardiac output and aortic pressure conditions monitored during the nine experiments are summarized in Table 5.1.

Table 5.1: Cardiac output and aortic pressure values measured downstream of the aortic valve cultured in the organ culture system at a cardiac rate of 70 beats/min.

Expt #	Cardiac output (L/min)	Mean Aortic pressure (Systolic/Diastolic) mmHg	
1	4.09	90	120/60
3	3.85	90	120/60
4	3.84	95	120/70
5	4.72	95	120/70
6	3.99	100	120/80
7	3.82	95	120/70
8	4.26	90	120/60
9	4.28	100	120/80
10	4.50	100	120/80

The mean values for flow rate and aortic pressure were in the range of 3.8-4.5 L/min and 90-100 mmHg suggesting that normal mechanical conditions have been maintained for all the valves cultured in the organ culture system.

5.4.1. Collagen content

The total collagen content in the leaflets was measured using the Sircol collagen assay kit as described in section 4.3.2.1. The results from this test are shown in Figure 5.10. The

data for individual valves are given in Table 5.2, and the p-values for the data are given in Table 5.3.

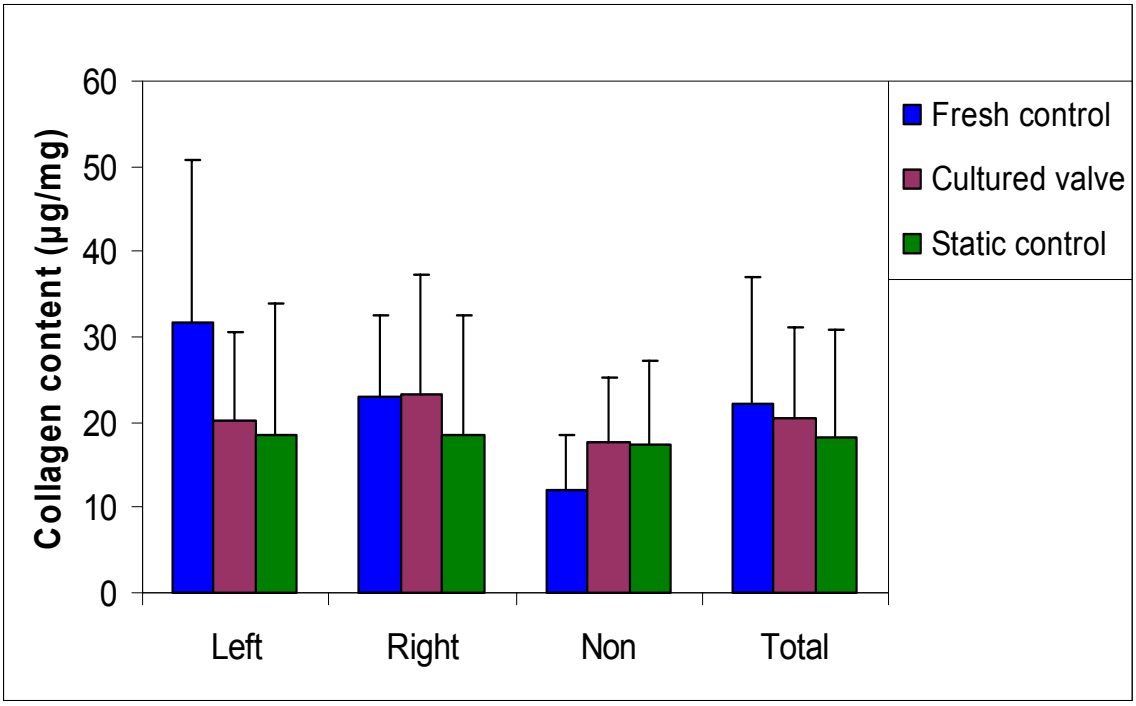

Figure 5.10: Collagen contents in left, right, non-coronary and mean content in all the three leaflets of the valve. The data are represented as average value + one standard deviation. No significant difference was observed between the three groups of the leaflets $p>0.05$ for $n = 9$.

Table 5.2: Collagen data from left, right and non coronary leaflets of fresh (F), cultured (C) and static (S) control valves used in the study. The data are expressed as μg of collagen present in mg of dry leaflet tissue.

Expt. No.	Left coronary leaflet			Right coronary leaflet			Non coronary leaflet		
	F	C	S	F	C	S	F	C	S
1	42.15	14.64	55.32	19.37	47.67	24.71	3.67	25.34	31.21
3	24.80	6.84	6.02	20.89	12.13	12.96	14.62	25.68	6.99
4	75.62	18.80	7.56	20.54	21.64	3.58	7.11	17.88	24.04
5	14.76	17.95	6.89	14.64	38.04	26.63	6.83	19.69	4.31
6	16.60	16.08	12.28	30.72	14.27	11.71	24.78	8.27	12.80
7	39.76	30.70	17.20	22.88	8.24	47.06	13.99	7.27	13.10
8	20.18	8.31	28.65	6.08	11.28	6.84	8.52	27.78	10.58
9	18.65	35.01	18.66	33.12	19.95	26.68	16.19	14.97	27.01
10	31.95	33.49	13.71	37.83	36.16	5.32	13.11	13.27	26.52
Avg.	31.60	20.20	18.48	22.90	23.26	18.39	12.09	17.79	17.40
Std. Dev.	19.26	10.50	15.54	9.76	14.00	14.13	6.37	7.52	9.85

Table 5.3: p-values for the collagen data comparisons between all three groups of the leaflets obtained using Mann-Whitney non-parametric statistical analysis at 95% confidence interval.

Leaflet	Fresh Vs Cultured	Fresh Vs Static	Cultured Vs Static
Left	0.1333	0.0521	0.3772
Right	0.8598	0.3772	0.4268
Non	0.0774	0.4268	0.7911
Total	0.5918	0.1772	0.3157

Results for each leaflet (left, right and non-coronary leaflets) from each group (fresh, cultured and static control) and mean collagen content for all the leaflets (total) were averaged for each group. Standard deviations for the results were calculated for all the leaflets in each group, and the data was expressed in the graph as average value + one standard deviation. From the figure and Table 5.3 it can be inferred that there is no significant difference in collagen content between the fresh, cultured and static control leaflets ($p>0.05$). This shows that the organ culture system is able to maintain collagen synthesis at native levels. Collagen content in the static control leaflet, although reduced compared to the fresh and cultured leaflets, was not statistically different from the two groups at $\alpha=0.05$. However if $\alpha=0.1$, then from the p-value of Table 5.3 a significant decrease ($p=0.0521$) in left coronary static leaflets compared to fresh leaflets can be observed. This result was different from that seen in previous studies on porcine aortic valve leaflets [Weston, 2001], where collagen synthesis during static incubation increased

significantly compared to fresh leaflets. This may be due to differences in analysis procedures. Measuring collagen synthesis is more sensitive than measuring collagen content in the leaflet as the latter test measures newly synthesized collagen, soluble by pepsin. Also, the leaflets differ biologically between the groups since they are from different animals although the statistical analysis method takes into account the differences between the populations. The large standard deviations seen with data are also due to the variability in collagen content seen between the individual data sets shown in Table 5.2.

5.4.2. sGAG content

Sulfated glycosaminoglycan (sGAG) content in the leaflet was measured using the Blysclan sGAG kit as described in section 4.3.2.2. The results shown in Figure 5.11 are expressed as the average value + one standard deviation for all the groups. The individual data sets for each valve involved in the study are given in Table 5.4 and the p-values obtained from comparing data sets between the three groups are given in Table 5.5.

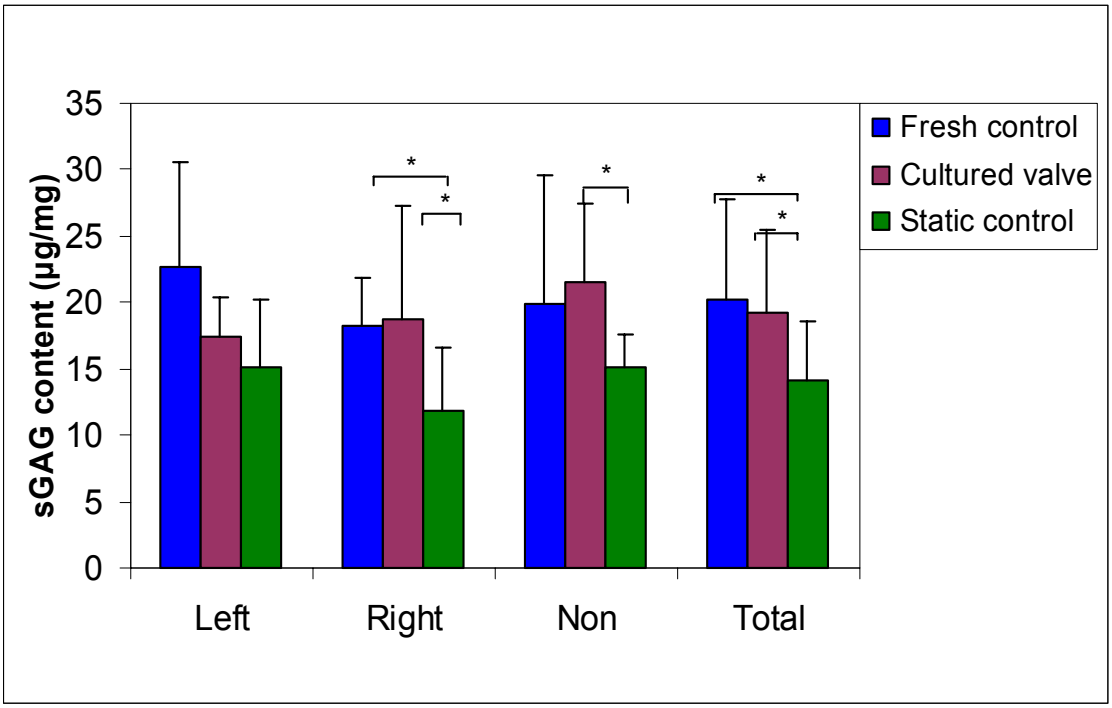

Figure 5.11: sGAG content in left, right, non-coronary and mean content in all the three leaflets of the valve. The data are represented as average value + one standard deviation. No significant difference was observed between the cultured and fresh control leaflets ($p>0.05$). Static control leaflets have significantly reduced sGAG content compared to both fresh and cultured leaflets ($p<0.05$ for $n = 9$).

Table 5.4: sGAG data from left, right and non coronary leaflets of fresh (F), cultured (C) and static (S) control valves used in the study. The data are expressed as μg of sGAG present in mg of dry leaflet tissue.

Expt. No.	Left coronary leaflet			Right coronary leaflet			Non coronary leaflet		
	F	C	S	F	C	S	F	C	S
1	16.31	18.22	11.15	18.40	15.18	4.02	12.96	17.08	17.05
3	27.05	12.23	14.17	23.30	10.23	8.48	32.59	12.07	15.26
4	37.16	17.40	17.59	18.10	15.71	8.06	33.89	21.77	11.35
5	21.00	21.99	14.74	22.56	20.92	10.96	30.14	22.83	14.08
6	13.96	19.81	10.49	13.37	18.05	15.04	11.06	15.45	15.32
7	25.51	14.10	7.88	18.31	12.15	14.75	18.54	22.77	11.61
8	30.72	15.94	24.79	20.49	20.32	19.29	9.31	27.27	18.69
9	15.72	18.08	18.94	16.12	17.03	9.55	17.39	31.52	16.33
10	16.69	18.77	16.78	13.09	39.36	16.36	13.76	22.42	16.95
Avg.	22.68	17.40	15.17	18.19	18.77	11.84	19.96	21.46	15.18
Std. Dev.	7.95	2.95	5.09	3.61	8.47	4.84	9.65	5.95	2.47

Table 5.5: p-values for the sGAG data comparisons between all three groups of the leaflets obtained using Mann-Whitney non-parametric statistical analysis at 95% confidence interval.

Leaflet	Fresh Vs Cultured	Fresh Vs Static	Cultured Vs Static
Left	0.2893	0.0637	0.2510
Right	0.4799	0.0171	0.0273
Non	0.5962	0.5962	0.0134
Total	0.7293	0.0028	0.0008

The results suggest that sGAG content in the cultured leaflets is not significantly different ($p>0.05$) from that in fresh valve leaflets. However, static controls show significantly less sGAG content compared to both fresh controls and cultured leaflets ($p<0.05$). The left coronary leaflets do not show a significant difference ($p>0.05$) between the three groups at $\alpha=0.05$, while the right and non coronary leaflets in the static controls have 35%, 37% and 24%, 29.3% less sGAG content compared to fresh control and cultured leaflets, respectively. A reduction of 30.65% and 26.8% in total sGAG content averaged over all the three leaflets of the valve was found in the static control leaflets compared to fresh control and cultured leaflets. When $\alpha=0.1$, the sGAG content is found to be significantly reduced in left coronary static leaflet when compared to fresh leaflet. This shows that mechanical forces are required for normal synthesis of GAG in the leaflets.

5.4.3. Elastin content

Elastin content results obtained using the Fastin elastin kit as described in section 4.3.2.3., are shown in Figure 5.12. Individual data sets for all the groups of the leaflets are given in Table 5.6, and the p-values for elastin data comparisons between the groups are given in Table 5.7.

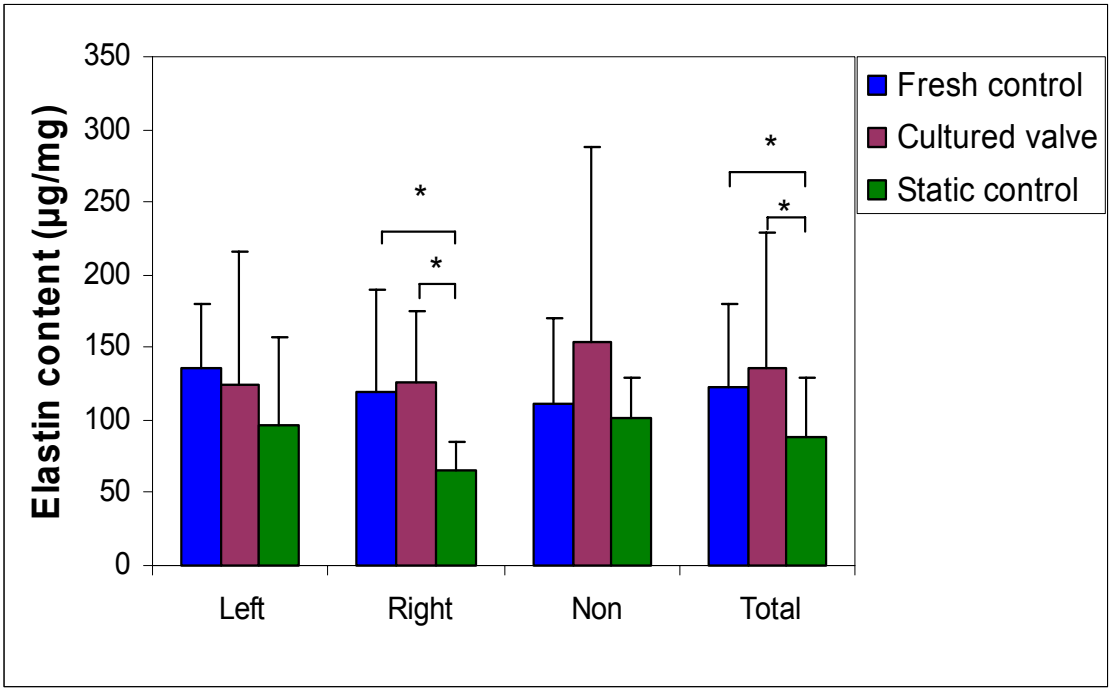

Figure 5.12: Elastin content in the left, right, non-coronary leaflets and mean content in all three leaflets of the valve. The data are represented as average value + one standard deviation. No significant difference was observed between the cultured and fresh control leaflets ($p>0.05$). Static control leaflets have significantly reduced elastin content compared to both fresh and cultured leaflets ($p<0.05$ for $n = 9$).

Table 5.6: Elastin data from left, right and non coronary leaflets of fresh (F), cultured (C) and static (S) control valves used in the study. The data are expressed as μg of elastin present in mg of dry leaflet tissue.

Expt. No.	Left coronary leaflet			Right coronary leaflet			Non coronary leaflet		
	F	C	S	F	C	S	F	C	S
1	108.86	336.79	115.6	85.57	232.6	107.2	88.72	137.3	92.72
3	77.57	116.09	70.45	147.65	91.13	47.67	83.71	133.4	105.4
4	118.86	70.82	172.3	152.49	117.5	56.65	67.58	115.8	39.98
5	160.93	109.43	52.35	69.38	166.5	50.43	132.6	503.2	79.19
6	173.84	53.11	47.19	278.40	98.90	65.15	211.7	77.44	104.4
7	144.54	59.79	54.09	131.04	75.29	74.11	64.79	127.7	107.2
8	216.82	92.34	216.7	92.45	138.6	65.12	202.2	123.4	139.6
9	134.65	201.94	57.72	64.50	90.81	46.64	87.34	82.24	113.3
10	88.08	84.30	81.00	52.90	117.3	79.37	59.32	90.06	123.6
Avg.	136.02	124.96	96.38	119.38	125.4	65.82	110.9	154.5	100.6
Std. Dev.	43.88	90.95	60.38	69.93	48.83	19.31	58.53	132.7	28.40

Table 5.7: p-values for the elastin data comparisons between all three groups of the leaflets obtained using Mann-Whitney non-parametric statistical analysis at 95% confidence interval.

Leaflet	Fresh Vs Cultured	Fresh Vs Static	Cultured Vs Static
Left	0.2164	0.0637	0.2893
Right	0.5365	0.0341	0.0020
Non	0.2893	0.6588	0.3314
Total	0.8627	0.0110	0.0043

It can be seen from the figure that the elastin content in the cultured and fresh control leaflets is not significantly different in total valve and in different leaflets ($p>0.05$). However, the static control leaflets do show a significant decrease in elastin content in the right coronary leaflet and in average elastin content for all three leaflets of the valve ($p<0.05$). Elastin content in the static control for the left and non coronary leaflets was not significantly different from that in the fresh and cultured leaflets. ($p>0.05$). However, for the right coronary leaflet, a significant reduction in elastin content of 44.87% and 47.52% was observed compared to fresh controls and cultured leaflets, respectively. A reduction of 28.25% and 35.1% for the static control versus the fresh control and cultured leaflets, respectively, was observed in total elastin content averaged over all three leaflets of the valve. At $\alpha=0.1$ significant reduction can be seen in the left leaflet of the static control compared to fresh leaflet, which suggests that static incubation of the leaflet alters the structural protein synthesis in the leaflets.

In conclusion, the total amount of ECM components of the cultured valve leaflets was maintained at native levels in the organ culture system, which suggests that the natural architecture of the leaflet is retained. Static controls showed reduced sGAG and elastin contents compared to fresh and cultured leaflets, which suggests that a dynamic environment is required by the leaflets in order to maintain the native synthetic activity of the valvular cells.

5.5. Qualitative studies of the leaflet

5.5.1. Hematoxylin and Eosin stain

Structural integrity of the leaflet was assessed by examining the morphology of the leaflets after staining with Hematoxylin and Eosin (H&E). As described in section 4.3.3.1, the stain was used to observe any remodeling in the tissue structures. Pictures of representative H&E stains for fresh, cultured and static control leaflets are shown in Figure 5.13, taken at 20X magnification. Cell nuclei in the tissue are stained blue and the cytoplasm is pink. Tissue structures such as collagen crimp in the fibrosa (F), and elastic fibers in the ventricularis (V) region have a dark pink color and hence are differentiated from the ECM. Spongiosa (S) has a loose tissue structure, which is characterized by light pink in the pictures.

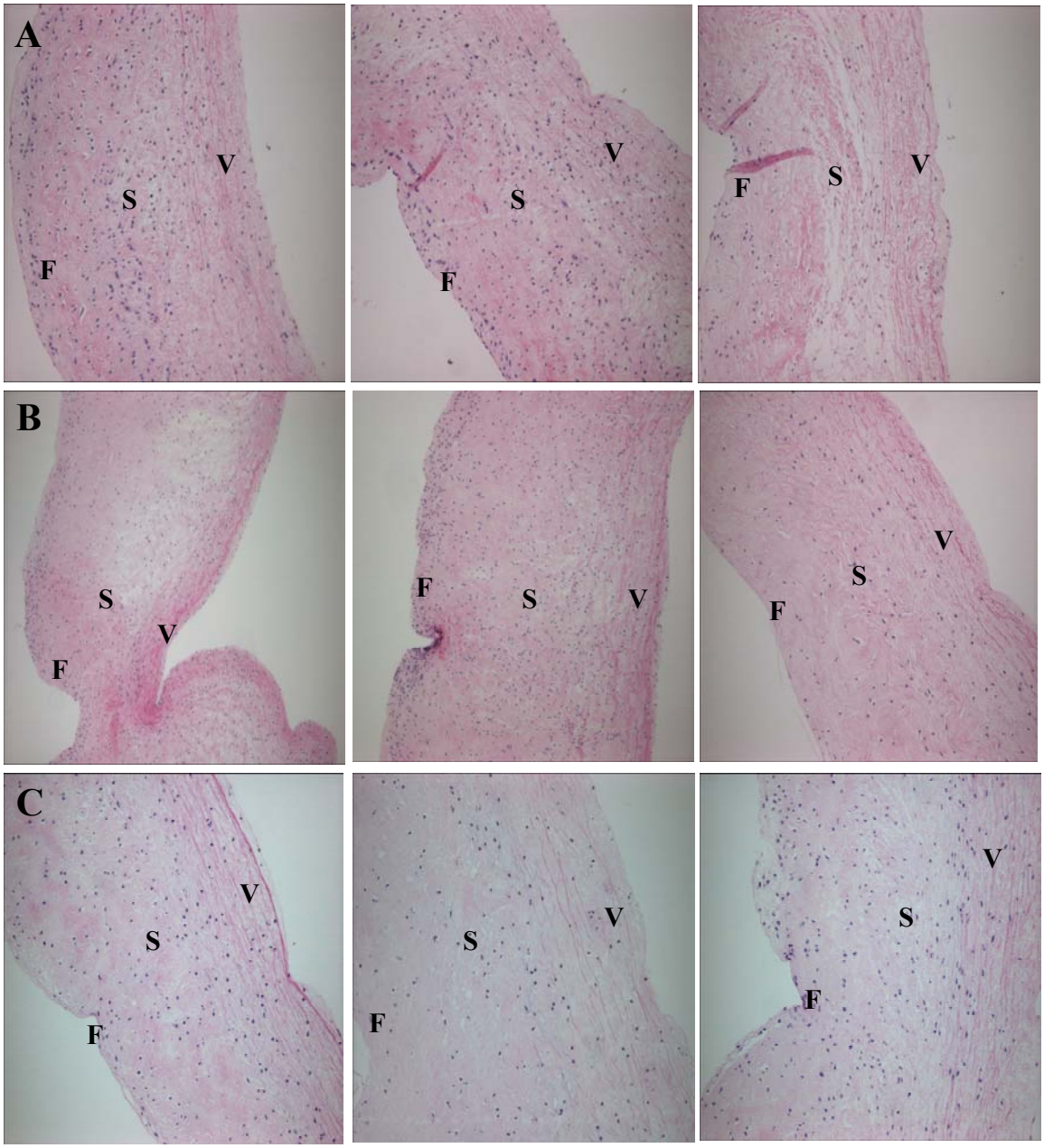

Figure 5.13: From left to right: Left, Right and Non coronary leaflets. H & E stains of fresh (A), cultured (B) and static (C) control leaflets. Cell nuclei are blue, and ECM are pink. Images were taken at 20X magnification. The morphology of the cultured leaflets was preserved in the system, which is comparable to the fresh and static control leaflets. (F-Fibrosa, S-Spongiosa, V-Ventricularis).

The images show that valve leaflets cultured in the organ culture system have a three layer tissue structure similar to fresh and statically incubated leaflets. There is no apparent change in the cellular distribution or thickness of the leaflet layers. The gross morphology of the leaflets suggests that there is no remodeling in the tissue structure when compared to the fresh and static controls. This suggests that the system is capable of preserving leaflet morphology when cultured under normal physiological conditions for a period of 48 hours.

5.5.2. Cell proliferation: 5-Bromo deoxyuridine stain

Cell proliferation in the valve leaflets was observed by marking proliferating cells with an anti- BrdU antibody. Proliferating cells show up as red nuclei while the rest of the cells are stained blue (Figure 5.14). Positive cells (indicated by black arrows) can be observed in both the cultured and static control leaflets with no specific distribution of the cells in the leaflets. All the images were taken under 20X magnification.

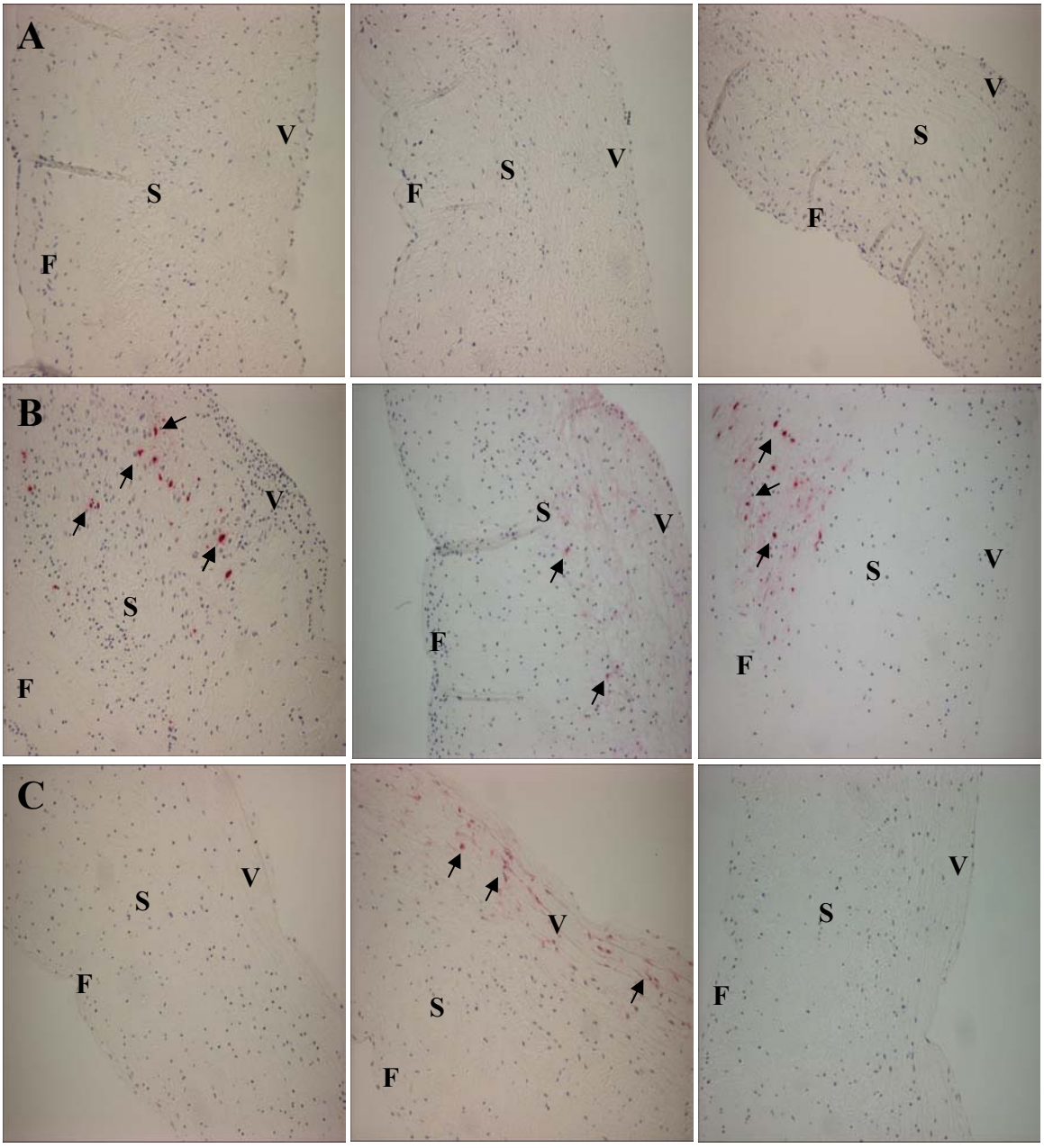

Figure 5.14: From left to right: Left, Right and Non coronary leaflets. BrdU IHC images of fresh (A), cultured (B) and static (C) control leaflets. Cell nuclei are shown in blue and proliferating cells as red nuclei. Images were taken at 20X magnification. Positive cells (indicated by black arrows) were found in cultured and static control leaflets scattered through the ECM of the leaflets. (F-Fibrosa, S-Spongiosa, V-Ventricularis).

Few cells compared to the total number of cells on the leaflets were found to be proliferating in both the cultured valve and static leaflets. The fresh control leaflets, shown in Figure 5.14, were fixed in formalin instead of incubation in medium containing BrdU. Thus, there was no BrdU incorporation in the cells, and no proliferating cells were identified in the fresh leaflets.

Proliferating cells in both groups were quantified by cell counting using Image Pro software, as detailed in the methods chapter. The number of proliferating cells in cultured leaflets was 0.17% ± 0.33% compared to 0.096% ± 0.11% in the static control leaflets. Data presented in Figure 5.15 shows that there is no statistically significant difference between the cultured and static control leaflets ($p>0.05$). Data sets corresponding to the graph shown below are given in Table 5.8, with p-values for data comparisons between the groups given in Table 5.9.

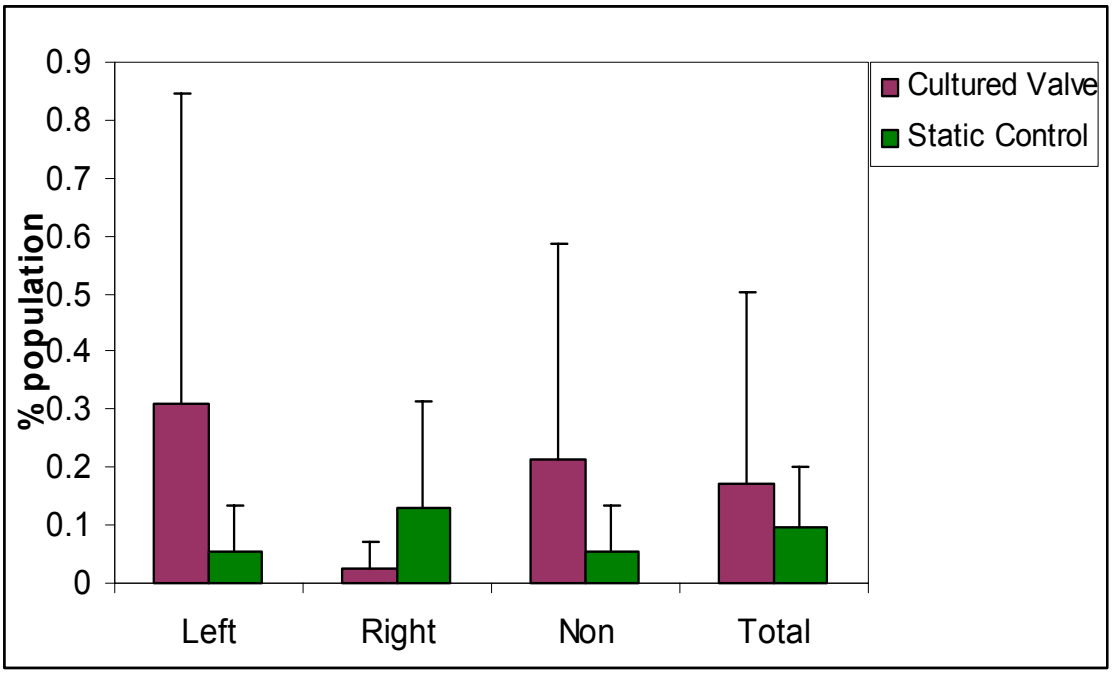

Figure 5.15: Percentage population of proliferating cells in the left, right, non-coronary leaflets and mean content in all three leaflets of the valve. The data are represented as average value + one standard deviation. No significant difference was observed between the cultured and static control leaflets ($p>0.05$), $n = 8$.

Table 5.8: Cell proliferation data from left, right and non coronary leaflets of fresh (F), cultured (C) and static (S) control valves used in the study. The data is expressed as percentage population of total cells that are proliferating. Blank cells specify that data has not been analyzed for that valve.

Expt. No.	Left coronary leaflet			Right coronary leaflet			Non coronary leaflet		
	F	C	S	F	C	S	F	C	S
1	0	0	0	0	0.079	0.26	0	0	0
3	0	0	0.109	0	0	0	0	0.645	0.110
4		0.927			0			0	
5					0.076				
Avg.	0	0.309	0.055	0	0.026	0.13	0	0.215	0.055
Std. Dev.	0	0.535	0.077	0	0.045	0.184	0	0.372	0.078

Table 5.9: p-values for the cell proliferation data comparisons between all three groups of the leaflets obtained using Mann-Whitney non-parametric statistical analysis at 95% confidence interval.

Leaflet	Cultured Vs Static
Left	1.000
Right	0.817
Non	1.000
Total	0.5815

5.5.3. Cell apoptosis: Caspase 3 stain

Leaflets cultured in the organ culture system were tested for apoptosis to ensure that there was no system-induced injury to the leaflets by adverse mechanical or biochemical factors. Apoptotic cells in the leaflet containing activated caspase 3 cleavage sites are marked by red nuclei using an activated caspase 3 antibody, and the rest of the cell nuclei are stained blue. The images, shown in Figure 5.16, were taken at 20X magnification.

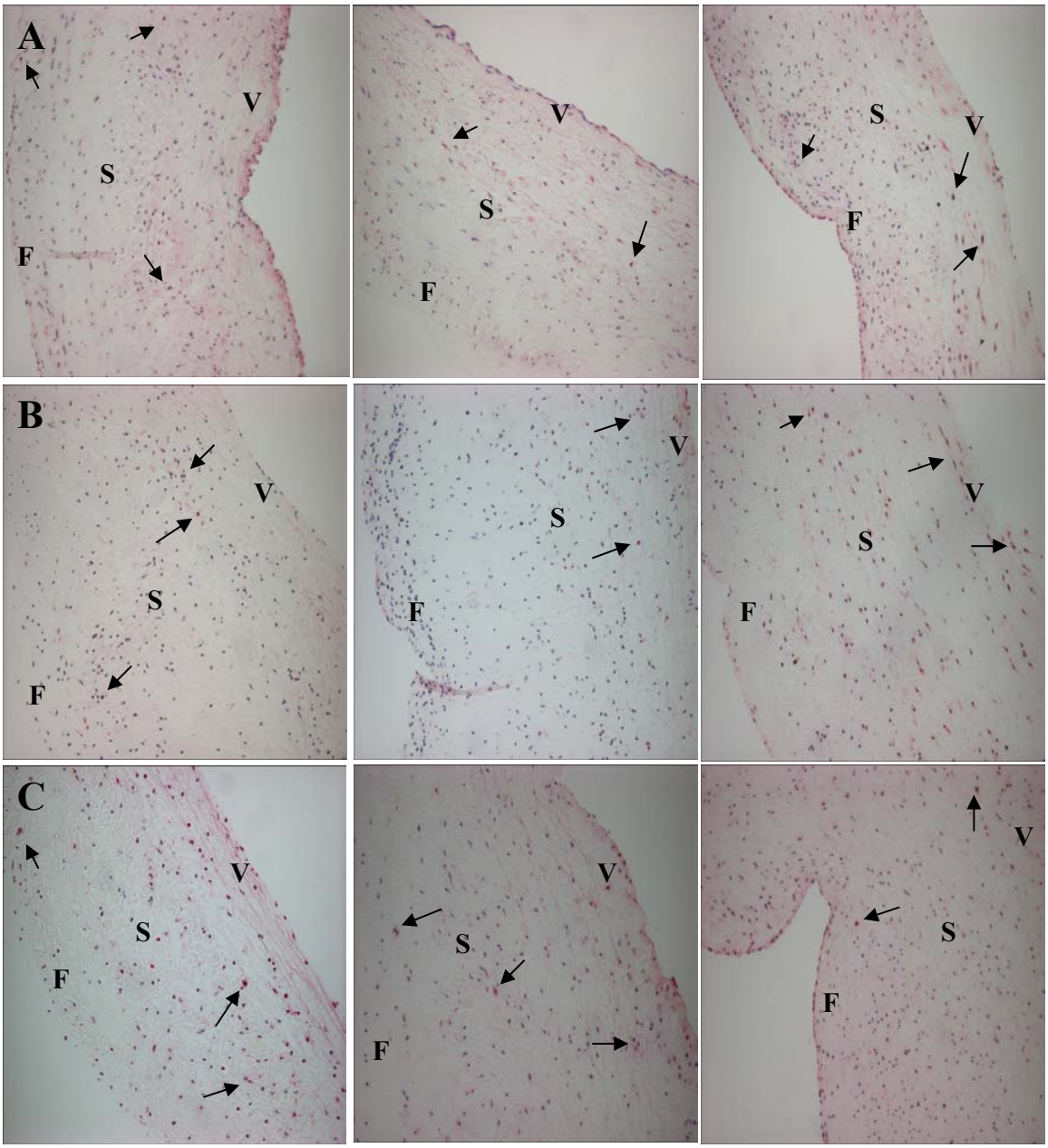

Figure 5.16: From left to right: Left, Right and Non coronary leaflets. Shown here are Activated caspase 3 IHC images of fresh (A), cultured (B) and static (C) control leaflets. Cell nuclei are shown in blue and apoptotic cells as red nuclei. Images were taken at 20X magnification. Positive cells (indicated by black arrows) were found in fresh, cultured and static control leaflets scattered through the ECM of the leaflets. (F-Fibrosa, S-Spongiosa, V-Ventricularis).

Apoptotic cells were found scattered in all three layers of the three groups of the leaflets. To provide an estimate of increase or decrease in number of apoptotic cells in cultured leaflets compared to fresh valve leaflets, cells were counted in the leaflets and the data was expressed as a percentage of the population of cells undergoing apoptosis. The apoptosis data is shown in Figure 5.17 and the corresponding data sets are given in Table 5.10. The p-values for all three leaflet group comparisons are given in Table 5.11. Apoptosis in the cultured leaflets (1.64% ± 1.04%) was not statistically different than that in the fresh control leaflets (1.96% ± 0.41%), but it was significantly less than in the static control leaflets (2.82% ± 0.96%).

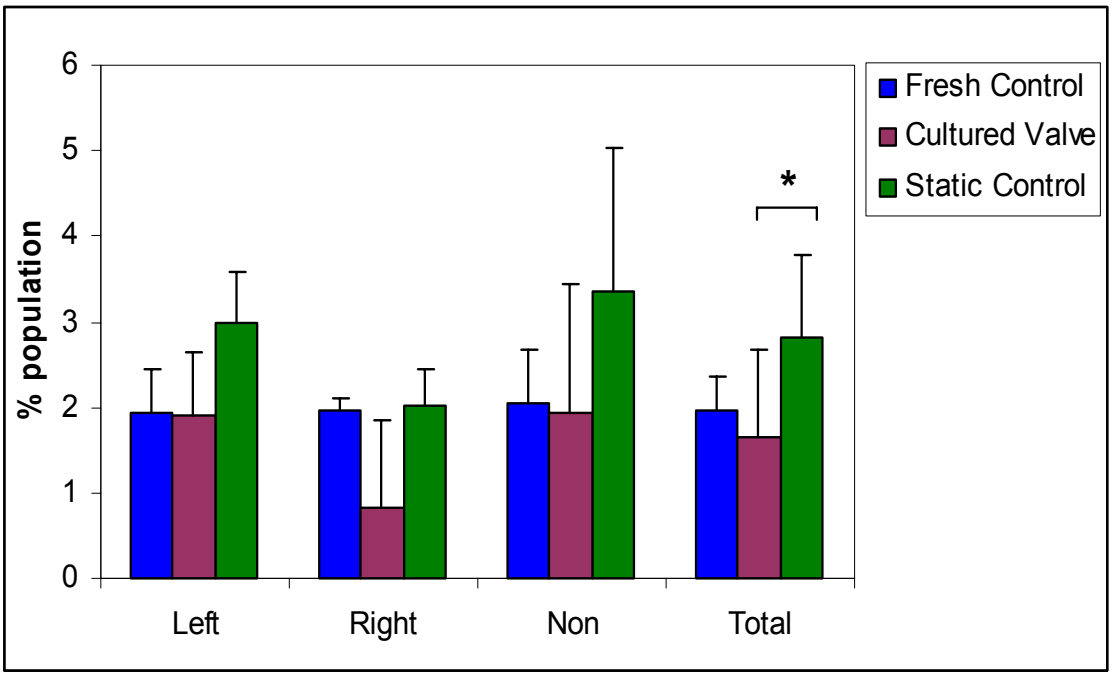

Figure 5.17: Percentage population of apoptotic cells in the left, right, non-coronary leaflets and mean content in all three leaflets of the valve. The data are represented as average value + one standard deviation. No significant difference was observed between fresh and cultured valve leaflets. Apoptosis in the static control leaflets was significantly greater than in the cultured valve leaflets ($p<0.05$) but not statistically different from fresh valve leaflets ($p>0.05$), $n = 8$.

Table 5.10: Cell apoptotic data from left, right and non coronary leaflets of fresh (F), cultured (C) and static (S) control valves used in the study. The data is expressed as percentage population of total cells that are undergoing apoptosis. Blank cells specify that data has not been analyzed for that valve.

Expt. No.	Left coronary leaflet			Right coronary leaflet			Non coronary leaflet		
	F	C	S	F	C	S	F	C	S
1	2.02	1.94	3.46	1.90	0.19	1.73	2.49	0.53	4.54
3	1.18	2.17	3.18	1.81	2.00	2.33	1.58	1.77	2.20
4	2.31	0.80	2.34	2.13	0.28			3.52	
5	2.44	1.32							
6	1.74	2.19							
7		2.93							
Avg.	1.94	1.89	2.99	1.95	0.82	2.03	2.04	1.94	3.37
Std. Dev	0.50	0.74	0.59	0.16	1.02	0.43	0.65	1.50	1.65

Table 5.11: p-values for the cell apoptosis data comparisons between all three groups of the leaflets obtained using Mann-Whitney non-parametric statistical analysis at 95% confidence interval.

Leaflet	Fresh Vs Cultured	Fresh Vs Static	Cultured Vs Static
Left	0.9273	0.0736	0.0528
Right	0.3827	1.000	0.3865
Non	1.000	0.6985	0.3865
Total	0.4483	0.0570	0.0251

5.5.4. α-Smooth muscle cell actin immunohistochemistry

Phenotypical changes in the leaflet were observed through the expression of α-SMC actin by interstitial cells in the leaflet. Immunofluoroscence images of the leaflet shown in Figure 5.18 were taken at a magnification of 20X. α-SMC actin expression was green (indicated by white arrows) and surrounded the cells expressing it. The cell nuclei were counterstained in blue.

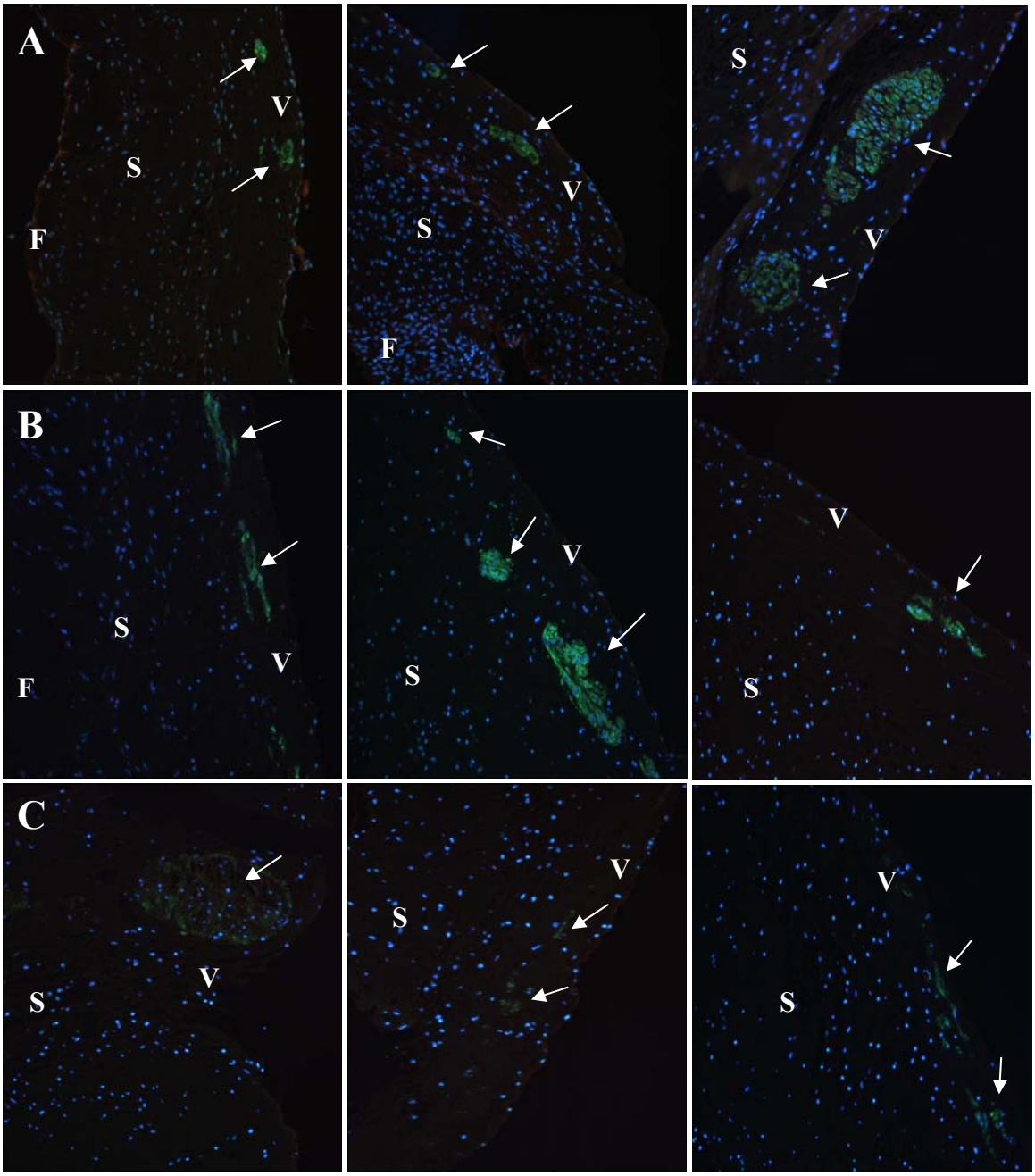

Figure 5.18: From left to right: Left, Right and Non coronary leaflets. α-SMC actin immunofluoroscence images of fresh (A), cultured (B) and static (C) control leaflets. Green indicates α-SMC actin expressed by interstitial cells and blue indicates cell nuclei. Images were taken at 20X magnification. Actin expression (indicated by white arrows) was comparable between fresh and cultured valve leaflets but was reduced in static control leaflets compared to the other two groups. (F-Fibrosa, S-Spongiosa, V-Ventricularis).

In the images it can be seen that α-SMC actin was expressed predominantly in the ventricularis region of all three leaflets in the three groups. Actin expression in the cultured valve leaflets was similar to that of fresh valve leaflets. However, expression in the static control leaflets was less than both the fresh and cultured valve leaflets. This suggests that the native phenotype of the leaflets was maintained in the cultured valves exposed to normal mechanical conditions for 48 hours.

5.5.5. Endothelial cells: von Willebrand factor stain

Double immunofluroscence was used to stain for both EC expressing vWF and IC expressing α-SMC actin. vWF in the EC marked using texas red fluorochrome is red in the images shown in Figure 5.19. Cell nuclei were counterstained blue, and the images were taken at a magnification of 20X. ECs are indicated with white arrows. It can be seen that the ECs on both cultured and static control leaflets were reduced compared to fresh control leaflets. To confirm this observation, SEM was performed on all leaflet samples.

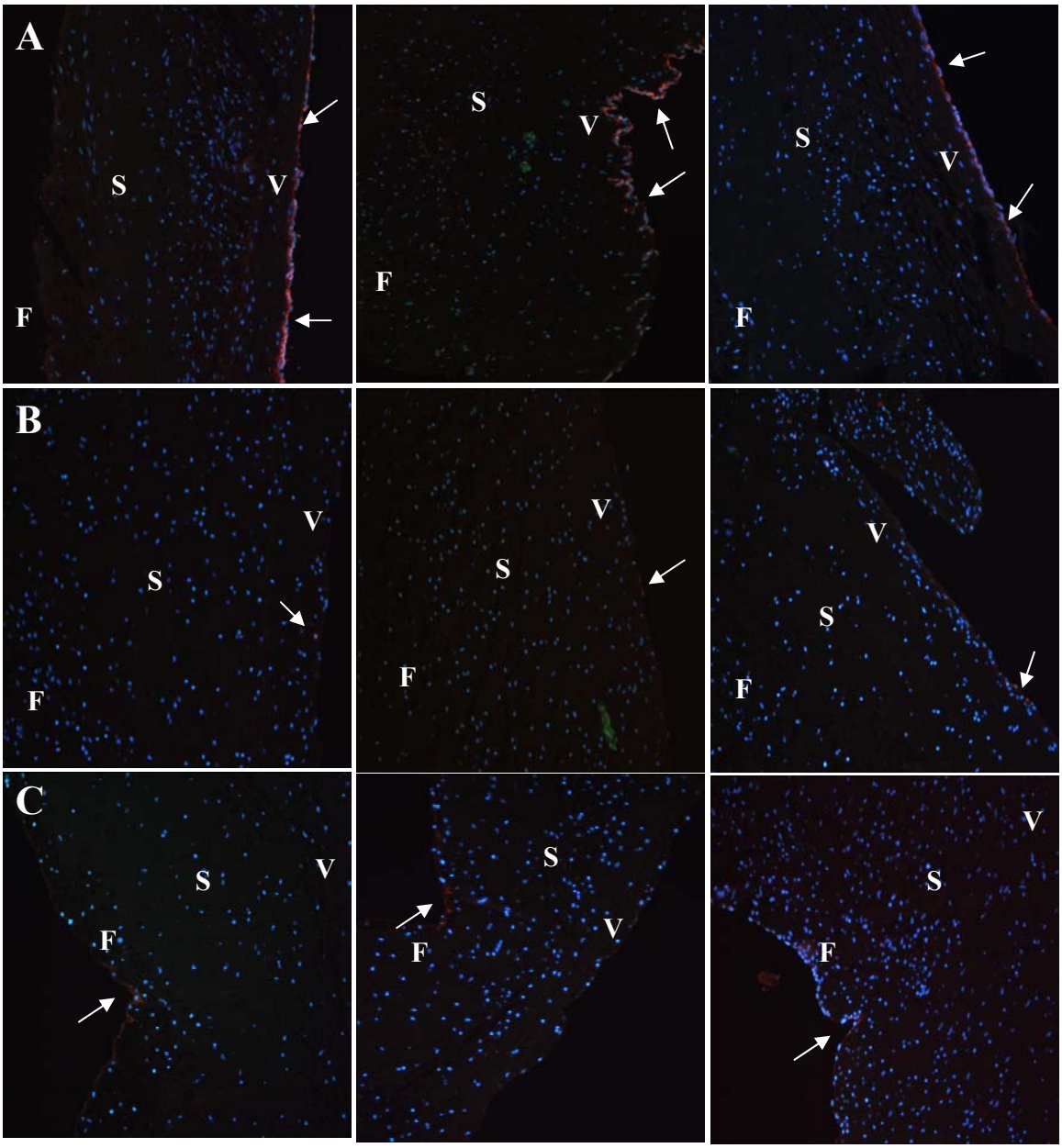

Figure 5.19: From left to right: Left, Right and Non coronary leaflets. vWF immunofluoroscence images of fresh (A), cultured (B) and static (C) control leaflets. EC are indicated by red and cell nuclei were counterstained with blue. Images were taken at 20X magnification. vWF expression (indicated by white arrows) is reduced in cultured and static control leaflets compared to fresh control leaflets. (F-Fibrosa, S-Spongiosa, V-Ventricularis).

5.5.6. Scanning electron microscopy: Endothelial cells

SEM was used to observe endothelial cells on the ventricularis surface of aortic valve leaflets. Images were taken at a magnification of 1000X and are shown in Figure 5.20.

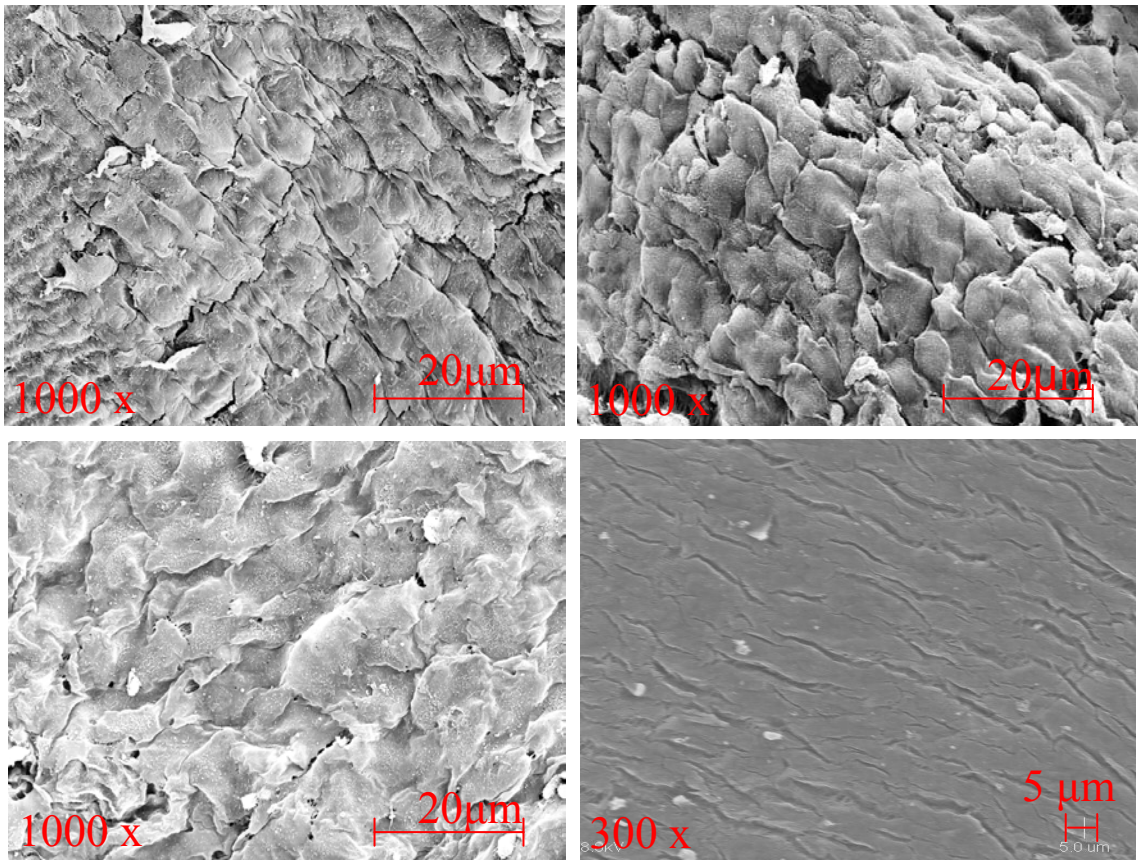

Figure 5.20: SEM images of the ventricularis surface of the aortic leaflets taken at 1000X resolution. EC were aligned in circumferential direction on cultured leaflets and looked similar to those on fresh leaflets. Shown from left to right and top to bottom are fresh, cultured, static and denuded leaflets, respectively.

EC on the cultured valve leaflets were found to be comparable to those on the fresh control leaflets. EC aligned in the circumferential direction of the leaflets, perpendicular to the flow. The EC on the static control leaflets were not as clearly defined as those on the fresh and cultured leaflets, but this may be an artifact that occurred during

leaflet processing. Shown in the images from left to right are fresh, cultured, static and denuded leaflets. The denuded image has been adopted from unpublished data generated in our laboratory from a different study and has been used here to provide a comparison between leaflets populated with and without EC. These images show that the EC were retained by the valve leaflets cultured in the organ culture system for a period of 48 hours. They also maintained their native morphology with respect to orientation.

CHAPTER 6

DISCUSSION

The experimental results presented in Chapter 5 demonstrate that the *ex vivo* organ culture system is capable of maintaining normal physiological pressure and flow conditions, and sterility for a period of 96 hours. The system has also been shown to maintain physiological pH and provide adequate oxygen for sustaining the viability of the porcine aortic valve. Biological studies of the valve leaflets cultured in the system indicate that collagen, sGAG and elastin content were maintained at native levels in the organ culture system. A significant decrease in sGAG and elastin content was observed in the static control leaflets compared to native levels. The cell phenotype of the cultured valve leaflets was comparable to that of fresh valve leaflets, and there were no gross changes in the morphology of the cultured leaflets. The ECs were retained on the leaflet surfaces after 48 hours of organ culture. A comparable amount of cell apoptosis between the fresh and cultured valve leaflets showed that the system was able to maintain the viability of the leaflet tissue without causing any adverse environmental changes, such as oxygen limitation or detrimental pH levels.

6.1. Mechanical performance of the system

The organ culture system was developed to simulate the physiological and mechanical environments experienced by the native aortic valve. The closed flow loop is constructed of biocompatible components that are capable of withstanding the high temperatures and pressures of repeated autoclave cycles. The system is compact to enable it to be contained

in an incubator in order to maintain the temperature at 37^{o}C. Silicone tubing, situated inside the compliance tank of the system, provides oxygen to the culture medium, thus ensuring that the nutritional requirements of the valve are met. The flow rate and pressure in the system could be controlled independently of each other, enabling a wide range of clinically relevant mechanical conditions to be studied aseptically [Warnock, 2005]. In addition, the flow and pressure waveforms shown in Figures 5.1-5.4 are very similar to the physiological waveforms shown in Figure 4.1. In the flow waveforms of Figures 5.1-5.4, the peak flow rates obtained were between 22.0-24.0 L/min, which is comparable to 29.0 L/min seen in Figure 4.1. The peak pressure was 120 mmHg, the same as that of a normal human adult heart under resting conditions. The duration of the systolic and diastolic phases in the pressure waveform was also comparable with the physiological values of 300 and 550 ms, respectively.

The flow waveform obtained by testing a ball and cage mechanical heart valve in the organ culture system showed negative flow rates during diastole due to paravalvular leakage. This was possibly due to a slight tilt of the valve in the valve holder caused by a mismatch between the size of the valve (25mm) and the inflow diameter (33mm) of the central component of the aortic valve holder, despite the use of a 35mm external diameter support ring to hold the valve in place. Additionally minimal fluid flow reversal was observed due to the backward movement (diastolic phase) of the piston causing negative flow rates. It can also be seen from the pressure waveforms in Figures 5.1 and 5.3 that the pressure gradient (i.e.magnitude of the waveforms) was large (60-65 mmHg) when compared to the waveforms obtained with the pericardial bioprosthetic valve or the native

porcine aortic valve. This may be to due to the lower effective orifice area of the valve causing larger pressure gradients.

The negative flow rates seen in the flow waveform for the pericardial bioprosthetic valve were due to backflow of fluid through a small coaptation gap between the closed leaflets and flow reversal causing the fluid to leak back along the inside wall of the valve holder during the diastolic phase of the cardiac cycle. The disturbances in the pressure waveform in this case were reduced when compared to the waveforms seen with the mechanical valve. The flow waveforms of the native porcine aortic valves, seen in Figure 5.4, showed reduced backflow compared to flow waveforms obtained with either the mechanical or the bioprosthetic valves, shown in Figures 5.1-5.3. The lower values of negative flow rates seen in the waveform may have been due to fluid flow reversal leading to leakage of the fluid between the aortic root and the inside wall of the aortic valve holder during backward movement of the piston. Leakage through the aortic valve was minimized by ligating the coronary arteries and also fixing the excess aortic tissue between the outflow side of the central component and outflow components of the valve holder. This also prevented the aorta from bending on to the leaflets. In all the pressure waveforms in Figures 5.1-5.4, fluctuations can be seen at the beginning of systole. This may be due to turbulence created by the forward movement of the piston to push the fluid through the flow loop. Overall, the flow and pressure waveforms were consistent throughout the experimental duration with minimal variation between the curves acquired at different time points. Thus, the organ culture system was able to maintain consistent physiological mechanical conditions for a period of 96 hours.

The system was shown to maintain a physiological pH level and provide sufficient oxygen transport to the valve. pH values outside of the physiological range of 7.2-7.4 induce significant cell death in the leaflet tissue, thus changing the biological properties of the leaflets. A lack of oxygen transport to the valves in the organ culture system decreased the viability of the cells as shown in Appendix D. The incorporation of a gas-exchanger in the system was able to maintain leaflet cell viability with cell apoptosis comparable to fresh leaflets as seen in Figures 5.16 and 5.17. The oxygen uptake rate obtained in this study compares well with the value obtained in the oxygen diffusion study of aortic valve leaflets conducted by Wend et al [Wend, 2001]. However, the method of calculating the oxygen uptake rate of the valve and oxygen transfer rate into the medium is not accurate since oxygen seepage into the closed systems will occur during DO_2 measurements with the probe. This is due to the presence of large oxygen concentration gradients between the inside of the system and the outside atmosphere. Further, the closed system used for oxygen uptake measurements may have allowed minimal oxygen exchange into the system through the polystyrene gasket located in the lid of the culture flask. The amount of leakage of oxygen into the culture flask may be determined by degassing the medium in the flask with N_2 and periodically recording the DO_2 values for long enough time. Thus, the error in measuring the oxygen uptake rate may be minimized. The gas-flow rate in the gas-exchanger was calculated based on normal cardiac pressure and flow conditions. This value depends upon the pressure and flow conditions in the system and changes to meet the oxygen uptake requirements of the valves due to changes in the convective mass transport rate. Additionally, the oxygen exchange rate into the medium contained in the organ culture system was 4.74×10^{-3}

mg/sec, which is two orders (i.e. 100 times) of magnitude greater than the oxygen uptake rate of the valve, 9.90×10^{-5} mg/sec. The oxygen uptake rate of the valve was established when it was cultured under static, atmospheric pressure with no mechanical loading. However, when the valve is cultured under dynamic conditions the oxygen requirement increases. This increase in demand for oxygen is met by gas that is transferred into the medium in the system. Hence, the gas-flow rate in the gas-exchanger was calculated such that the amount of oxygen supplied is greater than the uptake rate. Also, there was no increase in cell death, as seen in Figure 5.16, due to excess oxygen to the valve, suggesting that adequate amount of oxygen was provided to the organ culture system.

This organ culture system is the first system to address the issue of providing the required level of oxygen to maintain the viability of native aortic valves. Previous *in vitro* bioreactors that were used for producing and preconditioning tissue engineered valve constructs under dynamic conditions did not address the issue of oxygen transport in the closed set up of the systems [Dumont, 2002; Hoerstrup, 2000a; Hoerstrup, 2000b; Sodian, 2000]. The earliest of these bioreactors was developed by Hoerstrup et al to produce tissue engineered valvular constructs under aortic flow and pressure conditions. This bioreactor could attain a maximum flow rate of 2.0 L/min and a maximum pressure of 240 mmHg. Although the pressure could be adjusted to physiological ranges, the flow rate was much less than the physiological value. Also, since the constructs were not anchored to a support to simulate the physiological leaflet movement, they were not subjected to bending or cyclic flexure. When implanted *in vivo* in a lamb model, the tissue engineered valve leaflets produced in this bioreactor developed regurgitation within 4 months of implantation [Hoerstrup, 2000a; Sodian, 2000]. This result suggests

that the valve leaflets require greater mechanical strength to withstand *in vivo* hemodynamic conditions. Another recent study to develop an *in vitro* bioreactor for dynamic seeding and conditioning of tissue engineered constructs was undertaken by Hildebrand et al [Hildebrand, 2004]. The system was capable of operating under various mechanical loading conditions and visual examination of the medium showed that the system could be operated aseptically for 21 days. However, the study did not address maintenance of the pH level or nutrient sufficiency (specifically oxygen) as only 2L of culture medium was used in the closed system for 21 days without perfusion. The results from the current study suggest that an aortic valve weighing ~30 g will reach limiting oxygen conditions in 3 hours when cultured in 400 mL of medium. Hence, with an operating volume of 2 L in a closed system, oxygen transport to the tissue constructs will become limited within a short time. Furthermore, the medium may require periodic replenishment to prevent depletion of other nutrients such as glucose.

The *ex vivo* organ culture system developed in the current study provides consistent physiological loading conditions with independent control of the flow rate, pressure and frequency to reproduce clinically relevant mechanical conditions. In addition, the ability of the system to provide adequate oxygen transport to the valve at physiological pH level enables the system to culture native porcine aortic valves for a period of at least 48 hours.

6.2. Role of dynamic environment on leaflet biology

6.2.1. Extracellular matrix components

The results from the biological study of the valve leaflets show that the collagen, sGAG and elastin content of the cultured valve leaflets were not significantly different from that of the fresh control leaflets, while the sGAG and elastin content in the static leaflets were significantly lower when compared to both the fresh and cultured valve leaflets. These results highlight the importance of mechanical forces in maintaining the ECM. Cultured valve leaflets were subjected to a mean flow rate of 3.8-4.5 L/min, and systolic/diastolic pressure of 120/80 mmHg at a frequency of 1.167 Hz representing the normal mechanical/physiological conditions of the aortic valve. Since the cultured valve leaflets were exposed to the same physiological forces as the *in vivo* hemodynamic environment there was no change in the leaflet biology compared to fresh leaflets. However, the disturbances in fluid flow upstream of the aortic valve might have induced some changes in the biology of the three leaflets of the same valve as seen by the elastin contents of the right and non coronary leaflets as shown in Figure 5.12. However, these changes in ECM components within the leaflets of the cultured valve were not significant at a p-value of 0.05. The orientation of the three leaflets of the valve in the aortic valve holder was randomized during the study. Hence the effects of disturbed fluid flow were randomized over the three leaflets. Further, the ligation of left and right coronary arteries might have induced slight deviation in fluid flow on the aortic side of the left and right coronary leaflets leading to an altered shear stress distribution on the leaflets. This however, did not affect the cultured leaflets' biological properties as seen in Figures 5.10, 5.11 and 5.12.

Collagen, a structural protein of the valve leaflet, is synthesized by the valvular cells in the leaflets as a response to the flexure and bending that occur during the cardiac cycle. During this process they are exposed to pressure and shear stresses, which have been shown to regulate collagen synthesis in the leaflets [Weston, 2001; Xing, 2004a; Xing, 2004b]. Although the mechanisms by which mechanical forces affect cells are not fully understood, the observed biosynthetic activity of the leaflets is thought to be due to the synergetic action of the three components of the leaflets: ECs, ICs and ECM. As illustrated in Figure 6.1, the ECs are the prime receptors of the mechanical forces on the leaflets and they respond to the forces by releasing cytokines or growth factors that effect the metabolism of underlying ICs, which are responsible for matrix production. The ECM serves as a connection between the ECs and ICs via cell-cell and cell-ECM junctions and transmits the mechanical stresses to ICs. The ICs react by constantly producing ECM components in response to the mechanical forces experienced by the leaflets. This process may involve many biochemical factors. The observed similarity in ECM components between the fresh and cultured leaflets in the current study could be due to a balance between synthesis and degradation of the ECM components. The mechanism of this balance can be further elucidated by studying changes in gene expression as well as enzymatic activities in the valvular cells. Based on the results from this study and previous investigations conducted in our laboratory a pathway for changes in valvular biology under the influence of physiological mechanical forces can be proposed as shown in Figures 6.1 and 6.3. Mechanical forces such as shear stresses and pressure exert loading on leaflet tissue, which in turn are communicated to both ECs and ICs. In response, the ECs and ICs may undergo some cytoskeletal reorganization or open/close

their mechanosensitive ion-channels. Consequently, this may lead to a series of intracellular events such as stimulation/inhibition of lysosomal proteases in ICs (e.g. cathepsin S, L and D) as observed in studies carried out in our laboratory [Xing, 2004c]. The inhibition of lysosamal proteases leads to a slower degradation of collagen or other matrix proteins, eventually resulting in higher matrix synthesis and vice versa. Other mechanical forces, such as bending stresses and cyclic tensile stretch, on the valve leaflets are hypothesized to maintain the contractile phenotype of the leaflets. However, the mechanisms of cell signaling and phenotypical changes in myofibroblasts during leaflet contractility are poorly understood. ICs are a dynamic population of specific cell types, which communicate with each other, ECs, and ECM through the release of growth factors, integrin interaction, calcium signaling and intracellular tension as shown in Figure 6.1 [Taylor, 2003]. Further studies are required to understand these complex mechanisms of cell-cell and cell-matrix interaction that involve activation of ECM-regulated kinases and integrin-mediated mechanotransdcution, including activation of various kinases (i.e. FAK, c-Src, and Fyn), adaptor molecules (i.e. CAS and Shc), guanine nucleotide exchange factors (GEFs) (i.e. C3G and son of sevenless [Sos]), and small GTPases (i.e. Rap1 and Ras) [Xing, 2004c]. Additionally investigating the mechanisms of gene regulation within the valvular cells will help in understanding the contribution of these cells to maintain the physiological function of valves and re-establishing the normal structure of the valve following injury.

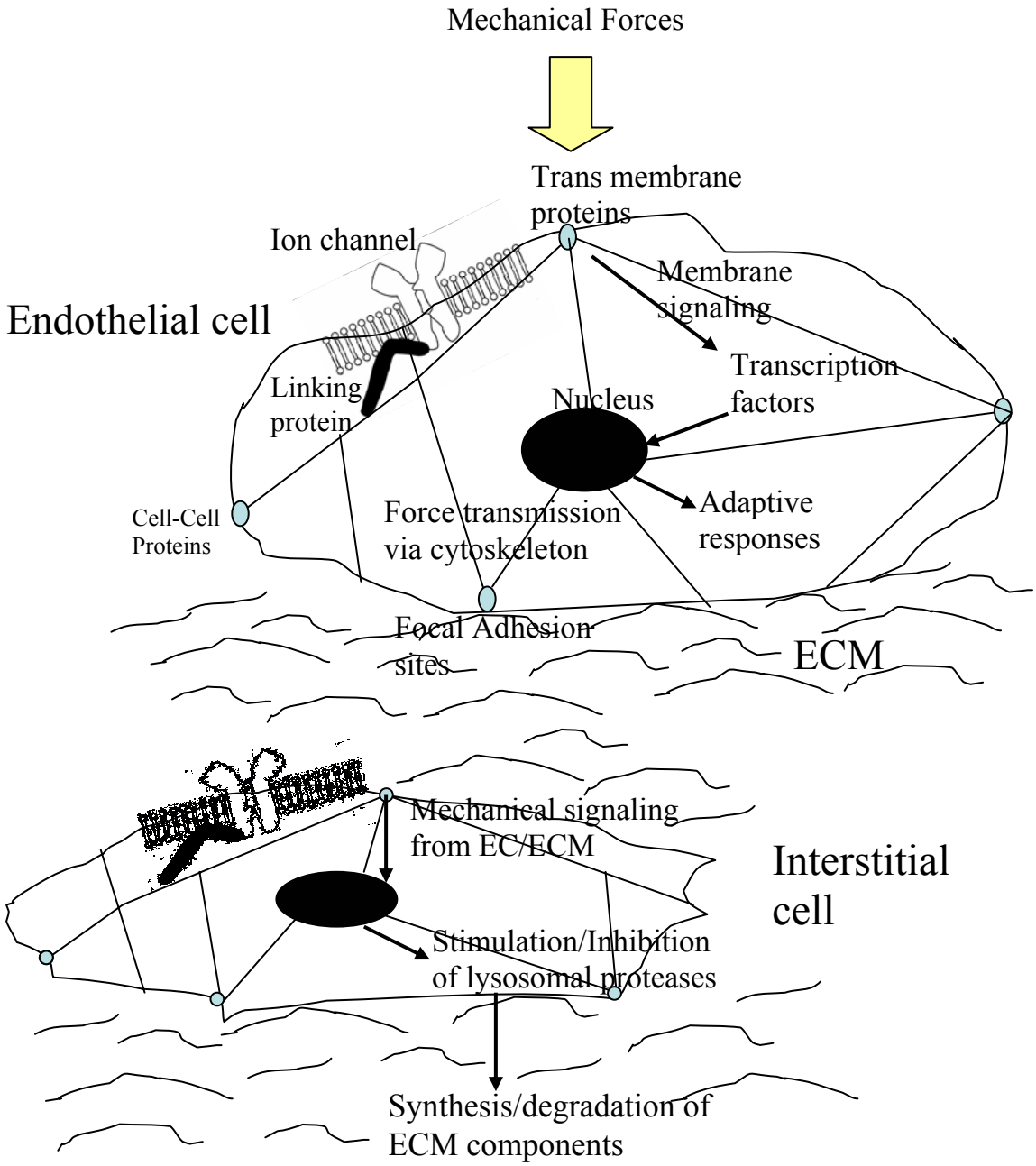

Figure 6.1: This is a schematic that illustrates the transduction of mechanical forces. Mechanical forces acting on the valve leaflets are communicated to ECs and ICs via cell-cell and cell-ECM junctions. The cells reorganize cytoskeleton or open/close mechanosensitive ion channels and consequently stimulate or inhibit lysosomal proteases to synthesize/degrade ECM components.

The valve leaflets in the organ culture system were exposed to physiological forces such as pressure, shear and bending stresses, flow, and cyclic flexure. These mechanical conditions maintained the collagen content in the cultured valve leaflets at comparable amounts to fresh leaflets as seen in Figure 5.10. The collagen content from individual leaflets of the cultured valves is not only comparable to each other but also is not significantly different from that of the fresh and static leaflets at $p=0.05$. However, large standard deviations in the collagen content were observed for all the leaflets in the three groups. This is because of the variation in collagen content between the valves from different animals. At a p-value of 0.1, there was a significant difference in collagen content between: (i) the non-coronary leaflets of the cultured and fresh valves, and (ii) the left coronary leaflets of static and fresh leaflets. The difference seen in the first case is due to the low collagen content seen in the fresh non-coronary leaflet of the first valve shown in Table 5.2. Since this value is very low compared to the rest of the values, the average value of collagen content in the leaflets is reduced causing a significant difference between the cultured and fresh leaflets. The non-coronary static leaflets also exhibit low collagen content causing the difference between the fresh and static non-coronary leaflets to be non-significant ($p>0.1$). The same trend is seen with the left coronary static leaflets. Due to low values of collagen content in valves 3, 4 and 5, a significant decrease can be seen in the leaflets when compared to the fresh leaflets. The results from the remaining types of the leaflets suggest that the collagen content of the cultured, fresh and static leaflets are comparable to each other when analyzed at a p-value of 0.1. The results from this study are consistent with the results seen in previous physiological flow and shear stress studies on porcine aortic valve leaflets. The previous

study showed that collagen synthesis was maintained at native levels when the leaflets were subjected to fluid flow and shear stress but increased under static incubation [Weston, 2001]. In another study, exposing the aortic valve leaflets to cyclic and static pressures at a mean value of 100 mmHg resulted in collagen synthesis comparable to that of static leaflets with collagen synthesis increasing at higher pressure in a magnitude dependent manner [Xing, 2004a; Xing, 2004b]. The current study has also shown that collagen data is comparable between the static and cultured valve leaflets ($p>0.05$), which is the same result as the pressure study. Another *in vitro* study on the effect of mechanical stretch on cardiac fibroblasts showed an increase in the ratio of collagen type III to collagen type I in mechanically stretched cells. Type III collagen mRNA levels increased in response to cyclic mechanical stretch for durations as short as 12 hours, while type I collagen mRNA levels were not found to change under the stretch conditions used in the study [Carver, 1991]. These results emphasize the potential regulatory role of mechanical stimulation in the expression of specific genes in cardiac cells. An *in vivo* study, complimentary to the above mentioned *in vitro* study, was performed to investigate the effect of hypertensive pressures on structural alterations of the aortic valve in rats. At aortic pressures of 160-180 mmHg there was an increase in the tensile strains within the valve leaflet. Hypertensive rats were found to posses greater mRNA for collagen types I and III, suggesting increased collagen turnover [Willems, 1994]. These results suggest that type I and type III collagen synthesis are both affected by pressure overload.

sGAG is predominantly present in the spongiosa and is constantly synthesized under the influence of normal hemodynamic forces. They function as a lubricant to reduce the internal shear between the ventricularis and the fibrosa during leaflet bending

and cyclic flexure. Mechanical forces in the organ culture system facilitate physiological movement of the leaflets, thus maintaining GAG synthesis at native levels. Table 5.5 shows that the sGAG content in the cultured and fresh valve leaflets were comparable within statistical significance at p-values of both 0.05 and 0.1. sGAG content in the right-coronary static leaflets was significantly decreased when compared to both the cultured and fresh leaflets ($p<0.05$), while sGAG in the non-coronary static leaflets was significantly decreased when compared to the cultured valves leaflets ($p<0.05$). The reduction in sGAG content in the right and non-coronary static leaflets led to an overall decrease in sGAG content of the static leaflets in comparison to both the fresh and cultured valve leaflets. This is because the sGAG content in the right coronary leaflets of static valves 1, 3, 4 and 9 (Table 5.4) is very low when compared to the rest of the valves, consequently decreasing the average value and increasing the standard deviation in comparison to the left and non-coronary static leaflets. The sGAG content of the cultured non-coronary leaflets has a higher average value than that of the fresh leaflet, although the difference is not significant ($p>0.05$). This increase in sGAG results in a significant difference between the cultured and static non-coronary leaflets ($p<0.05$). However, the difference in sGAG content between the fresh and static non-coronary leaflets was not statistically significant ($p>0.05$). At p-value=0.1, there is a significant difference between the left coronary static and fresh leaflets, which is again due to the large variations in the individual valves. The significant decrease in sGAG content seen in the statically incubated leaflets is due to the absence of a dynamic environment. This explanation is valid based on the results seen in the study by Weston et al wherein aortic valve leaflets subjected to fluid flow and shear stress maintained sGAG synthesis at native levels, but

significantly increased the synthesis when statically incubated [Weston, 2001]. The result with the static leaflets seen in the current study is contrary to that seen in Weston's study; however, both results draw the same conclusion that the absence of mechanical forces alters GAG synthesis in aortic valve leaflets. *In vivo* studies have been conducted using an autoradiography technique to identify sites of protein, GAG, and DNA synthesis in rat aortic valve leaflets [Schneider, 1981]. The attachment zone of the leaflet had the highest GAG synthesis, while the region between the attachment and the midpoint showed the greatest protein synthesis. They attributed the patterns of protein and GAG synthesis to difference in the functional stresses of the valve, suggesting that the structural components of the valve are constantly renewed *in vivo* in response to mechanical loading. These studies suggest that increased tensile forces increase collagen synthesis and GAG synthesis. Their study, however, did not show any variation in GAG synthesis between the three leaflets in response to mechanical forces. Hence, the reduction of sGAG content in the right and non-coronary static leaflets and not in left-coronary leaflets in comparison with fresh and cultured leaflets seen in the current study are due to variations in sGAG content of individual valves.

Elastin fibers maintain the structural integrity of the leaflets by stretching and recoiling during cyclic flexure. Similar to collagen and sGAG content, elastin content in the valve leaflets is also affected by mechanical forces. As shown in Figure 5.12, the leaflets cultured under normal physiological conditions in the organ culture system maintained their elastin content at levels comparable to fresh leaflets ($p>0.1$). However, the right coronary static leaflets showed a significant decrease in elastin content compared to both the cultured and fresh valve leaflets ($p<0.05$). This decrease in elastin

content resulted in an overall decrease in elastin content for the static leaflets compared to both the cultured and fresh valve leaflets ($p<0.05$). The reduced elastin content in the static leaflets is due to the absence of a dynamic environment during leaflet culture. The difference in responses seen between the three static leaflets is due to the large variability within the individual leaflets seen in the elastin data given in Table 5.6. At a p-value of 0.1, a significant difference was seen between the left coronary static and fresh leaflets in addition to the right coronary static leaflets. This observation was similar to that seen with the sGAG content in Table 5.5. Thus, lack of mechanical stimulus alters the structural composition of the aortic valve leaflets.

Heart valves leaflets have a complex tri-layered architecture composed of highly specialized, functionally adapted cells and ECM. The ECM elements (collagen, GAG and elastin) provide the mechanical characteristics vital for sustaining the dynamic behavior of the valve leaflets to accommodate cyclic changes in leaflet shape and dimensions throughout the cardiac cycle. ICs synthesize the ECM thereby mediating the ongoing repair and remodeling of the valve leaflets to provide durability. Aortic valves ICs, which are a mixed population of fibroblasts, myofibroblasts and smooth muscle cells, are interspersed throughout the ECM, while ECs are present only on the outer surfaces of the leaflets providing a non-thrombogenic surface. The ICs communicate with each other and the ECM through the release of growth factors, integrin interaction, calcium signaling and intracellular tension [Taylor, 2003]. Under normal conditions valvular cells are quiescent, and the ECM is well adapted to the surrounding hemodynamic environment. When stimulated by mechanical loading, the ICs are activated and mediate connective tissue remodeling to restore the normal stress profile in the tissue. In this process the IC

phenotype also changes in response to different mechanical forces. When equilibrium is restored in the mechanical environment, the cells return to the quiescent state [Aikawa, 2004]. During valvular pathologies IC dysfunction sometimes results in thickening of leaflets and a highly abnormal layered architecture, as seen in myxomatous leaflets. Under these conditions ICs exhibit activated myofibroblasts' features, express elevated levels of proteolytic enzymes, retain the ability to express interstitial collagen, and significantly increase in number in the spongiosa [Rabkin, 2001]. These findings suggest that matrix metabolism dysfunction modulates the abnormalities in collagen and other ECM components under pathological conditions.

The results obtained in the current study suggest that the normal physiological mechanical forces provided by the organ culture system are required to maintain the valvular cells' biosynthetic properties at native levels thereby increasing the durability of the leaflet tissue.

6.2.2. Hematoxylin and Eosin stain

Hematoxylin and Eosin (H & E) staining was used to observe any morphological changes in the valve leaflets. H & E staining of the tissue sections in Fig 5.15 shows that the three-layered aortic leaflet architecture was preserved in the cultured valve leaflets and was comparable to fresh leaflets. Elastic fibers can be observed along the ventricularis region, and the collagen crimp was observed in the fibrosa. The spongiosa layer can be seen as a loose tissue structure, distinctly separating the ventricularis and fibrosa. There was also no observable change in the thickness of the three layers compared to the fresh control leaflets. In a previous study, aortic valve leaflets when subjected to constant static

hypertensive and sever hypertensive pressures showed a decrease in thickness and cell number of the spongiosa layer compared to static control leaflets [Xing, 2004a]. The decrease in thickness was attributed to greater compression of the spongiosa (since it consists of 70% water) compared to the fibrosa or ventricularis. Cell numbers in the current study could not be compared between the valves of the three groups as they were from different animals with unique cellular distributions. The static control samples in the current study also had similar tissue architecture as compared to fresh and cultured valve leaflets. This observation was consistent with that seen in the previous studies.

Preserved leaflet morphology indicates structural integrity of the leaflets. Since there was no remodeling observed in the leaflets, it can be concluded that the system preserved the morphology of the leaflets.

6.2.3. Cell proliferation

Valve leaflets cultured in the *ex vivo* system were stained for proliferating cells to test whether the system provided a conducive environment for cell growth. Anti-BrdU stains of the leaflets, as seen in Figure 5.16, show proliferating cells distributed in all three layers of the cultured and static leaflets. This suggests that the system, apart from maintaining the viability of the cells, also provided the biochemical environment for cell proliferation. Cell proliferation in the aortic valve leaflets has not been demonstrated in the past. The result from the current study could not be compared to fresh leaflets since the leaflets were immediately fixed in formalin upon harvest. The cell proliferation protocol requires incubation of the leaflets in medium containing BrdU for at least 24 hours so that BrdU can be incorporated into proliferating cells. However, as this study

showed altered biological properties of the leaflet under static incubation, fresh leaflets were not incubated in the medium. Other methods previously studied in our laboratory to assess cell proliferation used a radio labeling technique. This method also requires incubation of the leaflets with the radiolabeled precursor. Hence, cell proliferation in fresh leaflets was not studied. Schneider and Deck have studied tissue and cell renewal, utilizing an autoradiography technique to identify DNA synthesis in rat aortic valve leaflets. They observed that DNA synthesis was more pronounced in growing rats than in mature rats. The pigs used in the study were mature pigs 2-3.5 years of age; hence only few cells were found proliferating. However, without any previous knowledge of valvular cell proliferation rate, a conclusion cannot be drawn on the total population size of proliferating cells in the current study. Additionally, it has been seen that ICs are quiescent when there are no changes in the surrounding mechanical environment of the cells [Aikawa, 2004]. ICs exhibit varied biological responses in accordance with changes in the surrounding mechanical environment and return to their quiescent state once they attain equilibrium in the new state. When cultured in the organ culture system valve leaflets experience a change from the previous *in vivo* environment to the new *ex vivo* environment. Thus, in this new mechanical environment, the cells might require longer than 48 hours to return to a quiescent state, which may explain the proliferation rates observed in this study.

Since the fresh leaflets in the current study did not contain BrdU in their proliferating cells, the leaflets were used as negative control to determine any background effects present in the cultured and static leaflets due to the staining. Quantitative analysis of the percent of proliferating *cells* showed that there was no significant difference

between the cultured and static leaflets suggesting that mechanical forces do not have any effect on the cell proliferation after 48 hours of ex vivo culture.

6.2.4. Cell apoptosis

Apoptosis in the valve leaflets was measured to test the ability of the system to maintain the viability of the valves without causing damage to the leaflet cells as a result of mechanical or biochemical conditions in the system. Figure 5.18 shows the presence of apoptotic cells distributed throughout the three layers of leaflets in the three study groups. Quantitative analysis of the percent population of apoptotic cells showed comparable levels of apoptosis between the fresh and cultured valve leaflets while static control leaflets showed a significant increase in apoptotic cells compared to the cultured ($p<0.05$) and fresh leaflets ($p<0.1$, $p=0.057$).

The absence of an increase in cell apoptosis in leaflets cultured in the organ culture system compared to the fresh leaflets suggests that there were no adverse changes in pH or nutrient transport, especially oxygen that would lead to cell death in the leaflet tissue. If there was insufficient oxygen in the system, ICs located in the interior of the leaflets would be less likely to survive as they are located farthest away from the oxygen and nutrient rich medium. Also, preliminary studies of valves cultured in the organ culture system without a gas exchanger showed increased cell death in all three layers of the leaflets compared to fresh control leaflets (data shown in Appendix D). In addition, cells from the interior of the leaflets appeared to be migrating towards either of the leaflet surfaces. Long term cell viability has always been an important design criterion for *in vitro* bioreactors. Hence, analysis of cell apoptosis is critical in the biological validation

of *ex vivo* organ culture systems. The small percentage of apoptosis seen in the cultured (1.64% ± 1.04%) and fresh valve leaflets (1.96% ± 0.41%) might have been induced during tissue harvest or handling while trimming and suturing the valve to the support ring. This is based on the argument that apoptosis in fresh valve leaflets can occur only during tissue harvesting and handling since the tissue was fixed within 3 hours after harvest. Comparable cell apoptosis between the fresh and cultured leaflets suggests that the apoptosis induced by the *ex vivo* organ culture system was negligible since tissue harvest and handling was performed using the same protocol for all the valves.

The increase in apoptotic cells observed in the static control leaflets is most likely due to the smaller volume of medium (10ml) used in the tissue culture plates, which possibly resulted in nutrient and/or oxygen limiting conditions. Also, altered metabolic activity in the valvular cells due to the absence of mechanical forces might have contributed to an increase in apoptosis compared to native tissue. Thus the amount of media and oxygen provided by the gas exchanger in the culture system was adequate and necessary for cell viability for a duration of 48 hours.

6.2.5. Cell phenotype

According to the current study's hypothesis, the cells in the cultured valve leaflets should not only maintain viability but also retain their native phenotype when subjected to physiological mechanical forces. An α- SMC actin immunofluoroscence stain of leaflet sections shown in Figure 5.20 suggests that the IC phenotype of the cultured valve leaflets was maintained at native levels in the organ culture system. Microscopic observation showed comparable actin expression in the ventricularis region of both fresh

and cultured leaflets. ICs exhibit different phenotypes depending on the surrounding microenvironment, and α- SMC actin is related to the contractile phenotype of SMC and myofibroblasts. α- SMC actin, which has an ability to polymerize under contraction, has two components; a monomeric form of globular protein called G-actin and a polymeric form of fibrous protein called F-actin. Since the leaflets *in vivo* have the ability to contract and relax, a dynamic equilibrium exists between polymerization of G-actin and depolymerization of F-actin to maintain the phenotype of the cells. The leaflets in the organ culture system, seen by visual observation, are subjected to similar movement as that experienced *in vivo*. Hence, the ICs in the cultured valve leaflets express actin in amounts comparable to those in fresh leaflets. Static leaflets, on the other hand, have no contractility once harvested from the body. Thus the equilibrium favors the depolymerization process, resulting in decreased F-actin. Also, polymerization of G-actin is absent in the cells leading to a low actin expression in the static leaflets as shown in the Figure 5.20. This observation was consistent with previous shear and pressure studies on valve leaflets [Weston, 2001; Xing, 2004a]. These studies showed that the effect of steady shear stress or pressure alone could not maintain the phenotype of the valvular cells at native levels, and the actin expression in these leaflets was comparable to statically incubated leaflets used in the studies. In another study cardiac fibroblasts were studied for α- SMC actin expression under the influence of mechanical stretch. The results showed that mechanical stretch down regulated α- SMC actin mRNA and protein content [Wang, 2001] in the fibroblasts. This suggests that mechanical forces others than pressure, shear stress or stretch must be affecting the cell phenotype of the leaflets. Studying the effects of isolated bending stresses or cyclic flexure on the leaflets may

provide information on the contractile phenotype of ICs. It has also been observed that SMC actin expression was altered by changes in culture conditions and mechanical and biochemical stimulation in cultured vascular cells [Stegemann, 2003a; Stegemann, 2003b]. Similar behavior was observed in a study with valvular ICs in 3D static collagen gel culture, which showed a reduction in α- SMC actin expression [Butcher, 2004a]. This suggests that matrix interaction plays a significant role in modulating cell phenotype. The results observed from 3D static culture of ICs were similar to those seen in the current study. Both studies noted a decrease in α-SMC actin compared to native levels, which suggests that mechanical forces are required to maintain the cell phenotype. Thus, another unique feature of the *ex vivo* organ culture system is that it provided the required mechanical environment to maintain the cell phenotype of the leaflets while preserving cell viability.

6.2.6. Endothelial cells

ECs on valvular surfaces provide a non-thrombogenic surface, transport nutrients, and facilitate transduction of mechanical and biochemical signals via the leaflet ECM. Presence of ECs on the leaflet surface was analyzed by immunohistochemical staining for vWF expressed by the cells. Figure 5.21 shows a weak stain for vWF on the valve leaflets in the three groups, which may be because of the choice of antibody used in the stain. Hence, scanning electron microscopy (SEM) was used to observe the surface of the leaflet tissue for the presence of ECs. SEM results presented in Figure 5.22, show ECs on all the three leaflet groups. ECs on the leaflet surfaces had a flattened morphology with a monolayer distribution of cells on the ventricularis surface The cells were

circumferentially aligned perpendicular to the flow direction, as observed in studies conducted by Deck [Deck, 1986]. All the SEM pictures taken were of the ventricularis surface of the valve leaflet because the fluid flow is in the radial direction on ventricularis surface thus providing a better representation of cell alignment with flow.

ECs on cultured valve leaflets appeared to be comparable to those on fresh control leaflets while those on static control leaflets lacked the flattened morphology of fresh leaflet ECs. This appearance of the cells might have been induced when the leaflets were placed in the culture plate for sectioning. Retention of ECs on the surface of the leaflets is important to provide appropriate cellular responses when culturing the tissue in the organ culture system. Absence or dysfunction of ECs adversely affects the biosynthetic, morphologic and metabolic functions of the valvular cells implicated in valvular diseases. Previous studies done in our laboratory have shown that denudation of the endothelium on valvular leaflets alters their biosynthetic response to shear stress. The denuded leaflets have shown an increase in sGAG synthesis with a concomitant decrease in collagen synthesis compared to leaflets with intact ECs. When subjected to steady laminar shear stress at 20 dyne/cm^2, valvular ECs showed different organization of focal adhesion complexes and cell alignment than those in static culture. This suggests that mechanical forces have a unique influence on the phenotype of valvular ECs [Butcher, 2004b]. Also, it was observed that the valvular ECs were aligned perpendicular to the flow unlike vascular cells, which align parallel to the flow. This alignment corresponds to the circumferential alignment of the ECs in valve leaflets, since the fluid flow is in radial direction. The EC alignment on valve leaflets cultured in the organ culture system in the current study is in agreement with the result seen above with valvular EC culture.

Additionally, no altered biological responses compared to fresh leaflets were observed in cultured valve leaflets in the current study. Hence, it can be concluded that normal function of ECs was maintained in the organ culture system. However, there might have been a change in EC function in static leaflets in the current study that may have lead to the differences in sGAG, elastin, α-SMC actin, cell apoptosis compared to cultured and fresh leaflets. Hence, it can be inferred from this study that the sterile *ex vivo* organ culture system preserved the native morphology of the leaflets by maintaining the valvular cells in their normal microstructural environment.

The valve leaflets are dense, heterogeneous, layered structures with cells within each layer having different viabilities and phenotypes. If these cells are cultured in a monolayer, they are unlikely to behave in a similar fashion as when cultured along with their native 3D ECM. *In vivo* studies, on the other hand, provide the advantage of studying various biological mechanisms in native mechanical and biomechanical environments. However, they are limited due to the expenses incurred in conducting the experiments. Also, the mechanical conditions involved in the study cannot be closely controlled or regulated. Organ culture studies incorporate advantages of both *in vitro* and *in vivo* studies and provide well-controlled biomimetic micro-environments resembling the native state. These systems are economical and provide independent control of mechanical forces facilitating the simulation of clinically relevant mechanical conditions to study valvular diseases pathogenesis and development to provide a comprehensive understanding of the physiology and pathology of heart valves.

6.3. Model of cellular responses to forces

The results from this study suggest that normal physiological forces are required by the aortic valve leaflets to maintain the native biosynthetic activity of the leaflets and preserve the normal interstitial cell phenotype without remodeling of the leaflet tissue. A schematic of the action of mechanical forces on the valve leaflet is shown in Figure 6.1, and a mechanism of interaction of valvular cells with the ECM in response to the mechanical forces is illustrated in Figure 6.2. Valve leaflets subjected to shear and bending stresses, pressure, fluid flow and cyclic flexure during each cardiac cycle transmit the forces to the cells within the ECM of the leaflet via cyclic tensile deformation of the matrix. Valvular cells are linked to the collagen fibers of the leaflet matrix, and when mechanical forces on the leaflet surface cause deformation of the leaflet matrix, the cells experience the tensile forces created by the deformation. Mechanical forces on the aortic and ventricular surfaces of the leaflet stretch the surfaces relative to each other creating a certain degree of tension within the fiber network of the tissue. These tensile forces may then be communicated to individual cells and, subsequently, to the cell nuclei. Thus, mechanical stimulation may affect the biosynthetic activity, cell proliferation and death, cell phenotype, tissue remodeling, cellular secretions and immune responses of tissues.

Since the cultured valve leaflets in the organ culture system experience similar mechanical conditions to *in vivo* valve leaflets, they also express similar biological responses to those of fresh control leaflets. Altered biological responses in the static control leaflets may thus be related to the absence of these mechanical forces.

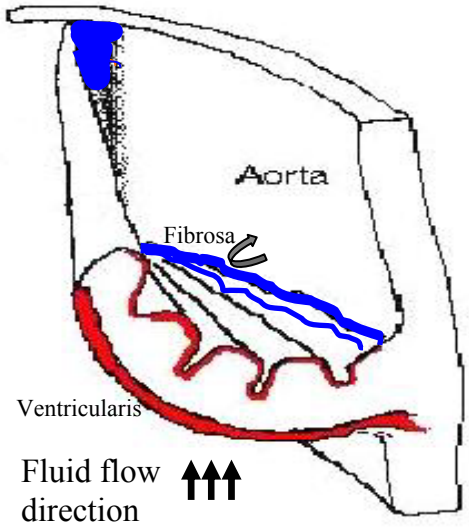

Figure 6.2: This schematic shows forces acting on the valve leaflet. Black arrows indicate fluid flow direction. Shear stresses act on both ventricularis and fibrosa surfaces (indicated by a curved arrow). Bending stresses on the leaflet are shown in blue. Pressure forces act on both the ventricularis and fibrosa surfaces during the diastolic and systolic phases of the cardiac cycle. Tensile strain on the leaflet is shown in red.

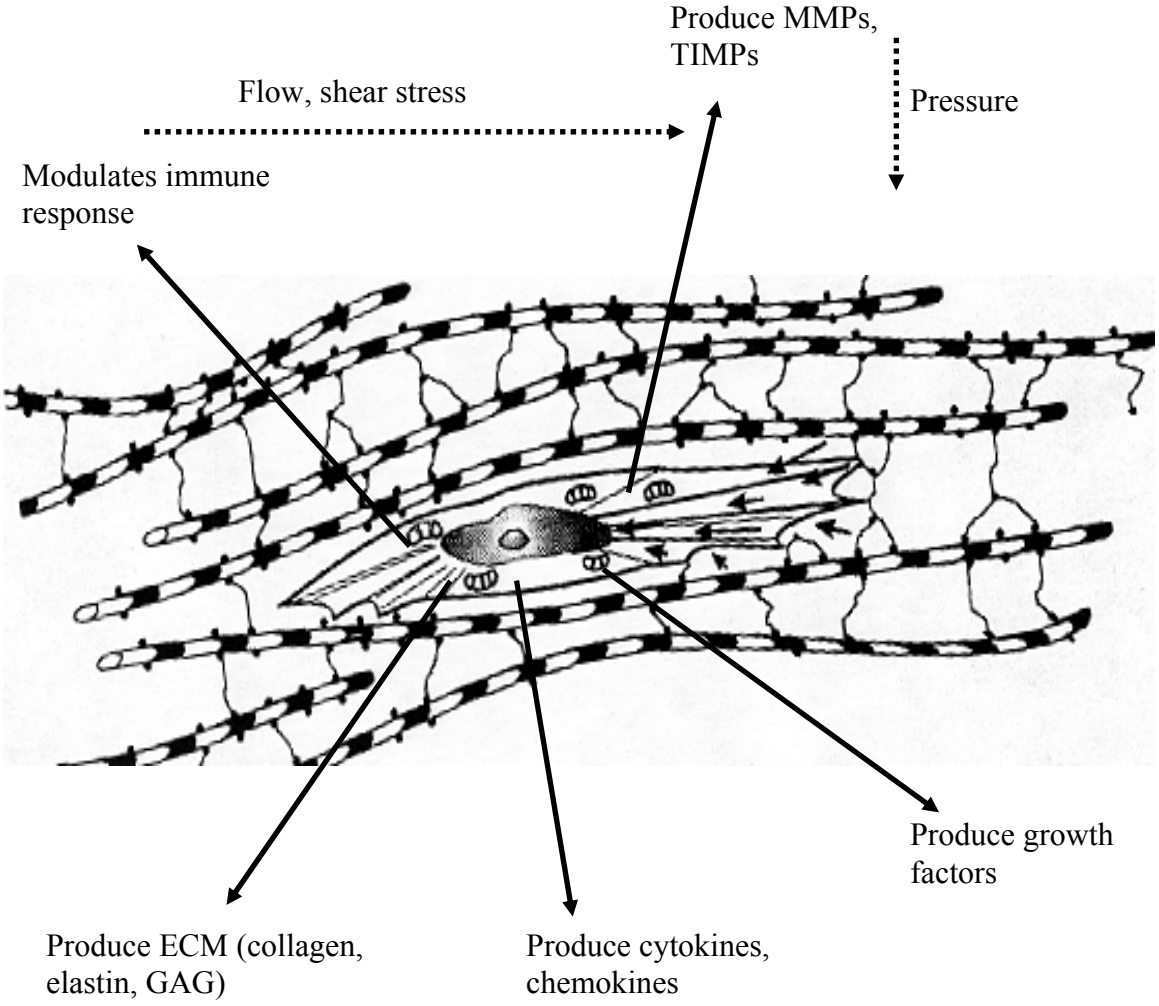

Figure 6.3: This schematic illustrates a cell within the tissue structure, which is mechanically linked to the connective tissue by fibers. The figure is a small section of the whole leaflet, which has many cells scattered throughout the matrix. When the leaflets are stretched, the cells mechanically linked to matrix by fibers, experience the tensile forces induced by the stretching. The cells respond to these forces by producing ECM components, cell proliferation and death, changes in cell phenotype, tissue remodeling, cellular secretions and immune responses.

6.4. Limitations of the study

The limitation of the current study can be divided into two areas: (1) Organ culture system; and (2) Cell proliferation and apoptosis.

The first limitation of the study was the complication in design of the organ culture system preventing periodic withdrawal of samples to check the pH, oxygen and glucose content in the medium. This limited a regulated control of pH and CO_2/O_2 level in the system. However, the pH readings of the medium at the end of the experiments showed the values were within the physiological range, and the histological results indicated that there were no adverse changes in the biochemical conditions of the system. But periodic check of the values will provide detailed information of the biochemical environment of the system. Another limitation was the size of the aortic valve holder. The holder was designed for 25 mm root diameter valves, which prevented valves having an aortic root diameter greater than 25 mm from being placed in the valve holder. The ligated coronary arteries of the aortic valve with bigger aortic root diameters created folds in the aorta when placed in the valve holder. These folds obstructed the aortic orifice area and thus restricted proper leaflet movement. The reduction in orifice area and impaired movement of the valve leaflets caused an increase in pressure load on the leaflets leading to tears in the leaflets. Hence, the valves used for the study were carefully chosen before suturing.

Cell proliferation in the current study could not be compared to that of fresh leaflets as it was undesirable to incubate fresh leaflets under static conditions. Hence, the study was limited in this aspect since there was no method of studying cell proliferation in fresh native leaflets. Apoptosis observed in the cultured leaflets is believed to be

induced during tissue harvest and suturing of the valve to the support ring for culture in the system. This assessment is based on comparison of the results with those of fresh leaflets. Fresh leaflets were fixed within 3 hours of harvest, and the percentage of apoptotic cells for the fresh and cultured leaflets was comparable. Thus, the apoptosis in the cultured leaflets most likely occurred during tissue harvest and was not system induced. The elevated level of apoptosis in the static leaflets is most likely due to nutrient limitation as opposed to a lack of mechanical stimulation, which is a drawback of the experimental protocol. Additionally, the activated caspase-3 IHC used for analyzing apoptotic cells might have underestimated the actual number of apoptotic cells, as caspase-3 belongs to a subclass of a wide range of caspases that are activated during apoptosis occurring via various pathways. This narrowed the study to apoptotic cells that follow the pathway leading to the activation of caspase-3. A live/dead stain would have provided more accurate results, but preliminary studies with such a stain overestimated the number of dead cells by staining cells positive for necrosis. Further studies to optimize the apoptosis stain should be done to obtain a closer approximation of apoptotic cells. Finally, the medium used for culture did not have the same viscosity as that of blood. It is known that changes in fluid viscosity alter the shear stresses acting on the valve leaflets. Experiments have not been conducted in the past or in the current study to investigate the effects of viscosity on changes in biological properties induced by shear stress. This is another limitation of the study.

6.5. Significance of the study

The *ex vivo* organ culture system developed in this study is novel with respect to the following features; (1) controllable flow and pressure conditions; (2) sterility for 96 hours; (3) provided adequate oxygen transport to the valve; (4) cell viability for 48 hours; and (5) preserved morphology and cell phenotype. Results from the study showed that under normal physiological conditions the cells maintain their native biosynthetic activity, morphology, and contractile phenotype compared to cells cultured under static atmospheric conditions. This suggests that physiological mechanical forces are required to maintain the structural integrity of the leaflet tissue and regulate cell signaling within the matrix for proper functioning of the leaflets. Further, the organ culture system can be used to simulate clinically relevant mechanical conditions to study the effects of altered mechanical forces or EC dysfunction on valve leaflets that are implicated in various aortic valve leaflet pathologies. Recent studies have shown that aortic cusp tissue has regional and directional contractile responses to different vasoactive agents [Kershaw, 2004]. Similar studies done in a circulation system mimicking the physiological conditions such as this organ culture system could provide a better understanding of the contractile effects to help predict *in vivo* valvular mechanisms. Such studies can then be extended to study the effect of pharmacological stimuli on the biology of native valve leaflets. Since native phenotypic characteristics of the leaflets can be maintained in the system for a minimum of 48 hours, and the system has been shown to sustain long term culture periods, the system can be used to improve the mechanical characteristics of tissue engineered valve constructs. This can be achieved either by dynamic seeding of acellular scaffolds in the system or mechanical conditioning of engineered constructs.

Also, the system can be used to test the structural integrity of different scaffolds or engineered constructs before implantation *in vivo*.

CHAPTER 7

CONCLUSIONS

The work done for this thesis successfully developed a novel *ex vivo* organ culture system that is capable of simulating normal physiological mechanical forces for a duration of 96 hours while maintaining consistency in the flow and pressure waveforms. The system was able to attain a cardiac output of 3.8-4.2 L/min with a peak flow rate of 24 L/min and systolic/diastolic pressures of 120/80 mmHg, 160/120 mmHg and 190/150 mmHg at a frequency of 1.167 Hz as well as a cardiac output of 7.5 L/min at a mean aortic pressure of 100 mmHg and heart rate of 2 Hz. Additionally, flow rate, pressure and heart rate can be controlled independent of each other to reproduce different clinically relevant mechanical conditions. Oxygen exchange in the system was also able to meet the required oxygen consumption by aortic valve leaflets while maintaining sterility to maintain the viability of the valvular cells. The pH at the end of experiments was found to be in the range of 7.3-7.5, which is in physiological range for the valve leaflets. The system did not induce any adverse mechanical and environmental effects on the native valve leaflets and provided sufficient nutrient transport to the valves under normal mechanical loading. This is the first work to address oxygenation of medium in a closed system to ensure sufficient transport of nutrients to the aortic valve for extended periods of operation. The system has also been shown to retain native morphology, ECM structural integrity, and cell phenotype of the leaflets for a period of 48 hours.

The results of the biological study prove that a dynamic mechanical environment is required to maintain the native biological characteristics of porcine aortic

heart valves when cultured under *ex vivo* conditions. In the absence of the appropriate mechanical signals, cells undergo a phenotypical change and loose their contractility. In addition, the ECM content undergoes significant changes, possibly due to a reduction in cellular biosynthetic activity. The current system preserved the morphology and leaflet architecture without any remodeling in the tissue. The cells were viable and retained their native phenotype in the leaflets. Finally, this study highlights the utility of dynamic *ex vivo* organ culture studies since cells are retained in their natural 3-D environment, and the mechanical conditions can be well defined and controlled.

CHAPTER 8

FUTURE WORK

The *ex vivo* organ culture system offers the ability to independently control flow rate, pressure, and heart rate in the system. This can potentially be used to operate the system at elevated mechanical conditions to simulate hypertensive, severe hypertensive, and elevated heart rate conditions *ex vivo*. Hypertensive and severe hypertensive blood pressures are related to heart failure, stroke, coronary and peripheral vascular diseases, valve calcification as well as other cardiovascular pathologies. Characterizing the biological properties of native aortic valves at such elevated conditions can provide insight into the biological changes of the leaflets following exposure to extreme conditions that may lead to valve failure. Experiments that subjected aortic valve leaflets to constant and mean pulsatile pressures of 140 and 170 mmHg showed increase in the protein and sGAG syntheses of the leaflets in response to increase in pressure [Xing, 2004a; Xing, 2004b]. This suggests that leaflets remodel in response to mechanical loading. An in-depth understanding of the biological changes in the leaflets can be attained by studying the valve leaflet biology in the pulsatile organ culture system at clinically relevant mechanical conditions. Further, carrying out the study at a genetic level in addition to a molecular level would enable an understanding of cross talk within the leaflets in response to physiological and pathophysiological forces. In addition knowledge on mechanotransduction within the cells, and changes in responses of the genes and protein expression, which are responsible for triggering the synthetic activity, protein degradation, and remodeling in the leaflets can be attained. Thus, these

experiments, apart from increasing the basic understanding of heart valve function, can be used to study the effects of hemodynamics on cell-cell interactions, cell-ECM interaction, ECM deformation affecting cell growth and gene expression.

Another area of study is to understand the effect of endothelial dysfunction on valvular pathogenesis. Endothelial dysfunction caused by mechanical forces, bacterial infection, autoantibodies, and circulating modulators of ECs has adverse effects on the biosynthetic, morphologic and metabolic functions of the valvular cells. Valvular diseases such as senile degenerative valve diseases, myxomatous (or floppy) valves, rheumatic and infective endocarditis valves are actively related to endothelial dysfunction. Disruption of ECs by mechanical stresses or other factors causes injury to the leaflets allowing inflammatory cells to enter and thus develop valvular diseases. Conditions of endothelial injury can be simulated *ex vivo* by denuding the leaflets and subjecting them to mechanical stresses. Preliminary studies in our laboratory have shown altered responses of denuded leaflets to shear stresses causing an increase in sGAG synthesis and decrease in collagen synthesis compared to leaflets with intact endothelium. Hence, studies done by denuding one, two or three of the leaflets of the aortic valve in a randomized manner would provide an understanding on changes in valvular responses to mechanical forces and physiological repair processes of the valve.

A third area of study is to investigate the mechanical forces responsible for maintaining the cell phenotype of the aortic valve ICs. It has been seen that the cell phenotype can be maintained at the native level in the leaflets cultured under physiological forces in the organ culture system. While valve leaflets subjected to isolated effects of shear stress, fluid flow, and constant and cyclic pressure decreased

their native content of α-SMC actin. Hence further experiments should be done to study the effects of bending stresses or cyclic flexure on cell phenotype of the valve leaflets. Previous studies on the effect of mechanical stretch on cardiac fibroblasts showed that α-SMC actin mRNA decreased in the *in vitro* cell culture compared to native amounts - [Wang, 2001]. However, cyclic tensile stretch of the leaflets is important in maintaining proper coaptation of the valve and is also known to regulate collagen synthesis in the valve leaflets [Carver, 1991]. Hence, the effect of cyclic tensile stretch at different frequencies should be studied to characterize the biological responses of the leaflet.

A recent study on the effects of vasoactive agents on contractility of aortic valves [Kershaw, 2004] suggests regional variation in leaflet contraction. Similar studies could be done in the organ culture system to investigate the effects of pharmacological stimuli on valve leaflets under physiological conditions. Further, the system could be used to test the structural integrity of acellular constructs under mechanical loading. The results from all these studies could be used as a standard of comparison while testing the performance of tissue engineered heart valves.

APPENDIX A

MACHINE DRAWINGS

A.1. Machine drawings of the aortic valve holder

This section includes machine drawings of aortic valve holder components. The inlet, center and outlet component drawings of the holder are shown respectively. All the dimensions in the drawings are given in inches.

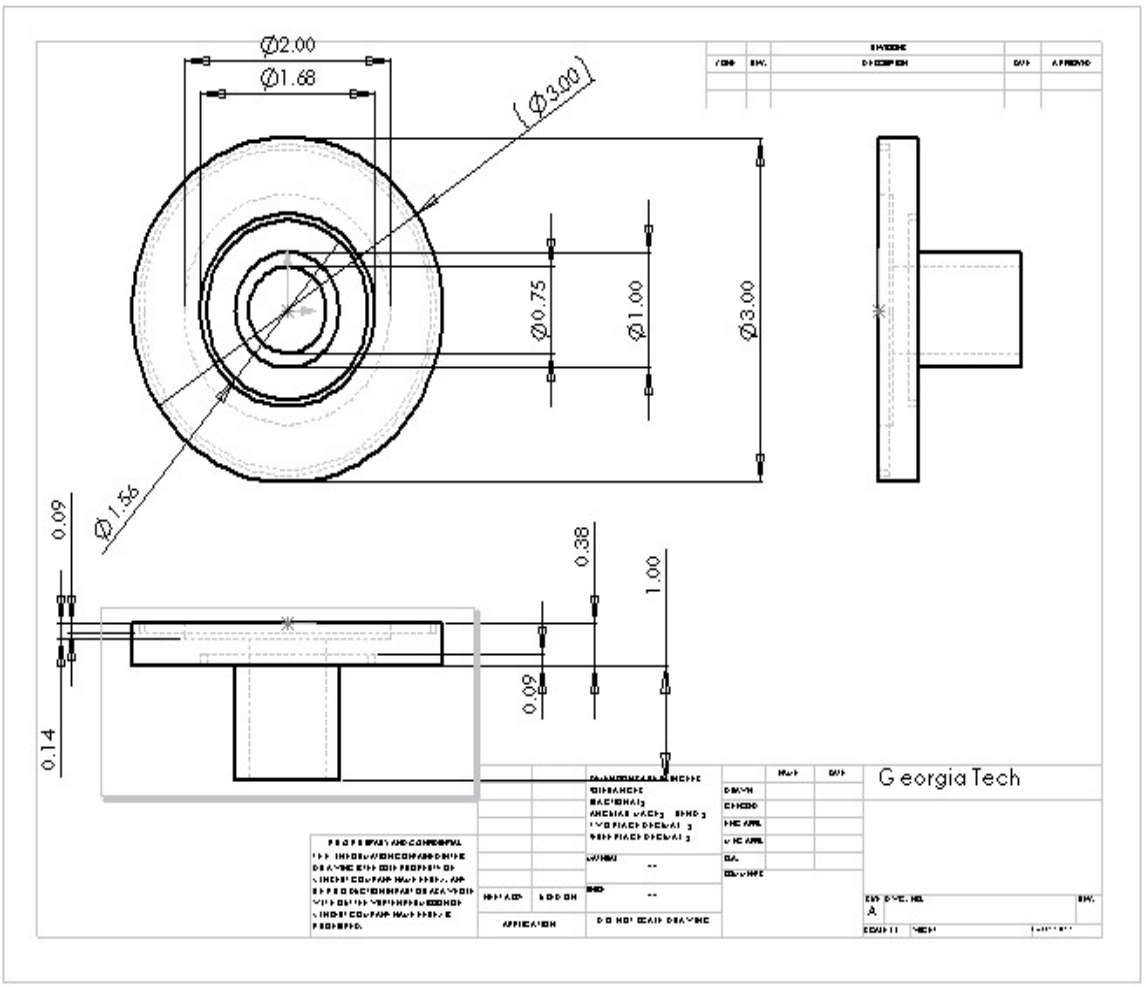

Figure A.1. Drawing shows inlet component of the aortic valve holder. All the dimensions are given in inches.

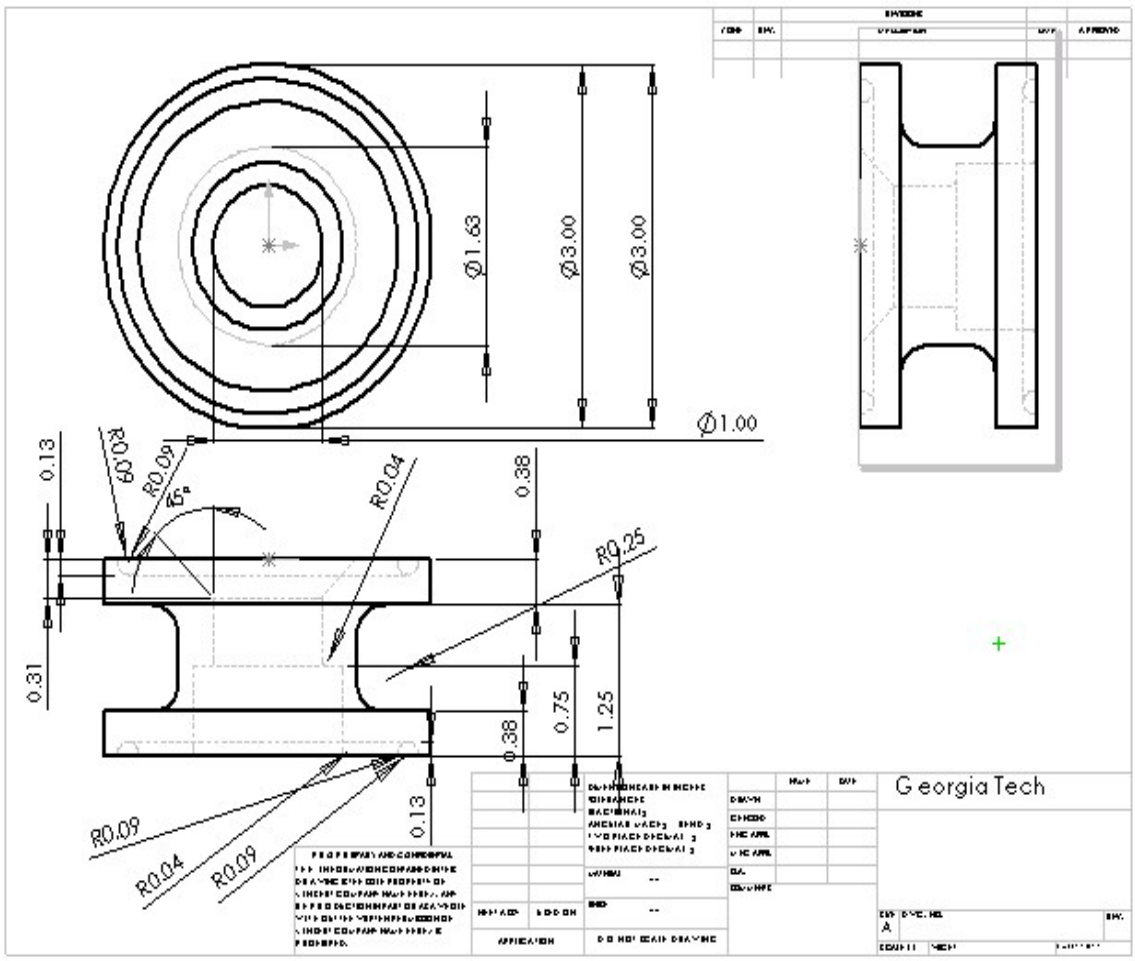

Figure A.2. Drawing shows center component of the aortic valve holder. All dimensions are in inches.

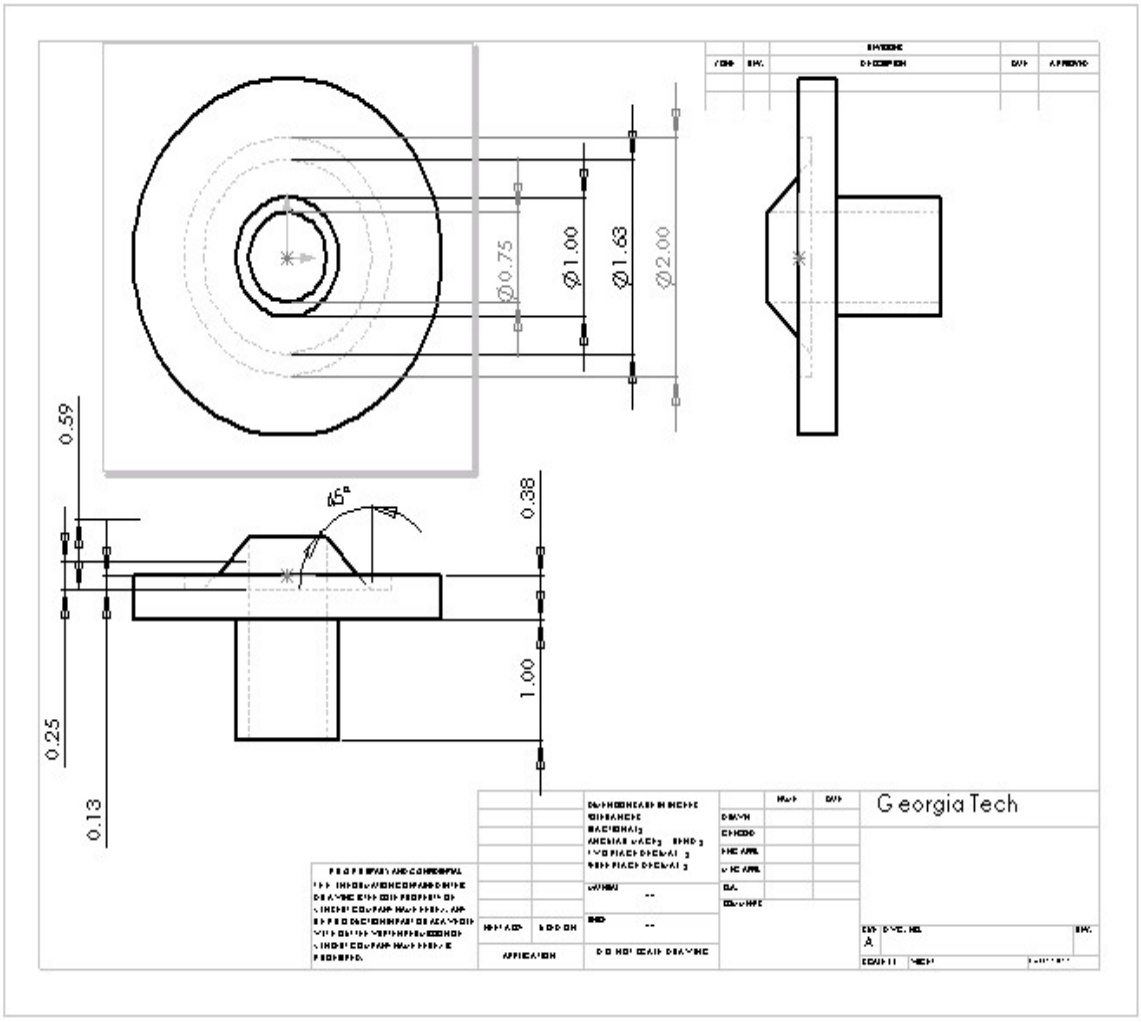

Figure A.3. Drawing shows outlet component of the aortic valve holder. All dimensions are in inches.

A.2. Machine drawings of the membrane chamber

The drawings of the water side and membrane side of the membrane chamber, respectively, are show in this section. All the dimensions are in inches.

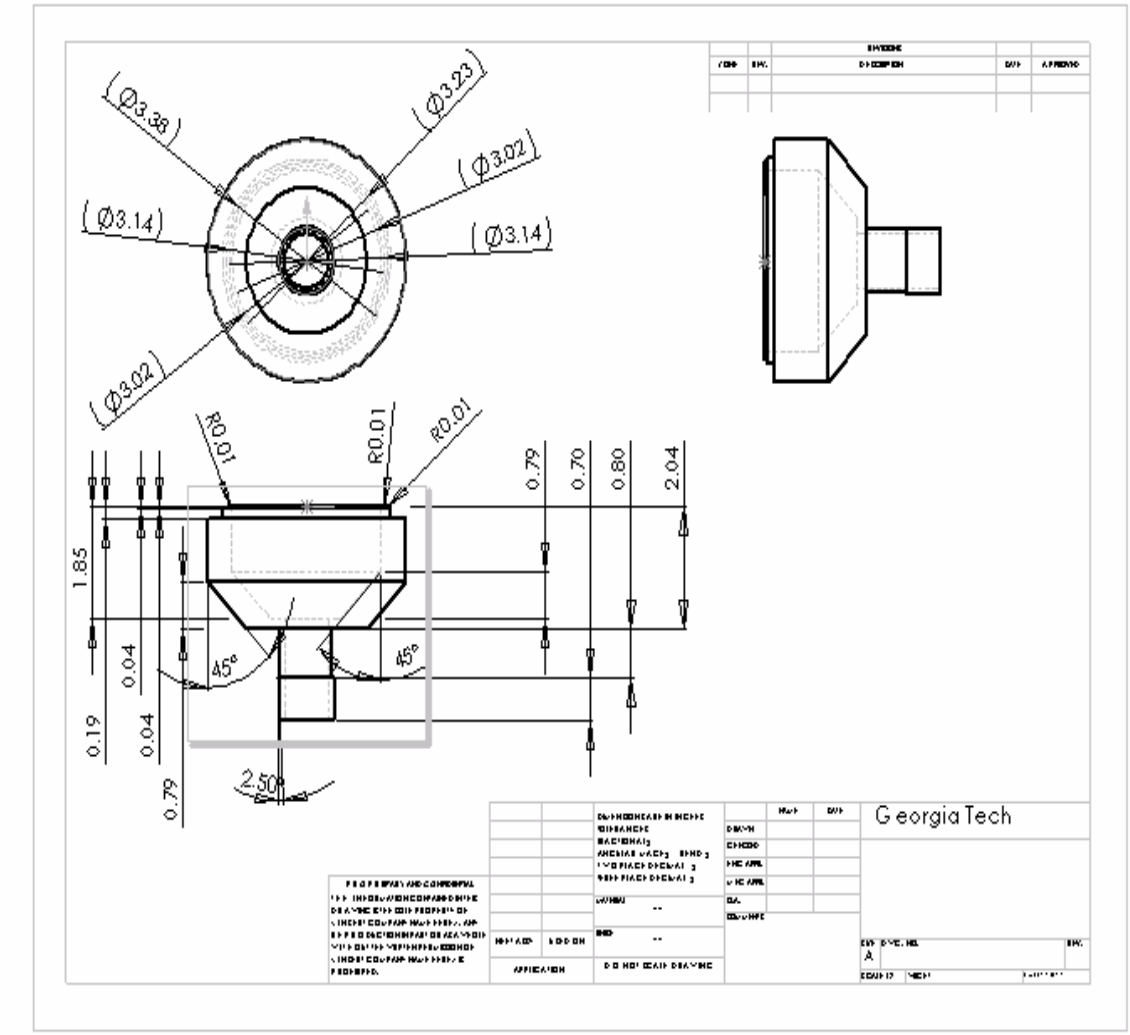

Figure A.4. Drawing of membrane chamber component on the water side of the organ culture system. All dimensions are in inches.

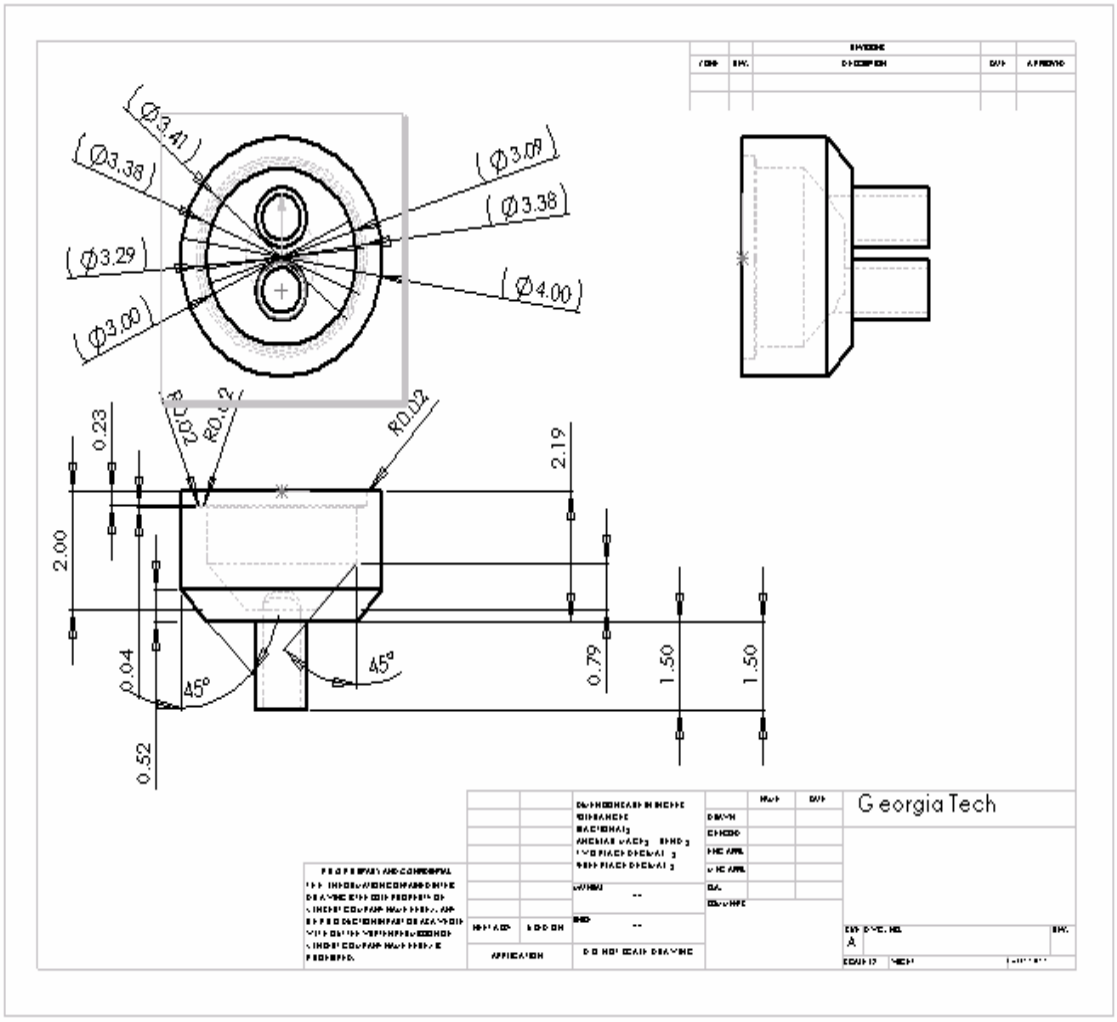

Figure A.5. Drawing of the membrane chamber component on the medium side of the organ culture system. All dimensions are in inches.

A.3. Machine drawing of the pump head

This section shows the drawing of pump head with all dimensions in the drawing in inches.

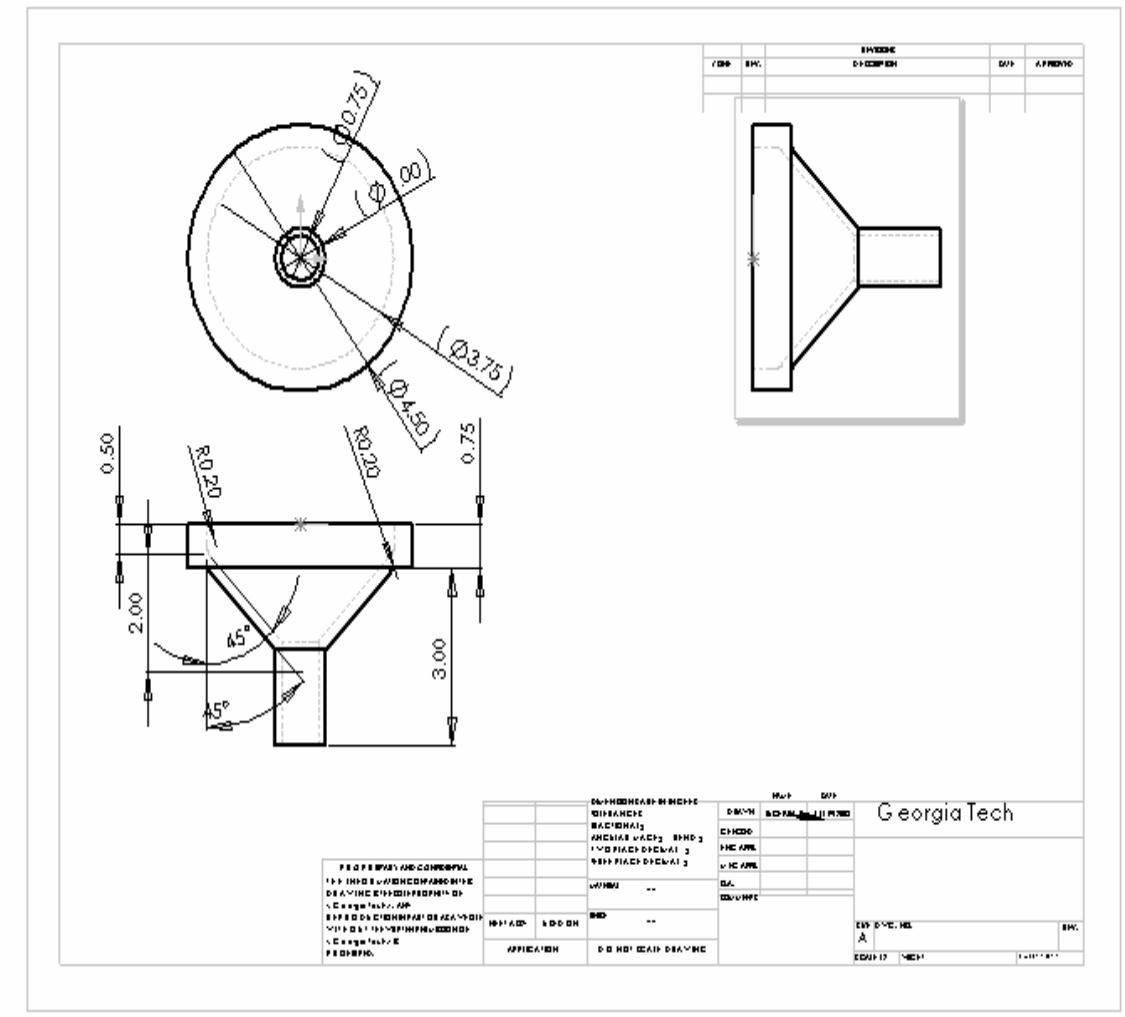

Figure A.6. Drawing of the pump head of the organ culture system. All dimensions are in inches.

APPENDIX B

ASSAY PROTOCOLS

The sections B.1, B.2, B.3 below outline the protocols used for estimating collagen, sGAG and elastin contents respectively in the valve leaflets.

B.1. Estimation of Collagen content

1) Determine dry weight of the tissue sample and digest the tissue with pepsin dissolved in 0.5M acetic acid (buffer) for 48 hours at 37^{o}C or 24 hours at 60^{o}C. The ratio of dry tissue weight : enzyme weight is 1:3.
2) Prepare reagent blank (0.5 M acetic acid), collagen standards (aliquots containing 5, 10, 25, 50µg) and test samples (100µl) and bring the solutions to 100µl using buffer in a 1.5ml micro centrifuge tubes.
3) To each tube add 1 ml of Sircol Dye reagent and cap all the tubes to mix the contents on a vortex mixer for 30 minutes at room temperature.
4) Transfer the tubes to micro centrifuge and spin the tubes at >10000 × g for a 10 minute period.
5) The unbound dye solution is removed by carefully inverting and draining the tubes. Any remaining droplets are removed from the tubes by gently tapping the inverted tube on a paper tissue, or a cotton wool bud is used for removing the droplets from the rim of the tubes.
6) To each tube add 1ml of alkali reagent and then mix the contents on a vortex mixture until the bound dye is dissolved.

7) Transfer 200µl aliquots of samples from tubes to the wells of a 96 well, multiwell plate and absorbance readings are taken using spectrophotometer set at a wavelength of 540nm.
8) Subtract the reagent blank reading from the standard and test sample readings.
9) Plot standards on graph and use the graph to calculate content of the test sample.

B.2. Estimation of sGAG content

1) Determine dry weight of the tissue sample and digest the tissue with protease dissolved in 0.1M tris- acetate with 10mM calcium acetate (buffer) for 48 hours at 37^{o}C or 24 hours at 60^{o}C. The ratio of dry tissue weight : enzyme weight is 1:30.
2) Prepare reagent blank (buffer), sGAG standards (aliquots containing 1, 2, 3, 4, 5µg) and test samples (100µl) and bring the solutions to 100µl using buffer in a 1.5ml micro centrifuge tubes.
3) To each tube add 1ml of Blyscan dye reagent and cap all the tubes to mix the contents on a vortex mixer for 30 minutes at room temperature.
4) Transfer the tubes to micro centrifuge and spin the tubes at >10000 × g for a 10 minute period.
5) The unbound dye solution is removed by carefully inverting and draining the tubes. Any remaining droplets are removed from the tubes by gently tapping the inverted tube on a paper tissue, or a cotton wool bud is used for removing the droplets from the rim of the tubes.
6) To each tube add 1ml of dissociation reagent and then mix the contents on a vortex mixture until the bound dye is dissolved.

7) Transfer 200µl aliquots of samples from tubes to the wells of a 96 well, multiwell plate and absorbance readings are taken using spectrophotometer set at a wavelength of 656nm.
8) Subtract the reagent blank reading from the standard and test sample readings.
9) Plot standards on graph and use the graph to calculate content of the test sample.

B.3. Estimation of Elastin content

1) Determine dry weight of the tissue sample and digest the tissue with protinase K dissolved in 50mM tris-HCl, 0.1M EDTA and 0.2M NaCl (buffer) for 48 hours at 37^{o}C or 24 hours at 60^{o}C. To each sample add 0.5mg/mL of enzyme and 0.1mg/mL of SDS.
2) Precool elastin precipitating reagent in fridge before use.
3) Prepare reagent blank (buffer), elastin standards (aliquots containing 12.5, 25, 50, 75µl) and test samples (100µl) and bring the solutions to 100µl using buffer in a 1.5ml micro centrifuge tubes.
4) Add 1ml of cold elastin precipitating reagent to each tube and incubate the tubes in ice-water overnight.
5) After incubation, change the tubes from ice-water to ice and incubate for 30 minutes to bring samples to 0^{o}C.
6) Centrifuge tubes and gently tap on paper towel to remove excess supernatant.
7) Add 1ml of Fastin dye reagent and 200µl of 90% saturated ammonium sulfate and cap the tubes to vortex the solution until elastin is back in solution.
8) Mix the contents at room temperature on a vortex mixer for 1 hour.

9) Transfer the tubes to micro centrifuge and spin the tubes at >10000 × g for a 10 minute period.
10) The unbound dye solution is removed by carefully inverting and draining the tubes. Any remaining droplets are removed from the tubes by gently tapping the inverted tube on a paper tissue, or a cotton wool bud is used for removing the droplets from the rim of the tubes.
11) To each tube add 1ml of dissociation reagent and then mix the contents on a vortex mixture until the bound dye is dissolved.
12) Transfer 200µl aliquots of samples from tubes to the wells of a 96 well, multiwell plate and absorbance readings are taken using spectrophotometer set at a wavelength of 513nm.
13) Subtract the reagent blank reading from the standard and test sample readings.
14) Plot standards on graph and use the graph to calculate content of the test sample.

APPENDIX C

QUALITATIVE STUDIES

This appendix outlines the protocols used for the various histological stains and SEM study for valve leaflet analysis.

C.1. Hematoxylin and Eosin stain

This stain is done automatically in an autostainer. The protocol is as follows:

1) Immerse the slides in xylene substitute three times for 5 minutes each at room temperature.
2) Immerse the slides to 100% alcohol three times at room temperature. The first treatment is for 3 minutes followed by 2 minutes for the other two treatments.
3) Immerse the slides in 95% alcohol for 2 minutes at room temperature.
4) Wash the slides in 70% alcohol for 2 minutes at room temperature.
5) Wash the slides in water for 2 minutes at room temperature.
6) Immerse the slides in hemotoxylin for 30 seconds at room temperature.
7) Wash the slides in water for 1 minute at room temperature.
8) Immerse the slides in acid alcohol for only 1 second at room temperature.
9) Wash the slides in water for 1 minute at room temperature.
10) Immerse the slides in Scott's solution for 30 seconds at room temperature.
11) Wash the slides in water for 2 minutes at room temperature.
12) Immerse the slides in 95% alcohol for 1 minute at room temperature.
13) Immerse the slides in alcoholic eosin for 30 seconds at room temperature.
14) Immerse the slides in 95% alcohol for 30 seconds at room temperature.

15) Immerse the slides in 100% alcohol three times at room temperature. The first treatment is for 1 minute and the other two are for 2 minutes each.
16) Immerse the slides in xylene substitute twice for 2 minutes each at room temperature.
17) Finally, immerse the slides in xylene for 1 minute at room temperature.

Reagents and Solutions

Hematoxylin

Dilute Gill's hematoxylin no.2 (Polysciences #04570) one to one with dH2O before use.

1% Acid Alcohol

2ml HCl (Fisher #A144s) in 198ml of 70% ethanol.

Scott's Solution

$NaHCO_3$	2g
$MgSO_4 \cdot 7H_2O$	20g
dH_2O	1000ml

Mix until dissolved.

Alcoholic Eosin

1% alcoholic eosin (VWR # VW3403-2).

C.2. 5-Bromo deoxyuridine immunohistochemistry

1) Deparaffinize slides in xylene substitute and rehydrate fixed paraffin embedded tissue in descending grades of alcohol. Wash sections in 1X PBS for 5minutes.

2) Proteolyse fixed, paraffin embedded sections by typically treating with 1µg/ml proteinase K for 10 minutes at room temperature.
3) Wash slides in 1X PBS twice for 5 minutes each at room temperature.
4) Immerse slides in 4N HCl for 10 minutes at room temperature.
5) Immerse slides in 1X TBE, pH 8.4 for 5 minutes at room temperature.
6) Immerse slides in 1X PBS. Check pH of buffer after 2 minutes. Apply primary antibody once pH is 7.0-7.5.
7) Prepare the working dilution of the primary antibody in 1% crystalline grade BSA in 1X PBS. Use anti-BrdU (Dako #M744) at 1:20 dilution. Blot off PBS and apply 150µl of working dilution. Incubate sections in a humid chamber for 1hour at room temperature.
8) Blot of excess antibody and wash slides in 1X PBS twice for 5 minutes each at room temperature.
9) Prepare working dilution of the secondary antibody (Vector #BA2001: biotinylated horse anti-mouse IgG) in 1% BSA/PBS and add 2% normal horse serum. Prepare the secondary antibody at a 1/400 dilution. Apply 150µl of antibody and incubate 30 minutes at room temperature in a humid chamber.
10) Prepare the working dilution of ABC-Vector Red complex from the alkaline phosphatase standard kit (Vector #AK-5000) after application of secondary antibody. Mix 5ml of 1X PBS, one drop of reagent A, and one drop of reagent B and allow to sit at room temperature, 30minutes prior to use.
11) Blot off excess antibody and wash slides in 1X PBS twice for 5 minutes each at room temperature.

12) Apply 150µl of prepared ABC mixture to each slide. Incubate in a humid chamber 1hour at room temperature.
13) Blot off excess solution and wash slides in 1X PBS twice for 5 minutes each, followed by one wash in 100mM tris pH 8.2 for 5 minutes.
14) Make up alkaline phosphatase substrate solution (Vector #SK-5100) immediately before use. Add 5ml of 100mM tris pH 8.2, one drop levamisole (Vector #SP-5000), two drops each of reagent one, two, and three to a foil wrapped bottle. Mix and apply 2-3 drops per section. Incubate slides in the dark for 20-30 minutes, checking color reaction periodically. Stop reaction by blotting off substrate and rinsing in tap water twice for 5 minutes each.
15) Lightly counter stain sections with Gill's hematoxylin (about 20 seconds). Rinse slides well in water until water is clear. Dip once in 1% acid alcohol and rinse well in water. Immerse in Scott's solution 20 seconds and rinse in water. Dehydrate through graded alcohols, then xylene and coverslip for viewing.

Reagents and Solutions

Anti-BrdU: DAKO #M0744 Clone Bu20a

Proteinase K

Dissolve proteinase K (Sigma # P-4914) in dH2O for a stock concentration of 20mg/ml. Aliquot and store at -20 C.

1%BSA/PBS

1g fraction V BSA (Sigma #A2153) in 100ml 1X PBS.

Mix until fully dissolved. Aliquot into 5ml volumes and store at -20 C.

C.3. Activated caspase 3 immunohistochemistry

1) Deparaffinize and rehydrate fixed paraffin embedded tissue in descending grades of alcohol. Wash sections in 1X PBS 5minutes.
2) Antigen retrieval: treat tissue sections with 1μg/ml proteinase K for 10 minutes at room temperature.
3) Wash slides in 1X PBS twice for 5 min. each at room temperature.
4) Block tissue using 1% gelatin/PBS mixture for 20 minutes at room temperature.
5) Prepare the working dilution of rabbit anti-human caspase 3, activated (Sigma#C8487) in 1%BSA in 1X PBS at a dilution of 1:400. Blot off gelatin/PBS and apply primary antibody. Incubate sections in a humid chamber for 1hour at room temperature.
6) Blot of excess antibody and wash slides in 1X PBS twice for 5 minutes each at room temperature.
7) Prepare working dilution of biotinylated goat anti-rabbit IgG antibody in 1%BSA in 1X PBS, and add 2% of normal goat serum. Prepare secondary antibody at 1/400 dilution. Apply antibody and incubate 30 minutes at room temperature in a humid chamber.
8) Prepare the working solution of ABC-alkaline phosphatase complex from the Vectastain ABC-alkaline phosphatase standard kit (Vector #AK-5000) after application of secondary antibody. Mix 5ml of 1X PBS, one drop of reagent A, and one drop of reagent B and allow to sit at room temperature 30 minutes prior to use.

9) Blot off excess antibody and wash slides in 1X PBS twice for 5 minutes each at room temperature.

10) Apply prepared ABC mixture to each slide. Incubate in a humid chamber for1hour at room temperature.

11) Blot off excess solution and wash slides in 1X PBS twice for 5 minutes each, followed by one wash in 100mM tris pH 8.2 for 5 minutes.

12) Make up alkaline phosphatase substrate solution (Vector Red #SK-5100) immediately before use. Add 5ml of 100mM tris pH 8.2, one drop levamisole (Vector #SP-5000), two drops each of reagent one, two, and three to a foil wrapped bottle. Mix and apply 2-3 drops per section. Incubate slides in the dark for 20-30 minutes, checking color reaction periodically up to 1 hour. Stop reaction by blotting off substrate and rinsing in tap water twice for 5 minutes each.

13) Lightly counter stain sections with hematoxylin. Rinse slides well in water until water is clear. Dehydrate through graded alcohols, then xylene and coverslip for viewing.

Reagents and Solutions

Proteinase K

Dissolve proteinase K (Sigma # P-4914) in dH2O for a stock concentration of 20mg/ml. Aliquot and store at -20ºC.

C.4. Double immunofluoroscence: von Willebrande Factor and α-smooth muscle actin

1) Deparaffinize and rehydrate fixed paraffin embedded tissue in descending grades of alcohol. Sections are washed in 1X PBS for 5minutes.
2) Antigen retrieval: Treat tissues with 100µg/ml protease for 10 minutes at room temperature.
3) Wash slides in 1X PBS twice for 5 minutes each at room temperature.
4) Block tissue using 1% gelatin/PBS mixture for 20 minutes at room temperature.
5) Prepare the working dilution of the primary antibody rabbit anti-vWF in 1% BSA in 1X PBS at a dilution of 1:800. Blot off gelatin/PBS and apply primary antibody. Incubate sections in a humid chamber for 1hour at room temperature.
6) Blot of excess antibody and wash slides in 1X PBS twice for 5 minutes, each at room temperature.
7) Prepare working dilution of the biotinylated secondary antibody, goat anti-rabbit in 1%BSA in 1X PBS at 1:400 dilution, and add 2% of normal goat serum. Apply antibody and incubate the section for 30 minutes at room temperature in a humid chamber. Prepare the working dilution of ABC-Vector Red complex from the alkaline phosphatase standard kit (Vector #AK-5000) after application of secondary antibody. Mix 5ml of 1X PBS, one drop of reagent A, and one drop of reagent B and allow to sit at room temperature 30 minutes prior to use.
8) Blot off excess antibody and wash slides in 1X PBS twice for 5 minutes each at room temperature.

9) Incubate sections with Avidin D- Texas red at 1:100 dilution in 1%BSA/PBS for 30 minutes. Incubate this step and all subsequent in the dark and preferably refrigerated.
10) Blot off excess solution and wash slides in 1X PBS for 5 minutes, twice in the dark.
11) Block tissue using 2% normal horse serum along with 8 drops of Avidin D and incubate for 20 minutes in the dark.
12) Prepare the working dilution of the second primary antibody, α- smooth muscle actin in 1%BSA in 1X PBS at 1:800 dilution along with 8 drops of biotin. Blot off serum, apply primary antibody, and incubate sections in a humid chamber in dark for 1hour at room temperature.
13) Blot off excess antibody and wash slides in 1X PBS twice for 5 minutes each at room temperature.
14) Incubate sections with horse anti- mouse secondary antibody at 1:400 dilution in 1%BSA/PBS and 2% normal horse serum in dark for 30 minutes.
15) Blot off excess solution and wash slides in 1X PBS for 5 minutes, twice.
16) Incubate with avidin D- fluoroscein in 1%BSA/PBS at a dilution of 1:100 for 30 minutes in the dark.
17) Wash the slides in 1X PBS twice for 5minutes each in the dark.
18) Counter stain with DAPI at a working dilution of 0.25μg/ml in 1%BSA/PBS for 5 minutes in the dark.
19) Rinse the slides in 1X PBS for 5 minutes in the dark.
20) Mount the slides with Aquamount mounting media and refrigerate.

C.5. Scanning electron microscopy

1) Harvest tissue and rinse briefly in 0.2 M sodium cacodylate buffer at a pH 7.2.
2) Fix tissue in 2.5% gluteraldehyde in cacodylate buffer at pH 7.2 for 1-2 hours. Dilute the stock of 8% gluteraldehyde using 0.2M cacodylate buffer at pH 7.2 immediately before use.
3) Rinse in 0.2M cacodylate buffer, pH 7.2 three times for 10 minutes.
4) Dehydrate tissue sample using the following protocol, each for 0.5-1 hour.

   25% alcohol, 50% alcohol, 70% alcohol, twice with 90% alcohol and twice with 100% alcohol.
5) Dry the sample using hexamethyldisilazane (HMDS). The protocol used is,

   100% ethanol: 100% HMDS = 2:1 for 30 minutes

   100% ethanol: 100% HMDS = 1:1 for 30 minutes

   100% ethanol: 100% HMDS = 1:2 for 30 minutes
6) Rinse in 100% HMDS three times for 30 minutes each.
7) Dry the tissue from the last 100% HMDS. The level of HMDS should just cover the tissue sample. Leave the tube containing the sample open in the fume hood and allow HMDS to evaporate and thus dry the tissue. Depending on the sample size, drying should occur overnight.
8) Adhere the sample to an aluminum stub using conductive, double sided carbon adhesive tape.
9) Sputter-coat the sample using gold to a thickness of approximately 100 A^{o}.
10) Desiccate the sample until ready to analyses. Keep tissue in desiccators before viewing under microscope.

APPENDIX D

PRELIMINARY STUDY

The data presented in this section was obtained during the preliminary studies conducted while developing the organ culture system for maintaining consistency in the mechanical conditions and viability of aortic valves for over a period of 48 hours.

D.1. Mechanical performance of the organ culture system

Mechanical performance of the system was tested with a Starr-Edwards ball and cage mechanical valve and a pericardial bioprosthetic valve before biologically validating the system with native porcine aortic valves. The system was operated at a cardiac output of 3.8-4.5 L/min, mean pressure of 100 mmHg and at a frequency of 1.167 Hz. Figure D.1 shows the initial flow and pressure waveforms obtained with a ball and cage mechanical valve and water as circulating fluid.

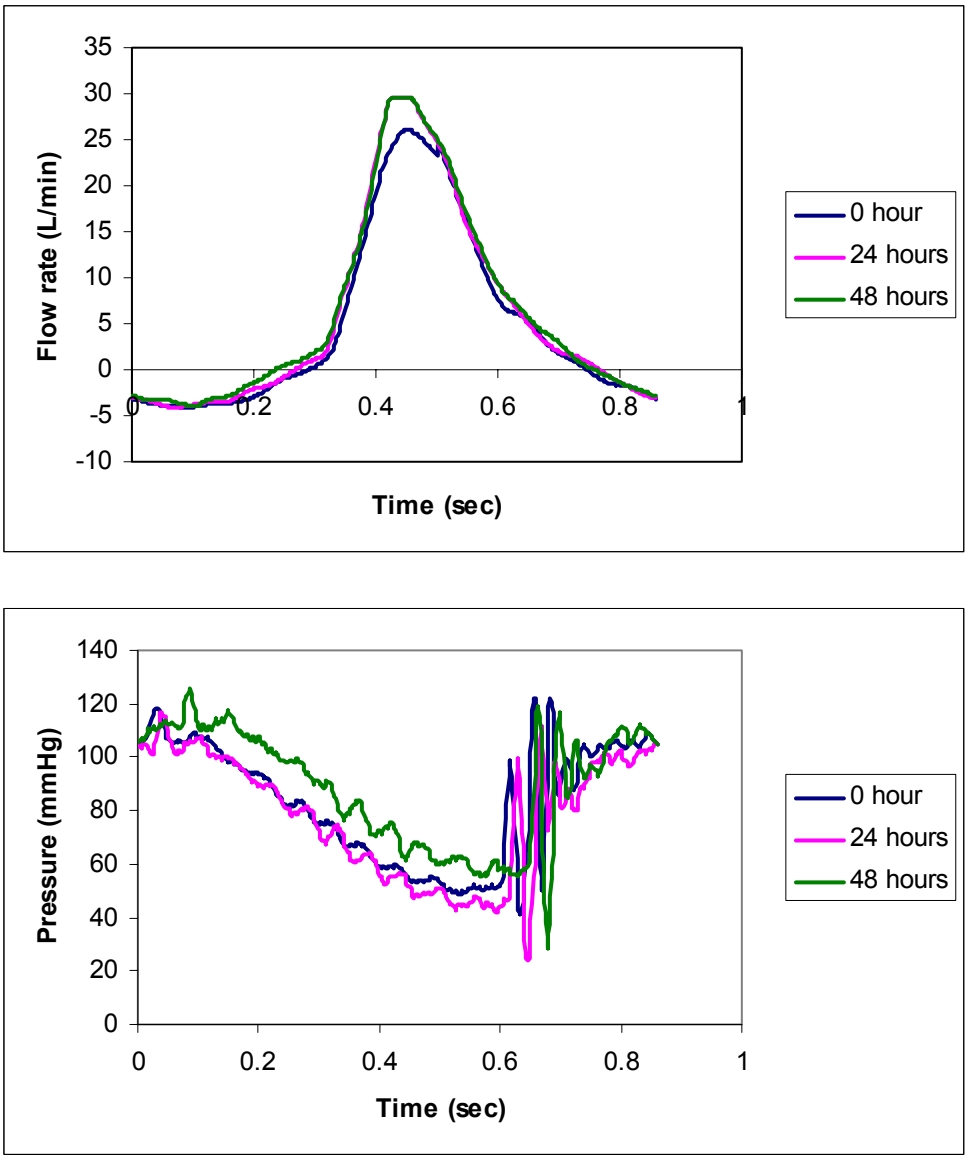

Figure D.1: Initial aortic flow and pressure waveforms of the Starr-Edwards ball and cage mechanical valve in the organ culture system with water as the circulating fluid. The curves were physiological and consistent over a period of 48 hours.

Observing the flow waveform, we can see that the waveforms were consistent over the period of 48 hours. Some amount of back flow is evident, which may be due to leakage when the valve closed. The waveforms were comparable to the physiological waveforms; however the pressure waveform had a much larger magnitude when

compared to the physiological pressure curve. Large pressure oscillations were also evident between 600-700 msec, and these were reduced by injecting air into the compliance tank, increasing the fluid volume in the system and tightening the clamps downstream of the compliance. The system was adjusted with the above mentioned changes, and the waveforms were recorded for the same duration of 48 hours. The new waveforms with the mechanical valve are shown in Figure D.2.

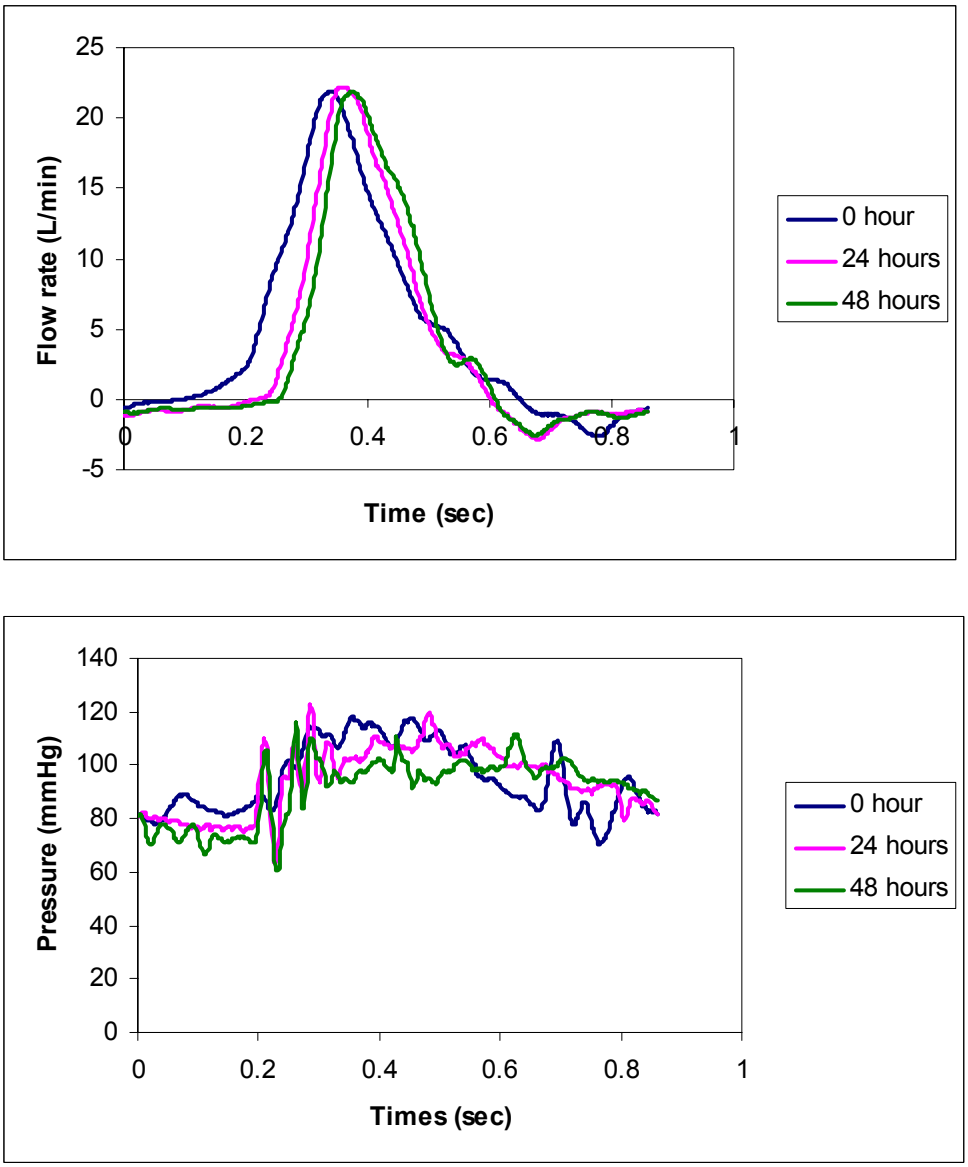

Figure D.2: Modified flow and pressure waveforms of the Starr-Edwards ball and cage mechanical valve in the organ culture system with water as the circulating fluid. The curves were physiological and consistent over a period of 48 hours.

The waveforms seen above are more comparable to physiological waveforms than those in Figure D.1. The backflow although present was less than in the earlier waveform, and the pressure oscillations are less severe. Thus, the adjustments enabled the flow loop to better approximate flow and pressure waveforms.

The system was then operated with a pericardial bioprosthetic valve, which was ultimately used to test the sterility of the system for a period of 96 hours. These waveforms are shown in Figure D.3.

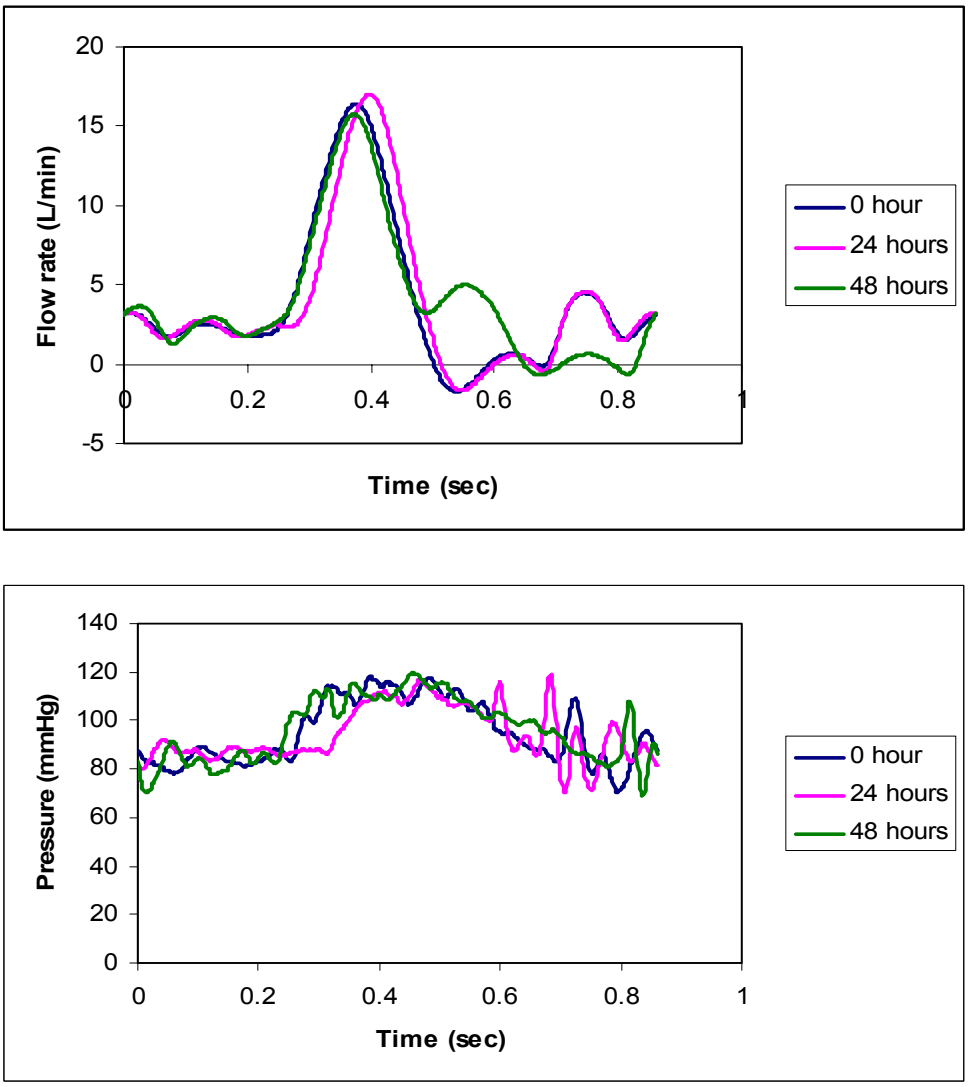

Figure D.3: Flow and pressure waveforms of a pericardial valve in the sterile organ culture system with DMEM as the circulating fluid. The curves were physiological and consistent over a period of 48 hours.

The waveforms were consistent and closely approximated physiological curves throughout the duration of the experiment. The backflow observed in the flow waveform was due to improper coaptation of the valve leaflets which was not system induced. After the consistency in mechanical conditions of the system was established, native porcine aortic valves were cultured in the system for a duration of 48 hours to characterize their biological properties under the influence of mechanical conditions. The flow and pressure waveforms with native aortic valve are shown in Figure D.4.

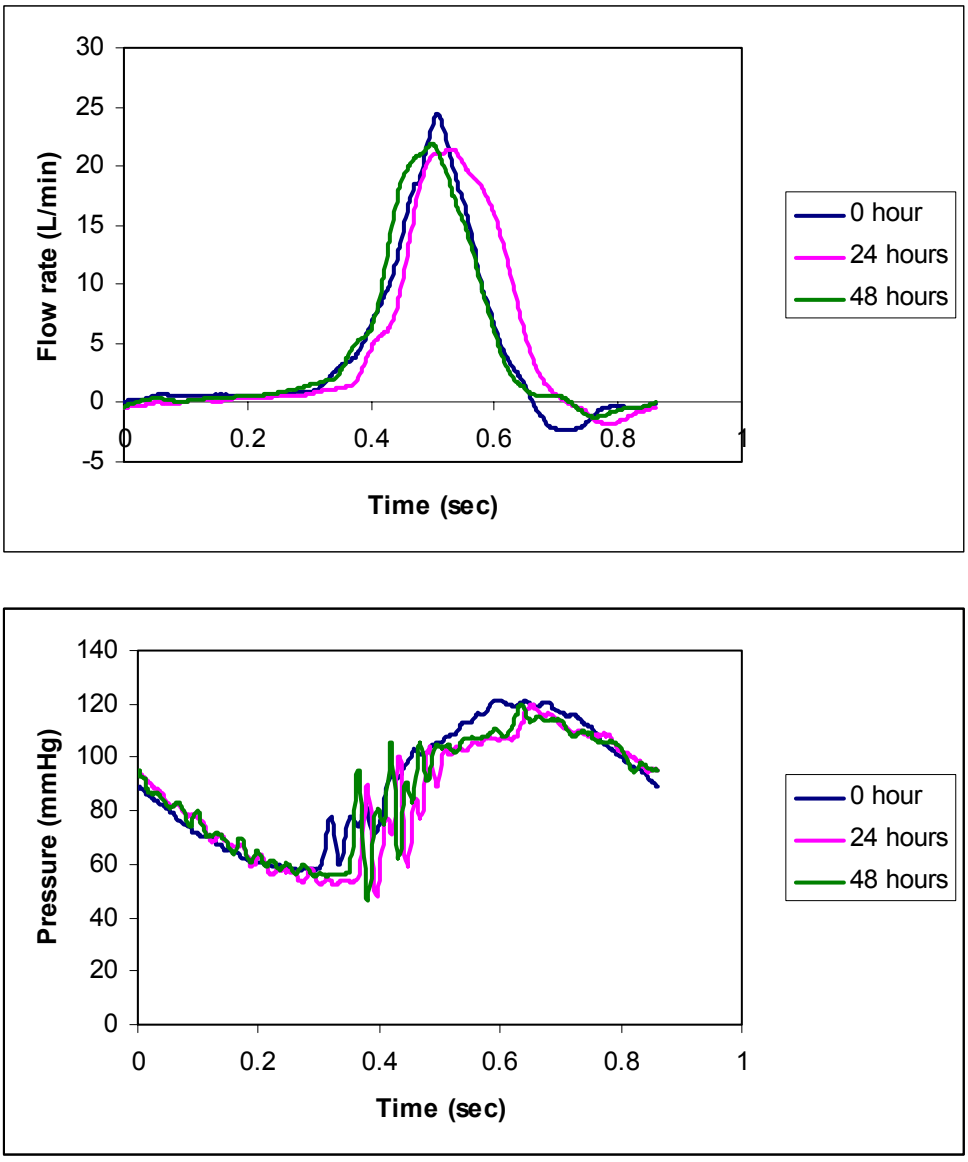

Figure D.4: Flow and pressure waveforms for the native porcine aortic valve in the sterile organ culture system with DMEM as the circulating fluid. The curves were physiological and consistent over a period of 48 hours.

The waveforms have been shown to consistent during the experimental time period. Preliminary experiments with native aortic valves showed the presence of oxygen transfer limitations in the system (which was studied by a Live/Dead stain shown in

section D.5). This was overcome by incorporating a gas permeable silicon tubing connected to a 5% CO_2 gas cylinder.

The biological data obtained by culturing native aortic valves is shown in the following sections.

D.2. Extracellular matrix components data

The methods used to obtain the biological data are same as those described in chapter 4. Figures D.4-D.6 show the differences in collagen, sGAG and elastin contents between the three groups of the leaflets from 5 experiments.

The differences in ECM components between cultured valve leaflets and control leaflets (fresh and statically incubated) was not statistically significant ($p>0.05$, $N=5$).

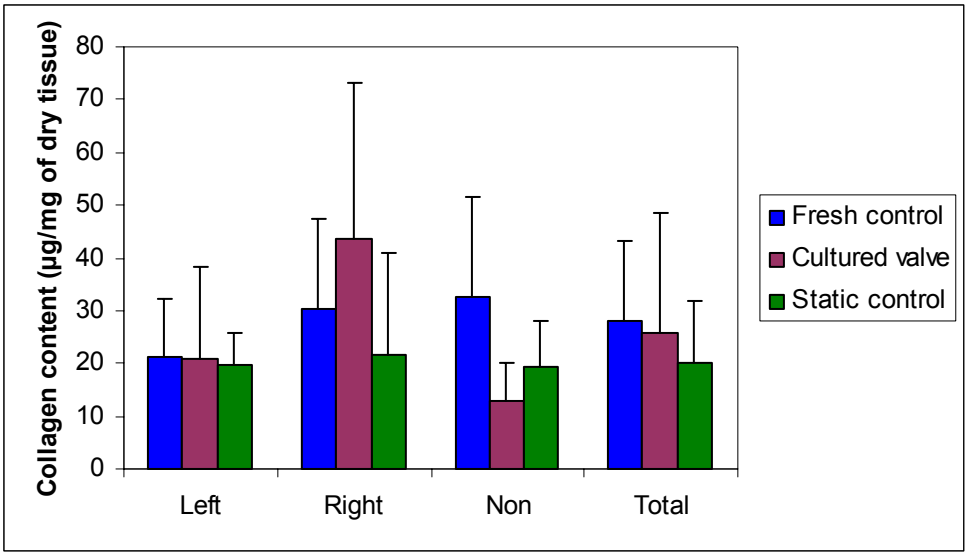

Figure D.5: Collagen content in the left, right, non-coronary leaflets and average value over the valve (total). Data is shown as average value + one standard deviation. (n=5). No difference is observed between cultured valve leaflets and control valves within statistical significance.

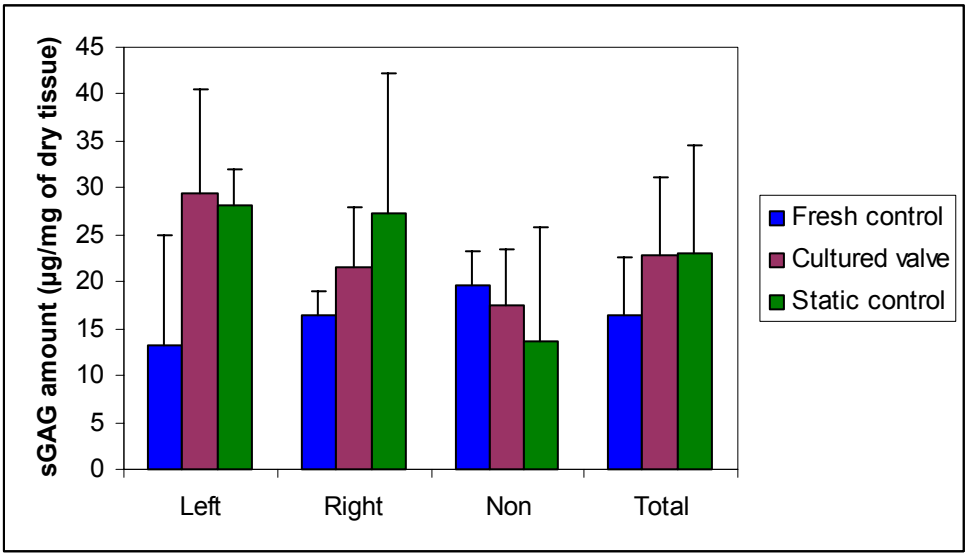

Figure D.6: sGAG content in the left, right, non-coronary leaflets and average value over the valve (total). Data is shown as average value + one standard deviation. (n=5). No difference is observed between cultured valve leaflets and control valves within statistical significance.

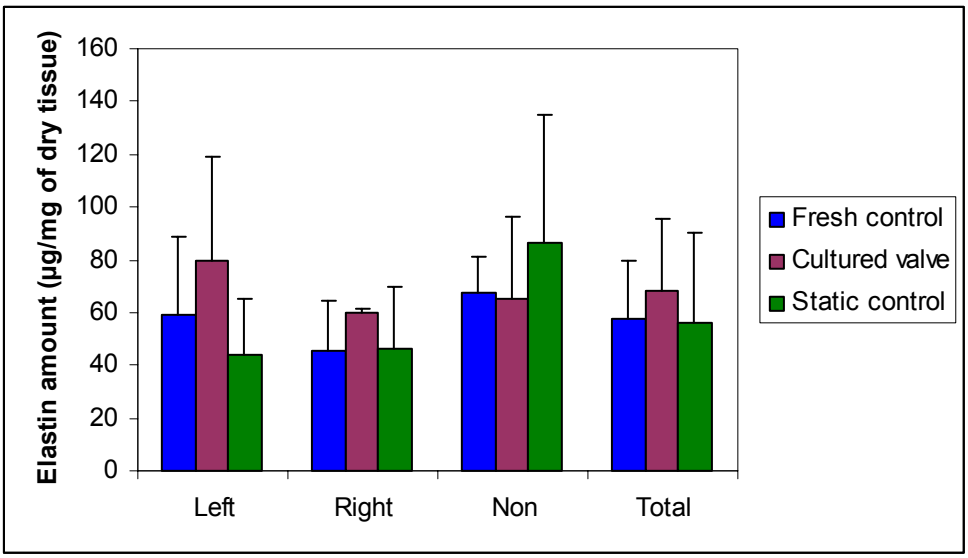

Figure D.7: Elastin content in the left, right, non-coronary leaflets and average value over the valve (total). Data is shown as average value + one standard deviation. (n=5). No difference is observed between cultured valve leaflets and control valves within statistical significance.

D.3. Hematoxylin and Eosin stain

This section shows the pictures of H & E stained sections of the cultured and control valves leaflets.

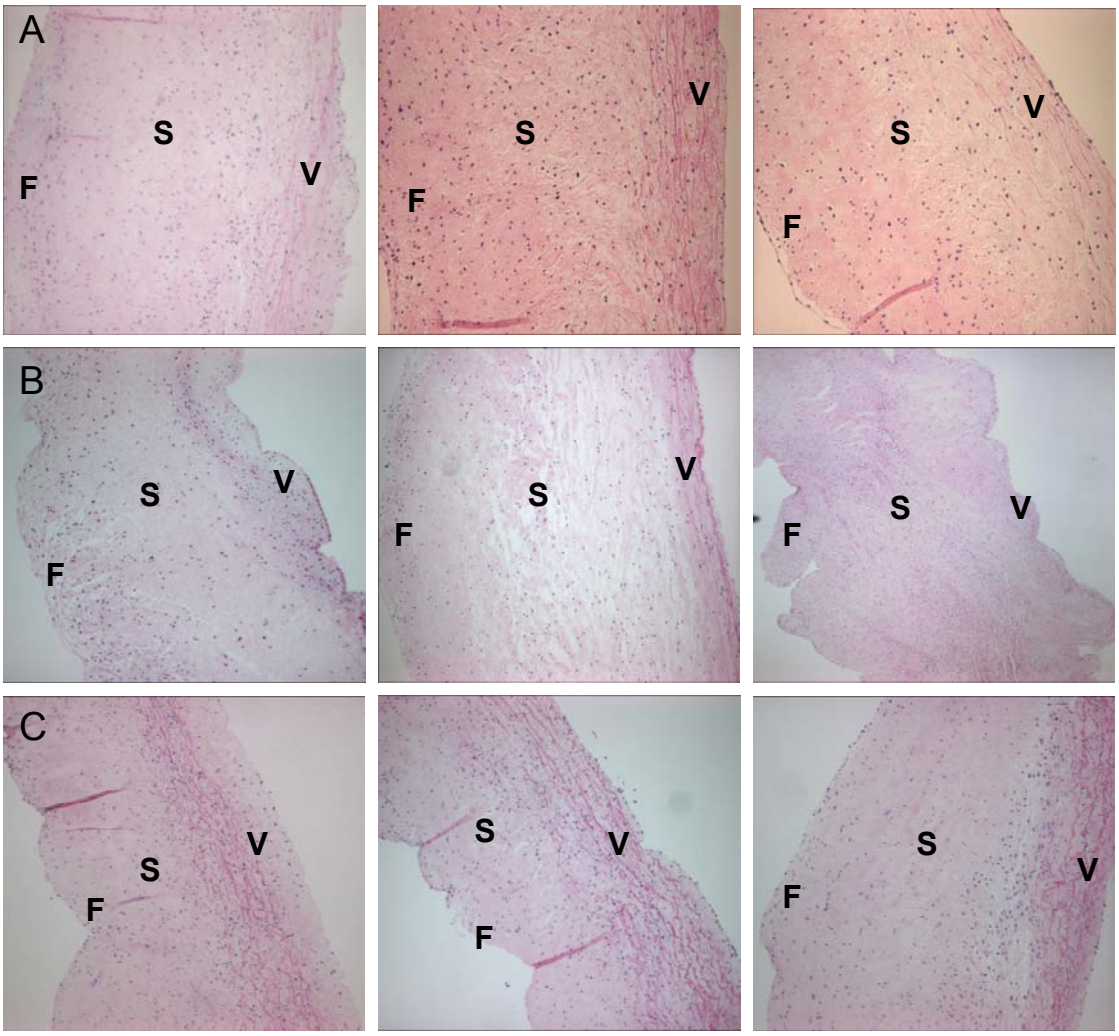

Figure D.8. From left to right: Left, Right and Non coronary leaflets. Shown here are the H & E stains of fresh (A), cultured (B) and static (C) control leaflets. Cell nuclei are shown in blue and ECM in pink. Images were taken at 20X magnification. The morphology of the cultured leaflets was preserved in the system, which is comparable to fresh and static control leaflets. (F-Fibrosa, S-Spongiosa, V-Ventricularis).

The leaflets showed no difference in morphology between the cultured and control valves leaflets. The leaflet cellularity and three-layered architecture of the leaflet was retained suggesting preservation of morphology of leaflets in the system.

D.4. α-smooth muscle actin immunohistochemistry

Leaflets cultured in the organ culture system were stained for presence of α-SMC actin in the leaflets and were compared to fresh valve leaflets. Static control leaflets were not used in the study. Shown in figure D.8 are the pictures of the α-SMC actin stain.

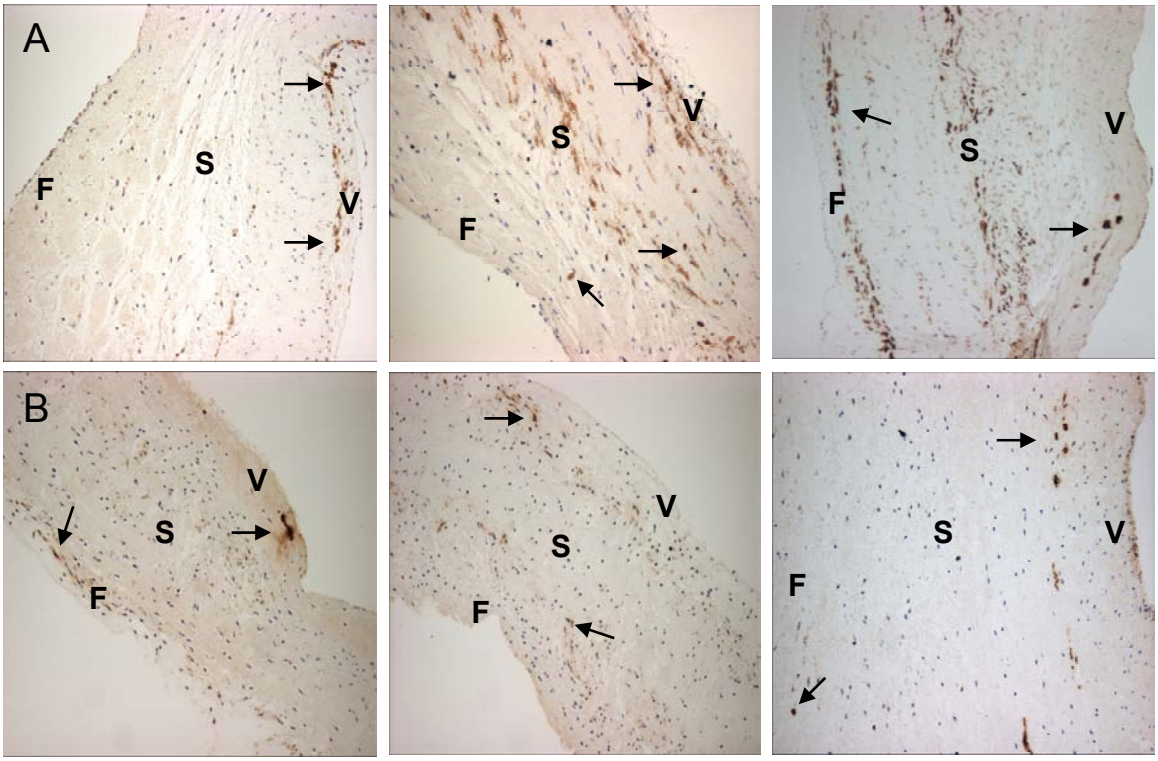

Figure D.9. From left to right: Left, Right and Non coronary leaflets. Shown here are α-SMC actin immunofluoroscence images of fresh (A), and cultured (B) valve leaflets. Brown indicates α-SMC actin expressed by interstitial cells and blue indicates cell nuclei. Images were taken at 20X magnification. Actin expressing cells are indicated by black arrows. (F-Fibrosa, S-Spongiosa, V-Ventricularis).

Since this stain produced a lot of back ground effects as seen in fresh control leaflets, no proper inference could be attained. Hence, immunofluoroscence technique was used for further analysis.

D.5. Ethidium homodimer immunofluoroscence

To see the presence of dead cells in the leaflets ethidium homodimer (Ethd) immunofluoroscence was used. The leaflets, after 48 hours of culture in the system, were harvested from the valves by cutting along the attachment region and incubated in DMEM containing ethidium homodimer. The sections were then counterstained by using

vectashield mounting media. Figure D.9, shows Ethd stained sections of fresh (A), cultured (B) and static control (C) valves leaflets. The dead cells are indicated by red color while blue indicates the live cells. Red cells were found in all the three layers of the leaflets for all the groups of the valves. Observing the pictures, it can be seen that the number of red cells are greater in cultured valve leaflets compared to fresh and static control leaflets and also static control leaflets have greater number of red cells than the fresh control leaflets. This suggests that increase in cell death in cultured valve leaflets was induced in the *ex vivo* system due to oxygen limiting condition in the system. Also the incubation of leaflets in a small volume of media (for Ethd) after the culture may have also increased the cell death as seen in static control leaflets. To prevent this, a gas exchanger was incorporated in the system which maintained the cells viable (shown in figure 5.17) and also cell death was analyzed by immediately fixing the leaflets in formalin after removing from the system.

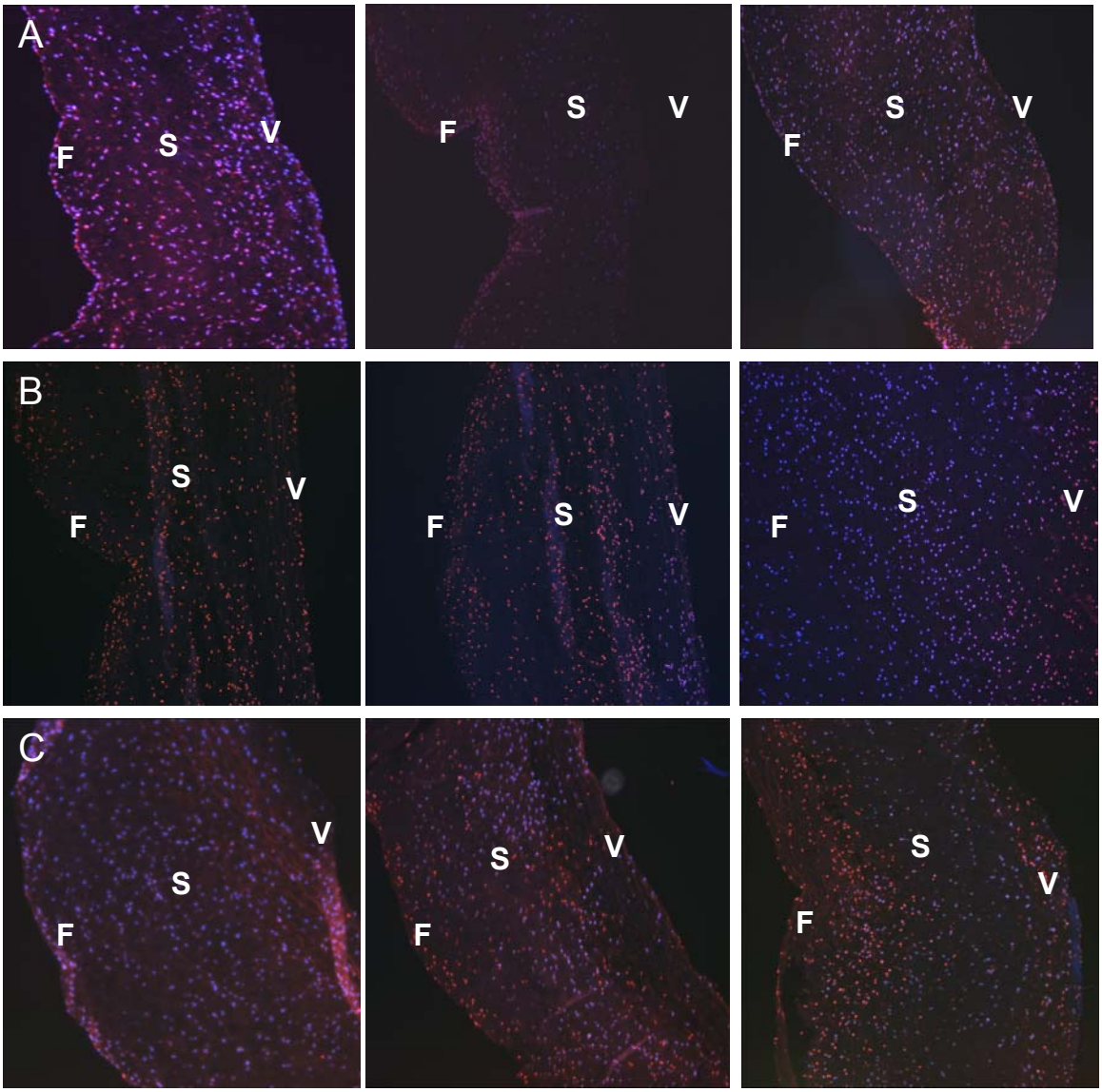

Figure D.10. From left to right: Left, Right and Non coronary leaflets. Shown here are ethidium homodimer images of fresh (A), cultured (B) and static (C) control leaflets. Dead cells are shown in red while live cells are shown in blue. Images were taken at 20X magnification. Positive cells (red cells) were found in fresh, cultured and static control leaflets scattered through the ECM of the leaflets. Cultured valve leaflets showed greater number of dead cells than the control (fresh and static) valves leaflets. (F-Fibrosa, S-Spongiosa, V-Ventricularis).

REFERENCES

Aikawa R.E., Farber M., Aikawa M., and Schoen F.J., "Dynamic and reversible changes of interstitial cell phenotype during remodeling of cardiac valves". *Journal of Heart Valve Disease*, 13, 841-847, 2004.

Angell W.W., Oury J.H., Lamberti J.J., and Koziol J., "Durability of the viable aortic allograft". *Journal of Thoracic and Cardiovascular Surgery*, 98, 48-55, 1989.

Bancroft J.D., and Gamble, M., "Theory and practice of histological techniques". 5th ed., *Churchill Livingstone*, Harcourt Place, London, UK, 2002.

Bernacca G.M., Mackay T.G., and Wheatley D.J, "*In vitro* function and durability of a polyurethane heart valve: material considerations". *Journal of Heart Valve Disease*, 5, 538-542, 1996.

Boulogne E., and Wick T.M., "Effect of shear stress on cardiac leaflet fibroblasts". *Bioengineering conference*, 1999.

Brown C.H.I., Leverett L.B., Lewis C.W., Alfrey C.P.Jr., and Hellums J.D., "Morphological, biochemical, and functional changes in human platelets subjected to shear stress". *Journal of Laboratory and Clinical Medicine*, 86, 462-471, 1975.

Butcher J. T., Penrod A.M., Garcia A.J., and Nerem R.M., "Unique morphology and focal adhesion development of valvular endothelial cells in static and fluid flow environments". *Arteriosclerosis, Thrombus and Vascular Biology*, 24, 1429-1434, 2004b.

Butcher J. T., and Nerem R.M., "Porcine aortic valve interstitial cells in three-dimensional culture: Comparison of phenotype with aortic smooth muscle cells". *Journal of Heart Valve Disease*, 13, 3 478-486, 2004a.

Cabalka A.K., Emery R.W., Petersen R.J., Helseth H.K., Jakkula M., Arom K.V., and Nicoloff D.M., "Long-term follow-up of the St. Jude Medical prosthesis in pediatric patients". *Annals of Thoracic Surgery*, 60, S618-S623, 1995.

Camp J.P., Smith M., and Szurgot M.A, "Lessons of the Björk-Shiley Heart Valve Failure". *http://www.me.utexas.edu/~uer/heartvalves/index.html*, (December), 1997.

Carson F.L., "Histotechnology: A self-instructional text". *American Society of Clinical Pathologies press*, Chicago, IL, USA, 1990.

Carver W., Nagpal M.L., Nachtigal M., Borg T.K., and Terracio L., "Collagen expression in mechanically stimulated cardiac fibroblasts". *Circulation Research*, 69, 116-122, 1991.

Cataloglu A., Gould P.L., Asce M., and Clark R.E., "Refined stress analysis of human aortic heart valves". *Journal of the Engineering Mechanics Division*, 102, 135-151, 1976.

Chaubey S., Latif N., Chester A.H., Taylor P.M., and Yacoub M.H., "Effect of stretch on the expression of cytoskeleton and extra cellular matrix proteins in aortic and pulmonary valve interstitial cells: relevance to the Ross procedure". *2nd Biennial meeting of the society for heart valve disease*, 2003.

Chen W., Schoen F.J., and Levy R.J., "Mechanism of efficacy of 2-Aminooleic acid for inhibition of calcification of glutaraldehyde-pretreated porcine bioprosthetic heart valves". *Circulation*, 90, 323-329, 1994.

Christie G.W., and Barratt-Boyes B.G., "Age-dependent changes in the radial stretch of human aortic valve leaflets determined by biaxial testing". *Annals of Thoracic Surgery*, 60, S156-159, 1995a.

Christie G.W., and Barratt-Boyes B.G., "Mechanical properties of porcine pulmonary valve leaflets: How do they differ from aortic leaflets?" *Annals of Thoracic Surgery*, 60, S195-199, 1995b.

Corden J., David T., and Fisher J., "*In vitro* determination of the curvatures and bending strains acting on the leaflets of polyurethane trileaflet heart valves during leaflet motion". *Proceedings of the Institute of Mechanical Engineers [H]*, 209, 243-253, 1995.

Cosgrove D.M., Lytle B.W., Gill C.C., Golding L.A., Stewart R.W., Loop F.D., and Williams G.W., "In vivo hemodynamic comparison of porcine and pericardial valves". *Journal of Thoracic and Cardiovascular Surgery*, 89, 358-368, 1985.

David A.O., Aldemire T.C., Denton A.C., and George J.R.Jr., "Ionescu-Shiley pericardial xenograft valve: Hemodynamic evaluation and early clinical follow-up of 326 patients". *Cardiovascular Disease*, 7, 137-148, 1980.

Deck J.D., "Endothelial cell orientation on aortic valve leaflets". *Cardiovascular Research*, 20, 760-767, 1986.

Del Rizzo D.F., Goldman B. S., Christakis G. T., and David T. E., "Hemodynamic benefits of the Toronto Stentless valves". *Journal of Thoracic and Cardiovascular Surgery*, 112, 143-145, 1996.

Dewey C.F., Bussolari S.R., Gimbrone M.A., and Davies P.F., "The dynamic response of vascular endothelial cells to fluid shear stress". *Journal of Biomechanical Engineering*, 103, 177-185, 1981.

Driessen N.J.B., Peters G.W.M., Huyghe J.M., Bouten C.V.C., and Baaijiens F.P.T., "Remodeling of continuously distributed collagen fibers in soft connective tissues". *Journal of Biomechanics*, 36, 1151-1158, 2003.

Dumont K., Yperman J., Verbeken E., Segers P., Meuris B., Vanderghe S., Flameng W., and Verdonck P.R., "Design of a new pulsatile bioreactor for tissue engineered aortic valve formation". *Artificial Organs*, 26, 710-714, 2002.

Edwards Life sciences, "Edwards's life sciences tissue valve products". *http://www.lifeisnow.com/MyHeart/EdwardsLifesciencesTissueValveProducts*, 2004.

Einav S., Stolero D., Avidor J.M., Elad D., and Talbot L., "Wall shear stress distribution along the cusp of a tri-leaflet prosthetic valve". *Journal of Biomedical Engineering*, 12, 13-18, 1990.

Elkins R.C., "Is tissue-engineered heart valve replacement clinically applicable?" *Current Cardiology Reports*, 5, 125-128, 2003.

Englemayr G.C.J., Hildebrand D.K., Sutherland F.W.H., Mayer J.E. Jr., and Sacks M.S., "A novel bioreactor for the dynamic flexural stimulation of tissue engineered heart valve biomaterials". *Biomaterials*, 24, 2523-2532, 2003.

Freed L.E., Vunjak-Novakovic G., Biron R.J., Eagles D.B., Lesnoy D.C., Barlow S.K., and Langer, R., "Biodegradable polymer scaffolds for tissue engineering". *Biotechnology*, 2, 689-693, 1994.

Fullerton D.A., Fredericksen J.W., Sundaresan R.S., and Horvath K.A., "The Ross procedure in adults: intermediate-term results". *Annals of Thoracic Surgery*, 76, 471-477, 2003.

Gilbert S., "Collagen Types". *http://zygote.swarthmore.edu/cell6.html*, (October), 1996.

Goldstein S., Clarke D.R., Walsh S.P., Black K.S., and O'Brein M.F., "Transpecies heart valve transplant: advanced studies of a bioengineered xeno-autograft". *Annals of Thoracic Surgery*, 70, 1962-1969, 2000.

Gott J.P., Girardot M.N., Girardot J.M.D., Hall J.D., Whitlark J.D., Horsely S.W., Dorsey L.M.A., Levy R.J., Chen W., Schoen F.J., and Guyton R.A., "Refinement of the alpha amino oleic acid bioprosthetic valve anticalcificattion technique". *Annals of Thoracic Surgery*, 64, 50-58, 1997.

Gross C., Harringer W., Beran H., Mair R., Sihorsch K., Hofmann R., and Brucke P., "Aortic valve replacement: Is the stentless xenograft an alternative to the homograft? Midterm results". *Annals of Thoracic Surgery*, 68, 919-924, 1999.

Guyton A.C., "Textbook of Medical Physiology". 8th ed. *W.B. Saunders Co.*, Philadelphia, PA, USA, 1991.

Hafizi S., Taylor P.M., Chester A.H., Allen S.P., and Yacoub M.H., "Mitogenic and secretory responses of human valve interstitial cells to vasoactive agents". *Journal of Heart Valve Disease*, 9, 454-458, 2000.

Hasirci V., Berthiaume F., Bondre S.P., Gresser J.D., Trantolo D.J., Toner M., and Wise D.L., "Expression of liver-specific functions by rat hepatocytes seeded in treated poly(lactic-co-glycolic) acid biodegradable foams". *Tissue Engineering*, 7, 385-394, 2001.

Hilbert S.L., Ferrans V.J., Tomaita Y., Eidbo E.E., and Jones M.M., "Evaluation of explanted valves: performance and blood compatibility". *Life Support Systems*, 4, 130-132, 1987.

Hilbert S.L., Luna R.E., Zhang J., Wang Y., Hopkins R.A., Yu Z., and Ferrans V.J., "Allograft heart valves: the role of apoptosis-mediated cell loss". *Journal of Thoracic and Cardiovascular Surgery*, 117, 454-462, 1999.

Hildebrand D.K., Wu Z.J., Mayer J.E.Jr., and Sacks M.S., "Design and hydrodynamic evaluation of a novel pulsatile bioreactor for biologically active heart valves". *Annals of Biomedical Engineering*, 32, 1039-1049, 2004.

Hishikawa K., Nakaki T., Marumo T., Hayashi M., Suzuki H., Kato R., and Saruta T., "Pressure promotes DNA synthesis in rat cultured vascular smooth muscle cells". *Journal of Clinical Investigation*, 93, 1975-1980, 1994.

Hoerstrup S.P., Sodian R., Sperling J.S., Vacanti J.P., and Mayer J.E., "New pulsatile bioreactor for *in vitro* formation of tissue engineered heart valves". *Tissue Engineering*, 6, 75-79, 2000.

Hoerstrup S.P., Sodian R., Daebritz S., Wang J., Bacha E.A., Martin D.P., Moran A.M., Gulesrian K.J., Sperling J.S., Kaushal S., Vacanti J.P., Schoen F.J., and Mayer J.E.Jr., "Functional living trileaflet heart valves grown *in vitro*". *Circulation*, 102, III 44-49, 2000.

Ingham E., and Fisher J., "Development of physically interactive bioreactors for study of cell and tissue responses to biomechanical stimulation in vitro". *European Cells and Materials*, 6, 5, 2003.

Iwatsuki K., Cradinale G.J., Spector S., and Udenfriend S., "Hypertension: Increase of collagen biosynthesis in arteries but not in veins". *Science*, 198, 403-404, 1977.

Jin Y.X., and Pepper J.R, "Do stentless valves make a difference?" *European Journal of Cardio-thoracic Surgery*, 22, 95-100, 2002.

Jockenhoevel S., Zund G., Hoerstrup S.P., Schnell A., and Turina M., "Cardiovascular tissue engineering: A new laminar flow chamber for in vitro improvement of mechanical tissue properties". *ASAIO Journal*, 48, 8-11, 2002.

Jones T.K., and Lupinetti F.M., "Comparison of Ross procedures and aortic valve allografts in children". *Annals of Thoracic Surgery*, 66, S170-173, 1998.

Jonge H.W.D.E., Dekkers D.H.W., Tilly B.C., and Lamers J.M.J., "Cyclic stretch and endothelin-1 mediated activation of chloride channels in cultured neonatal rat ventricular myocytes". *Clinical Science*, 103, S148-151, 2002.

Joris I., Zand T., and Majno G., "Hydrodynamic injury of the endothelium in acute aortic stenosis". *American Journal of Pathology*, 106, 394-408, 1982.

Jouret C., "Effects of matrix and phenotype on human dermal fibroblast attachment under laminar shear stress: implications for the development of tissue-engineered heart valves". *MS Thesis*.(Georgia Institute of Technology), 1997.

Kada K., Yasui K., Naruse K., Kamiya K., Kodama I., and Toyama J., "Orientation change of cardiocytes induced by cyclic stretch stimulation: Time dependency and involvement of protein kinases". *Journal of Molecular Cell Cardiology*, 31, 247-259, 1999.

Kershaw J.D.B., Misfeld M., Sievers H.H., Yacoub M.H., and Chester, A.H., "Specific regional and directional contractile responses of aortic cusp tissue". *Journal of Heart Valve Disease*, 13, 798-803, 2004.

King M.W., "Glycosaminoglycans".*http://www.indstate.edu/thcme/mwking/glycans.html*, (August), 2003.

Kitagawa T., Masuda Y., Tominaga T., and Kano M., "Cellular biology of cryopreserved allograft valves". *Journal of Medical Investigation*, 48, 123-132, 2001.

Klabunde R.E., "Cardiovascular Physiology Concepts". *http://www.cvphysiology.com/Heart%20Disease/HD002.htm*, 1999.

Koolbergen D.R., Hazekamp M.G., Kurvers M., de Heer E., Cornelisse C.J., Huysmans H.A., and Bruijn J.A., "Tissue chimerism in human cryopreserved homograft valve explants demonstrated demonstrated by hybridization". *Annals of Thoracic Surgery*, 66, S225-232, 1998.

Lee C.H., Vyavahare N., Zand R., Kruth H., Schoen F.J., Bianco R., and Levy R.J., "Inhibition of aortic wall calcification in bioprosthetic heart valves by ethanol pretreatment: Biochemical and biophysical mechanisms". *Journal of Biomedical Materials Research*, 42, 30-37, 1998.

Levesque M.J., and Nerem R.M., "The elongation and orientation of cultured endothelial cells in response to shear stress". *Journal of Biomechanical Engineering*, 107, 341-347, 1985.

Levesque M.J., Liepsch D., Moravec S., and Nerem R.M., "Correlation of endothelial cell shape and wall shear stress in a stenosed dog aorta". *Arteriosclerosis*, 6, 220-229, 1986.

L'heureux N., Pâquet S., Labbé R., Germain L., and Auger F.A., "A completely biological tissue-engineered human blood vessel". *The FASEB Journal*, 12, 477-486, 1998.

Lupinetti F.M., Kneebone J.M., Rekhter M.D., Brockbank K.G.M., and Gordon D., "Procollagen production in fresh and cryopreserved aortic valve grafts". *Journal of Thoracic and Cardiovascular Surgery*, 113, 102-107, 1997.

Maier G.W., and Wechsler A.S., "Pathophysiology of aortic valve disease". *http://www.ctsnet.org/edmunds/Chapter28.html*, 2003.

Martin I., Wendt D., and Heberer M, "The role of bioreactors in tissue engineering". *Trends in Biotechnology*, 22, 80-86, 2004.

Mayo Clinic, "Heart Disease". *http://www.cnn.com/HEALTH/library/DS/00418.html*, (December), 2003.

Missirlis Y.F., and Chong M., "Aortic valve mechanics-Part I: Material properties of natural porcine aortic valves". *Journal of Bioengineering*, 2, 287-300, 1978.

Mitchell R.N., Jonas R.A., and Schoen F.J., "Pathology of explanted cryopreserved allograft heart valves: comparison with aortic valves from orthotopic heart transplants". *Journal of Thoracic and Cardiovascular Surgery*, 115, 118-127, 1998.

Nandy S., and Tarbell J.M., "Flush mounted hot film anemometer measurements of wall shear stress distal to a trileaflet valve for Newtonian and non-Newtonian blood analog fluids". *Biorheology*, 24, 483-500, 1987.

Ng K.W., Hutmacher D.W., Schantz J.T., Ng C.S., Too H.P., Lim T.C., Phan T.T., and Teoh S.H., "Evaluation of ultra-thin poly(epsilon-caprolactone) films for tissue-engineered skin". *Tissue Engineering*, 7, 441-455, 2001.

Niklason L.E., Gao J., Abbott W.M., Hirschi K.K., Houser S., Marini R., and Langer R., "Functional arteries grown *in vitro*". *Science*, 284, 489-493, 1999.

Nishimura R.A., "Aortic Valve Disease". *Circulation*, 106, 770-772, 2002.

Novaro G.M., and Mills R.M., "Aortic Valve Disease". *http://www.clevelandclinicmeded.com/diseasemanagement/cardiology/aortic_valve/aortic_valve.htm*, (May), 2002.

O'Brien M.F., Stafford E.G., Gardner M.A., Pohlner P.G., and McGiffin D.C., "A comparison of aortic valve replacement with viable cryopreserved and fresh allograft valves, with a note on chromosomal studies". *Journal of Thoracic and Cardiovascular Surgery*, 94, 812-823, 1987.

Owen G.K., and Reidy M.A., "Hyperplastic growth response of vascular smooth muscle cells following induction of acute hypertension in rats by aortic coarctation". *Circulation Research*, 57, 695-705, 1985.

Passerini A.G., Polacek D.C., Shi C., Francesco N.M., Manduchi E., Grant G.R., Pritchard W.F., Powell S., Chang G.Y., Stoeckert C.J. Jr., and Davies P.F., "Coexisting proinflammatory and antioxidative endothelial transcription profiles on a disturbed flow region of the adult porcine aorta". *Proceedings of the National Academy of Sciences of the United States of America*, 101, 2482-2487, 2004.

Pettersson G., "Aortic Valve Surgery in the Young Adult Patient". *http://www.clevelandclinic.org/heartcenter/pub/guide/disease/valve/youngvalve.htm*, (November), 2003.

Purinya B., Kasyanov V., Vololakov J., Latsis R. and Tetere G., "Biomechanical and structural properties of the explanted bioprosthetic valve leaflets". *Journal of Biomechanics*, 27, 1-11, 1994.

Rabkin E., Aikawa M., Stone J.R., Fukumoto Y., Libby P., and Schoen F.J., "Activated Interstitial Myofibroblasts Express Catabolic Enzymes and Mediate Matrix Remodeling in Myxomatous Heart Valves". *Circulation*, 104, 2525-2532, 2001.

Sacks M.S., and Schoen F.J., "Collagen fiber disruption occurs independent of calcification in clinically explanted bioprosthetic heart valves". *Journal of Biomedical Materials Research*, 62, 359-371, 2002.

Schneider P.J., and Deck J.D., "Tissue and cell renewal in the natural aortic valve of rats: an autoradiographic study". *Cardiovascular Research*, 15, 181-189, 1981.

Scott M., "Background on heart valves and their function". *http://heartlab.robarts.ca/what.is.1.html*, (July), 1998.

Seliktar D., Black R.A., Vito R.P., and Nerem R.M., "Dynamic mechanical conditioning of collagen-gel blood vessel constructs subjected to cyclic strain". *Annals of Biomedical Engineering*, 29, 923-934, 2001.

Sell S., and Scully R.E., "Aging changes in the aortic and mitral valves. Histological and biochemical studies, with observations in the pathogenesis of calcific aortic stenosis and calcification of the mitral annulus". *American Journal of Pathology*, 46, 345-365, 1965.

Shappell S.D., "Valvular heart diseases". *http://www.heartcenteronline.com/myheartdr/common/articles.cfm?ARTID=187*, (May), 2004.

Shinoka T., Breuer C.K., Tanel R.E., Zund G., Miura T., Ma P.X., Langer R., Vacanti J.P., and Mayer J.E.Jr., "Tissue engineering heart valves: autologous valve leaflet replacement study in lamb model". *Annals of Thoracic Surgery*, 60, S513-516, 1995.

Silverthorn D.U., "Human Physiology: An Integrated Approach". 2nd ed. *Prentice Hall*, Upper Saddle River, NJ, USA, 2001.

Simon P., Kasimir M.T., Seebacher G., Weigel G., Ullrich R., Salzer-Muhar U., Reider E., and Wolner E., "Early failure of the tissue engineered porcine heart valve Synergraft in pediatric patients". *European Journal of Cardio-thoracic Surgery*, 23, 1002-1006, 2003.

Sipkema P., Van der Linden P.J.W., Westerhof N., and Yin F.C.P., "Effect of cyclic axial stretch of rat arteries on endothelial cytoskeletal morphology and vascular reactivity". *Journal of Biomechanics*, 36, 653-659, 2003.

Sodian R., Hoerstrup S.P., Sperling J.S., Daebritz S.H., Martin D.P., Schoen F.J., Vacanti J.P., and Mayer J.E.Jr., "Tissue engineering of heart valves: *In Vitro* experiences". *Annals of Thoracic Surgery*, 70, 140-144, 2000.

Solan A., Mitchell S., Moses M., and Niklason L., "Effect of Pulse Rate on Collagen Deposition in the Tissue-Engineered Blood Vessel". *Tissue Engineering*, 9, 579-586, 2003.

Song Y.C., Yao L.Y., Kneebone J.M., and Lupinetti F.M., "Effect of cryopreservation and histocompatibility on type I procollagen gene expression in aortic valve grafts". *Journal of Thoracic and Cardiovascular Surgery*, 114, 421-427, 1997.

Sotoudeh M., Jalali S., Usami S., Shyy J.Y.J., and Chien S., "A strain device imposing dynamic and uniform equi-biaxial strain to cultured cells". *Annals of Biomedical Engineering*, 26, 181-189, 1998.

St.PatrickHospital, "Ross procedure and registry". *http://www.saintpatrick.org/ihi/ross.html*, 2004.

Stegemann J.P., and Nerem R.M., "Altered response of vascular smooth muscle cells to exogenous biochemical stimulation in two- and three- dimensional culture". *Experimental Cell Research*, 283, 146-155, 2003.

Stegemann J.P., and Nerem R.M., "Phenotype modulation in vascular tissue engineering using biochemical and mechanical stimulation". *Annals of Biomedical Engineering*, 31, 391-402, 2003.

Takkenberg J.J.M., Van Herwerden L.A., Eijkenmans M.J.C., Bekkers J.A., and Bogers A.J.J.C., "Evolution of allograft aortic valve replacement over 13 years: results of 275 procedures". *European Journal of Cardio-thoracic Surgery*, 21, 683-691, 2002.

Talman E.A., and Boughner D.R., "Glutaraldehyde fixation alters the internal shear properties of porcine aortic heart valve tissue". *Annals of Thoracic Surgery*, 60, S369-S373, 1995.

Talman E.A., and Boughner D.R., "Effect of altered hydration on the internal shear properties of porcine aortic valve cusps". *Annals of Thoracic Surgery*, 71, S375-378, 2001.

Taylor P.M., Batten P., Brand N.J., Thomas P.S., and Yacoub M.H., "The cardiac valve interstitial cell". *The International Journal of Biochemistry and Cell Biology*, 35, 113-118, 2003.

Teebken O.E., and Haverich A., "Tissue engineering of small diameter vascular grafts". *European Journal of Vascular and Endovascular Surgery*, 23, 475-485, 2002.

Thubrikar M., "The Aortic Valve". CRC Press, Boca Raton, FL, USA, 1990.

Tokunaga O., and Watanabe T., "Properties of endothelial cell and smooth muscle cell cultured in ambient pressure". *In vitro Cellular and Developmental Biology*, 23, 528-534, 1987.

Travis B.R., Leo H.L., Shah P.A., Frakes D.H., and Yoganathan A.P., "An analysis of turbulent shear stresses in leakage flow through a bileaflet mechanical prostheses". *Journal of Biomechanical Engineering*, 124, 155-165, 2002.

Tziampazis E., and Sambanis A., "Tissue engineering of a bioartificial pancreas: modeling the cell environment and device function". *Biotechnology Progress*, 11, 115-126, 1995.

Vagale D., Hruska C, Kaufmann J, and Summerscale I., "Prosthetic Valves". *http://cape.uwaterloo.ca/che100projects/heart/files/testing.htm#intro*, 2004.

Vorp D.A., Peters D.G., and Webster M.W., "Gene expression is altered in perfused arterial segments exposed to cyclic flexure *ex vivo*". *Annals of Biomedical Engineering*, 27, 366-371, 1999.

Vouyouka A.G., Powell R.J., Ricotta J., Chen H., Dudrick D.J., Sawmiller C.J., Dudrick S.J., and Sumpio B.E., "Ambient pulsatile pressure modulates endothelial cell proliferation". *Journal of Molecular and Cellular Cardiology*, 30, 609-615, 1998.

Walburn F.J., and Stein P.D., "Wall shear stress during pulsatile flow distal to a normal porcine aortic valve". *Journal of Biomechanics*, 17, 97-102, 1984.

Wang J., Lukse E., Seth A., and McCulloch C.A., "Use of conditionally immortalized mouse cardiac fibroblasts to examine the effect of mechanical stretch on alpha-smooth muscle actin". *Tissue and Cell*, 33, 86-96, 2001.

Warnock J.N., Suchitra K., He Z., and Yoganathan A.P., "Design of a sterile organ culture system for the *Ex Vivo* study of aortic heart valves". *Journal of Biomechanical Engineering*, Under review, 2004.

Weinberg C.B., and Bell E., "A blood vessel model constructed from collagen and cultured vascular cells". *Science*, 231, 397-400, 1986.

Welgus H., "Elastin". *http://www.aad.org/education/elastin.htm*, 2003.

Wend K.L., Boughner D.R., Rigutto L., and Ellis C.G., "Oxygen diffusion and consumption of aortic valve cusps". *American journal of physiology- Heart and Circulatory Physiology*, 281, H2604-H2611, 2001.

Weston M.W., LaBorde D.V., and Yoganathan A.P., "Estimation of the shear stress on the surface of an aortic valve leaflet". *Annals of Biomedical Engineering*, 27, 572-579, 1999.

Weston M.W., and Yoganathan A.P., "Biosynthetic activity in heart valve leaflets in response to *in vitro* flow environments". *Annals of Biomedical Engineering*, 29, 752-763, 2001.

Wheatley D.J., Fisher J., Reece I.J., Spyt T., and Breeze P., "Primary tissue failure in pericardial heart valves". *Journal of Thoracic and Cardiovascular Surgery*, 94, 367-374, 1987.

Wheatley D.J., Raco L., Bernacca G.M., Sim I., Belcher P.R., and Boyd J.S., "Polyurethane: material for the next generation of heart valve prostheses?" *European Journal of Cardio-thoracic Surgery*, 17, 440-448, 2000.

Wick T.M., and Jouret C., "Flow chamber to mimic the environment in artificial heart valves". *International Conference on Cellular Engineering*, 1997.

Willems I.E., Havenith M.G., Smits J.F., and Daemen M.J., "Structural alterations in heart valves during left ventricular pressure overload in the rat". *Laboratory Investigation*, 71, 127-133, 1994.

Willems I.H.A., "The design of an in vitro flow loop for evaluating the effects of persistent mechanical forces on porcine aortic valves". Atlanta, 2002.

Wilson G.J., Courtman D.W., Klement P., Lee J.M., and Yeger H., "Acellular matrix: A biomaterials approach for coronary artery bypass and heart valve replacement". *Annals of Thoracic Surgery*, 60, S353-358, 1995.

Woo Y.R., and Yoganathan A.P., "An instrument for the measurement of in vitro velocity and turbulent shear stress in the immediate vicinity of prosthetic heart valves". *Life Support Systems*, 4, 47-62, 1986.

Xing Y., He Z., Warnock J.N., Hilbert S., and Yoganathan A.P., "Effects of Constant Static Pressure on the Biological Propertiesof Porcine Aortic Valve Leaflets". *Annals of Biomedical Engineering*, 32, 555-562, 2004.

Xing Y., Warnock J.N, He Z., Hilbert S., and Yoganathan A.P., "Cyclic pressure affects the biological properties of porcine aortic valve leaflets in a magnitude- and frequency-dependent manner". *Annals of Biomedical Engineering*, 32, 1461-1470, 2004.

Xing Y., "Effects of mechanical forces on the biological properties of porcine aortic valve leaflets". *PhD Thesis*.(Georgia Institute of Technology), 2004c.

Zeltinger J., Landeen K.L., Alexander H.G., Kidd I.D., and Sibanda B., "Development and characterization of tissue-engineered aortic valves". *Tissue Engineering*, 7, 9-22, 2001.

Zhang J., Doll B.A., Beckman E.J., and Hollinger J.O., "A biodegradable polyurethane-ascorbic acid scaffold for bone tissue engineering". *Journal of Biomedical Materials Research*, 67A, 389-400, 2003.

Zund G., Breuer C.K., Shinoka T., Ma P.X., Langer R., Mayer J.E., and Vacanti J.P., "The in vitro construction of a tissue engineered bioprosthetic heart valve". *European Journal of Cardio-thoracic Surgery*, 11, 493-497, 1997.